Matt Hutton Major Project Final Report

by Matthew David Alexander Hutton

FILE	7338_MATTHEW_DAVID_ALEXANDER_HUTTON_MATT_HUTTON_MAJOR_PROJECT_FINAL_REPORT_128469_730205230.DOCX (28.66M)		
TIME SUBMITTED	30-APR-2019 05:58PM (UTC+0100)	WORD COUNT	12189
SUBMISSION ID	105879418	CHARACTER COUNT	57156





Prifysgol Cymru
Y Drindod Dewi Sant
University of Wales
Trinity Saint David

University of Wales Trinity St David

Matt Hutton

IMPROVEMENTS TO AN INLET PORTS FLOW COEFFICIENT BY MANIPULATION OF PORT SHAPE, SEAT CONFIGURATION AND COMBUSTION CHAMBER DESIGN

Major Project

M6X00417

Malcom McDonald



I wish to express my appreciation for my project supervisor, Mr Malcom McDonald for his guidance and wizardry throughout the project, he has steered me along the right path, helped me with elements of the project I didn't understand and been a great mentor throughout the year. Without him, my project would have not been completed to the standards it has been.

I would also like to thank my family for their support and assistance not only through the final year at university, but the last three years as well. Without their moral, physical and financial support the course would have much more challenging and would have been hard to complete throughout its entirety.

This thesis is the result of the author's original research. It has been composed by the author and has not been previously submitted for examination which has led to the award of a degree.

Signed: *Date:* 30/4/19

TABLE OF CONTENTS

List Of Figures 3
Chapter 1 7
1.1 Abstract 7
1.2 Introduction 7
1.3 Project Background 10
1.4 Background Research 11
1.5 What is cfm? 22
1.6 Flow coefficient 23
1.7 Aims 26
1.8 Methodology 26
1.9 Gaant Chart 27
1.10 References 28

Chapter 2 29
2 Mini Cooper Engine 29
2.1 12g202 cylinder head 30
2.2 Cleaning the head 31
2.3 Making a valve opening tool 32
2.4 Setting up Flow Bench with the 12g202 Head 35
2.5 Flow Testing standard Head 39
2.6 Effect of carbon build up on the valve 41
2.7 Chapter 2 References 42

Chapter 3 43
3 Creating a CAD Model of the port phase 1 43
3.1 Creating a CAD Model of the port phase 2 45
3.2 Setting up the 3D Printer 47
3.3 Printing the CAD Components 52
3.4 Using silicone to model the port geometry 53
3.5 Creating a CAD Model of the port phase 3 54
3.6 Creating a CAD Model of the port phase 4 55
3.7 Printed parts flow test results 63

Chapter 4 ..... **86**
4 Flow Testing using Computation fluid Dynamics **86**
4.1 Results Comparison **95**
4.2 Further Work **96**
4.3 Conclusion **96**
4.3 Evaluation **97**
4.4 Bibliography **97**

LIST OF FIGURES

Figure 1: Simple example of Inlet port and Combustion Chamber 8
Figure 2: [1] Cylinder head porting 9
Figure 3: Example of CAD software (Solidworks 2019) 9
Figure 4: [2] 3D Printer halfway through a print 10
Figure 5: 1983 Mini Cooper 997 11
Figure 6: [3] structural parameters of an inlet port 15
Figure 7: [5] Air passing over short and long turn radius 16
Figure 8: [5] CFD Image of air flow through inlet port 17
Figure 9: [5] Seat and Port Velocity as Valve lift increases 18
Figure 10: [5] Flow efficiency increase as valve seat curvature increases 19
Figure 11: Seat Cut angles and lengths 20
Figure 12: Simplified example of poor valve shrouding 20
Figure 13: Simplified version of one sided valve shrouding 20
Figure 14: Simplified version of no valve shrouding 21
Figure 15: [5] How air flow exits different sections of the valve 21
Figure 16: Austin 9F/Sa/H 101 29
Figure 17: Austin 9F/SA/H 101 engine data 30
Figure 18: 12G202 Combustion Chambers 30
Figure 19:Top of 12G202 Cylinder Head 30
Figure 20: 12G202 Ports and Chambers 30
Figure 21: Exhaust Valve 31
Figure 22: Inlet Valve 31
Figure 23: Sand Blasting Cabinet 31
Figure 24: Image showing lack of threaded holes to bolt into head 32
Figure 25: Typical valve opening tool 32
Figure 26: Front view of CAD Valve Opening Tool 33
Figure 27: Side view of CAD Valve Opening Tool 33
Figure 28: Top view of CAD Valve Opening Tool 33
Figure 29: Bottom view of CAD Valve Opening Tool 33
Figure 30: Front view of CAD of 12G202 Cylinder head 33
Figure 31: Rear View of 12G202 Cylinder head 33
Figure 32: View of bottom of CAD cylinder head 34

Figure 33: View of bottom and rear of CAD cylinder head 34
Figure 34: top, front view of CAD cylinder head with valve opening tool 34
Figure 35 top front view of CAD cylinder head with added valve opening tool 34
Figure 36: Rear view of CAD cylinder head with added valve opening tool 34
Figure 37: Side view of CAD cylinder head with added valve opening tool 34
Figure 38: Aluminium legs for valve opening tool 34
Figure 39: Top plate for valve opening tool 34
Figure 400: Securing bolt and bolts used to push down valve 35
Figure 41: Valve tool on top of cylinder head 35
Figure 42: Valve tool sat on top of valve guides 35
Figure 43: Simplified drawing of a flow bench 36
Figure 44: Superflow CFM conversion chart 36
Figure 45: Creating a seal on the cylinder head 37
Figure 46: Cylinder head and clamp 37
Figure 47: Clamping the cylinder head down 37
Figure 48: Sitting the head on the adaptor plate 37
Figure 49: Bolting on valve opening tool 38
Figure 50: Valve opening tool from the side 38
Figure 51: Close up of DTI Gauge 38
Figure 52: Adding the DTI gauge 38
Figure 53: DTI with valve closed 38
Figure 54: DTI with valve open 0.5mm 38
Figure 55: Final setup of test equipment 39
Figure 56: Final setup of test equipment 39
Figure 57: Standard Flow test results 39
Figure 58: Average standard flow test results 40
Figure 59: Standard flow test coefficient results 40
Figure 60: Standard flow test results with carbon Build up 41
Figure 61: Standard flow coefficient results with carbon build up 42
Figure 62: Front view of first design 43
Figure 63: Rear view of first design 43
Figure 64: Mini Port without short side radius 43
Figure 65: Mini Port without short and long side radius 43
Figure 66: Mini port with increase floor height and reduced ceiling 44
Figure 67: Mini Port with curved floor and ceiling 44
Figure 68: Mini port with extreme curved floor and ceiling 44
Figure 69: Mini port with increased short and long side radius 44
Figure 70: 3 Angle Seat 44
Figure 71: 1 Angle Seat 44
Figure 72: 5 Angle Seat 45
Figure 73: 4 Angle Seat 45
Figure 74: Valve guide 45
Figure 75 : Seat and valve 45
Figure 76: rear view of mini port 45
Figure 77 Side view of mini port 45
Figure 78: Front view of mini port 46
Figure 79: bottom view of mini port 46
Figure 80: CAD of Mini inlet valve 46

Figure 81: CAD of Mini inlet valve with thread 46
Figure 82: Creatility Ender 3 Assembly Guide part 1 47
Figure 83: Creatility Ender 3 Assembly Guide part 2 47
Figure 84: Creatility Ender 3 Assembly Guide part 3 48
Figure 85: Creatilty Ender 3 Assembly Guide Part 4 48
Figure 86: Creatilty Ender 3 Assembly Guide Part 5 48
Figure 87: Creatilty Ender 3 Assembly Guide Part 6 49
Figure 88: Creatilty Ender 3 Assembly Guide Part 7 49
Figure 89: Creatilty Ender 3 Assembly Guide Part 8 49
Figure 90: Creatilty Ender 3 Assembly Guide Part 9 50
Figure 91: Creatilty Ender 3 Assembly Guide Part 10 50
Figure 92: Creatilty Ender 3 Assembly Guide Part 11 50
Figure 93: Creatilty Ender 3 Assembly Guide Part 12 51
Figure 94: Completed side view of printer 51
Figure 95: Completed front view of printer 51
Figure 96: Completed top view of printer 51
Figure 97: First test print 51
Figure 98: Bottom view of first 3D print 52
Figure 99: Top view of first 3D print 52
Figure 100: Top view of second 3D print 52
Figure 101: Top view of second 3D print 52
Figure 102: Bottom view of flanged port 53
Figure 103: Top view of flanged port 53
Figure 104: Bottom view of silicone mould 53
Figure 105: Top view of Silicone mould 53
Figure 106: Bottom view of the phase 3 port 54
Figure 107: Front view of the phase 3 port 54
Figure 108: Top view of the phase 3 port 54
Figure 109: Side view of the phase 3 port 54
Figure 110: Print of phase 3 design 54
Figure 111: 1 Angle seat 55
Figure 112: 2 Angle seat 55
Figure 113: 3 Angle seat 55
Figure 114: 4 Angle seat 56
Figure 115: 5 Angle seat 56
Figure 116: Port 1 Mini port 56
Figure 117: Port 2 reduced cross sectional area 56
Figure 118: Port 3 reduced long turn radius 57
Figure 119: Port 4 Reduced short turn radius 57
Figure 120: Port 5 Smoothed valve guide 57
Figure 121: Port 6 Increased short turn radius 58
Figure 122: Port 7 Increased short turn rad and long turn radius 58
Figure 123: Port 8, Increased short rad, increased long rad and smoothed guide 58
Figure 124: Combustion chamber 2 , reduced shroud 1 59
Figure 125: Combustion chamber 1 59
Figure 126: Combustion chamber 2 , reduced shroud 3 59
Figure 127: Combustion chamber 2 , reduced shroud 2 59
Figure 128: Printed 2 angle seat 59

Figure 129: Printed 1 angle seat 59
Figure 130: Printed 4 angle seat 60
Figure 131: Printed 3 angle seat 60
Figure 132: Printed 5 angle seat 60
Figure 133: Printed port 2 60
Figure 134: Printed port 1 60
Figure 135: Printed port 3 61
Figure 136: Printed port 4 61
Figure 137: Printed port 5 61
Figure 138: Printed port 6 61
Figure 139: Printed port 7 61
Figure 140: Printed port 8 61
Figure 141: Printed chamber 2 62
Figure 142: Printed chamber 1 62
Figure 143: Printed chamber 3 62
Figure 144: Printed chamber 4 62
Figure 145: Printed parts being flow tested 63
Figure 146: Printed parts being flow tested 63

CHAPTER 1

1.1 ABSTRACT

The design of inlet ports, valves, valves seats and combustion chambers greatly affect's the combustion performance of an internal combustion engine. This study investigates how these individual parameters aid or reduce the flow of air into the combustion chamber. By testing a Mini 997-cylinder head using a SF-110 flow bench baseline results for the project can be obtained. A silicone mould of the inlet port can be taken and converted into a CAD drawing on Solidworks 2019. By 3d printing the computer drawing using a Creatility Ender 3. And testing it on the flow bench, a comparison of the results can be drawn between the CAD drawing and the real cylinder head port design. From this, a degree of accuracy can be attained from the two designs, which can then be further validated by the use of the computational fluid dynamics add in on solid works. What once took many hours of prototype porting and physical flow testing, can now be done in a matter of minutes. These results of these changes can then be analysed, the design tweaked, and the new design tested again. This reduces the overall cost and time spent on the area of study and is one of the main reasons CAE (Computer Aided Engineering) has become so popular in design and engineering. By 3d printing the drawings, a physical test can be conducted and 'real life results' can be found. The use of the 3d printing also greatly reduces the time and cost involved in investigating flow increases, as printing a port and changing the design takes much less time than carving and sculpting a cylinder head. Once the CFD testing and the 3d printing tests show good increases in flow where desired. Physical porting can be conducted on the cylinder head to the exact specification of the CAD design.

1.2 INTRODUCTION

On a global scale, interests into Engine efficiency's, emissions and performance is on the increase. An engines performance in these areas is greatly affect by the quality of the combustion process. Cylinder heads are a vital component in an engine assembly. The cylinder head, houses passage ways for charged gases to enter, and exhaust gases to exit the engine. These passage ways are key in an engine's combustion outcome. These ports are important as they can restrict or heighten flow, manipulate the flow and direction of gases into and out of the combustion chamber, direct swirl and ultimately greatly affect the engines performance. Great amounts of research have been conducted into how port design and valve seat composition aid the flow of air into the cylinder. Work carried out by 'M. H. Shojaeefard' [1] states that:

‘” In any efficient design of the engine intake system, in order to have a high volumetric efficiency the energy losses of the inlet flow should be minimized.”

Ports need to be designed so that maximum air flow is available to enter the combustion chamber. As well as port efficiency, a new focus is being directed towards how combustion chamber and valve + seat design, aids the mixture of air and fuel in the combustion chamber. Swirl or turbulence is the term used to describe the vortex of gases entering or exiting a cylinder. The mixing and swirling of the path and the direction of the intake charge in the port effects how fast the chemical reaction of the charged gases occurs. Better atomisation ‘homogenous’ charge will result in more power fewer emissions and an increased efficiency.

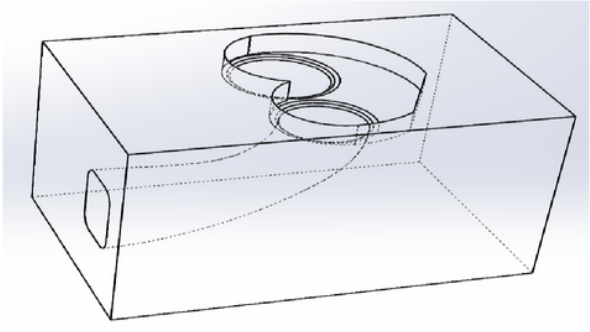


FIGURE 1: SIMPLE EXAMPLE OF INLET PORT AND COMBUSTION CHAMBER

Before the use of computers, trying to improve flow through a cylinder head was conducted traditionally by experience in cylinder head porting. This is where a grinding stone was taken to the inside of the port and removed metal from areas that restricted flow. The ported head could then be tested and compared to the original port results to see whether improvements have been made or not. The process has a few fundamental flaws, grinding away at ports takes a considerable amount of time and labour, especially when the work being done onto the head is unknown whether to be beneficial to the flow or not. By using this technique improvements to flow can be made, however if the work has been un able to show enhancements, many hours of grinding and testing has been wasted. Furthermore, the cost of labour will have been for nothing and additional money will have to be spent re- investing into a new cylinder head, as once metal has been removed from the port, it cannot be replaced easily.

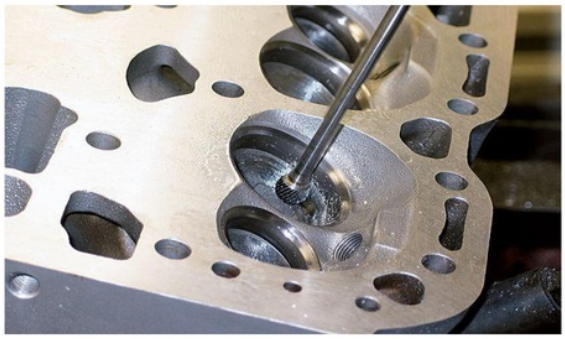


FIGURE 2: [1] CYLINDER HEAD PORTING

The use of Computer aided drawing (CAD) software programmes have become widely used throughout the engineering sector since the 1990's. Being able to draw, and change dimensions and shapes within a few clicks of a mouse has significantly reduced the amount of time and cost taken in designing components. As well as CAD packages the use of Computational Fluid Dynamics (CFD) software's have been on the increase as computer power and processing becomes more advanced. Being able to examine the flow of a fluid (or gas) by looking at specific properties such as temperature, pressure, density, velocity and more. These can then be calculated simultaneously giving highly accurate results whilst greatly reducing the amount and cost of physical prototypes.

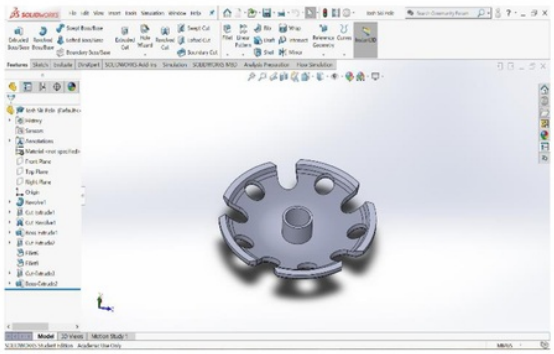


FIGURE 3: EXAMPLE OF CAD SOFTWARE (SOLIDWORKS 2019)

A relatively new and rapidly developing technology, which is gaining popularity throughout the manufacturing industry is 3D printing. 3D printing allows a CAD drawing to be turned into a physical 3d object by adding layers of material on top of each other. Compared to traditional methods of manufacturing components such as injection moulding and CNC machining 3D printing is cheaper and quicker, as no moulds or cutting tools are needed to create the object. Prototype parts, can be easily be made, tested

changed, reproduced and compared to simulation results, quicker and cheaper than other manufacturing methods.

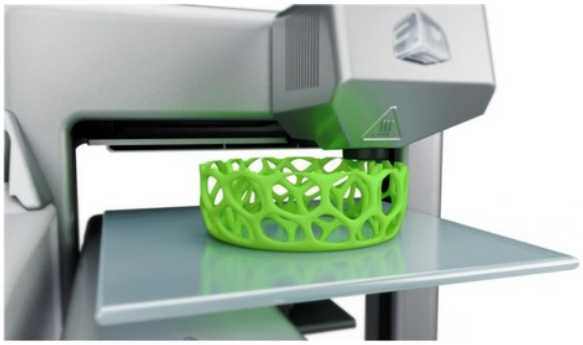


FIGURE 4: [2] 3D PRINTER HALFWAY THROUGH A PRINT

1.3 PROJECT BACKGROUND

Ever since the author was a child, he has had an obsession with creating fire and power from the explosions of gases. As he grew up and moved through education. his interest and knowledge of this subject area increased as well. At 18, whilst studying for a level 3 Motorsport Engineering qualification, he managed to obtain work experience at a performance engine building and re manufacturing company. Throughout his time there, he learnt a great deal from fellow employees and took their advice and years of experience on board. Apparently one of the best ways to help increase engine performance was increasing flow into and out of the cylinder head. Watching older co-workers use the flow bench he was always intrigued as to what it did and how it helped aid performance but even with continuous asking and pestering, he was never allowed to use it. So even though he had been told how to improve power, he was unable to physically create and test anything to confirm that their procedures and techniques actually aided increased performance. After two years at college he then went to study at University of Wales Trinity St David. To complete his final year, he was asked to complete a major project. This was a perfect opportunity to practise create and verify not only what he was taught at work, but also his own ideas and also others ideas in the same area of study. Before University the author and his brother had joint purchased a 1983 Mini Cooper 997. The car was driven about for around a year until ultimately it failed its MOT, and university and other jobs prevented the work being carried out. With this project being the final piece of work before finish university, the author thought that it would be a good idea to start working on the mini. With a view to increasing the engine performance and then restoring the car when the academic year had finished.



FIGURE 5: 1983 MINI COOPER 997

As the original mini engine was still running, pulling it apart and conducting experiments on it would have been a step backwards therefore a donor cylinder head needed to be found. This way it could be modified and experimented on but also have its performance compared to the original.

1.4 BACKGROUND RESEARCH

Plenty or papers and books have been produced on the subject of inlet port flow. Research conducted by Lei Cui [3] concludes that a well-designed inlet port, needs a suitable tumble intensity and a large flow coefficient. Although performance gains of the two parameters, are hard to obtain, as they contradict each other when trying to improve them both simultaneously. They can both be improved however by reducing the pressure loss in the port. On a flow bench under steady state conditions, the pressure drop (ΔP) through the system can be constructed from four characteristics.

- Local resistance loss $(\Delta \rho_\zeta)$
- Tumble Kinetic energy in the cylinder $(\frac{1}{2}\ \rho V_\tau^2)$
- Frictional drag loss $(\Delta \rho f)$
- Axial Kinetic Energy $(\frac{1}{2}\ \rho V_a^2)$

Under ideal conditions, the energy conservation can be denoted as

$$\Delta P = \Delta \rho_\zeta + \frac{1}{2}\ \rho V_\tau^2 + \Delta \rho f + \frac{1}{2}\ \rho V_a^2$$

The assumption above uses the total pressure drop to create V_0. This is the ideal flow velocity without any loss of flow. It produces

$$\Delta P = \frac{1}{2}\rho V_0^2$$

By combining the two equations above the result is

$$\left(\frac{V_a}{V_0}\right)^2 + \left(\frac{V_\tau}{V_0}\right)^2 + 2\frac{\Delta\rho f + \Delta\rho_\zeta}{\rho V_0^2} = 1$$

According to Lu, Z [4] The axial velocity V_a and the radial velocity V_t can be shown as

$$V_a = \frac{A C_f V_0}{\pi D L}$$

$$V_\tau = \frac{B N_r V_0}{4 D n}$$

C_f = Flow Coefficient

N_r = Tumble Intensity

B = Engine Bore

D = Intake Valve Diameter

L = Valve lift

n = Number of intake valves

If the previous two equations are substituted into the third equation, rearranging the terms gives

$$\left(\frac{A C_f V_0}{\pi D L}\right)^2 + \left(\frac{\mathrm{BNr}}{4\mathrm{Dn}}\right)^2 + 2\frac{\Delta\rho f + \Delta\rho_\zeta}{\rho V_0^2} = 1$$

The first term represents the flow coefficient with the second referring to the tumble intensity. The last term is the flow resistance. Looking at the equation above, it is fair to say that by making the flow resistance as small as possible, a larger flow energy throughout the port can then be shared between the flow coefficient and tumble intensity.

The Darcy- Weisbach formula can be used to calculate the frictional drag loss through the port.

$$h_f = \lambda \frac{l}{d} \frac{V^2}{2g}$$

The Darcy Weisbach formula expressed as differential pressure loss is

$$\Delta p_f = \lambda \frac{l}{d} \frac{\rho V^2}{2}$$

λ= Frictional drag factor
l = Length of intake port
Δ = Roughness
d = Diameter of port

The Nikuradse formula shows the how the frictional drag factor is found for the rougher zone of the turbulent pipe flow.

$$\lambda = \frac{1}{\left(2\, l\, g\, \frac{d}{2\Delta} + 1.74\right)^2}$$

The two equations above show that by having a smooth, short and large cross-sectional area intake port, the flow resistance can be reduced. The sudden changes in port shape direction and size are what contributes to local flow resistance in the port. This local resistance loss is calculated by using the Boda – Canow formula.

$$h_\zeta = \zeta \frac{V^2}{2g}$$

This can also be expressed as a differential pressure loss

$$\Delta p_\zeta = \zeta \frac{\rho V^2}{2}$$

ζ is the factor of local resistance and is determined by the port geometry. The biggest contributors to a high local resistance factor is a large bend angle in the port, a small cross sectional area and a large angle at the entrance of the port.

To calculate the local resistance at the entrance of the port, the equation below can be used.

$$\zeta = 0.5 + 0.303\ sin\ \alpha + 0.226\ sin^2\ \alpha$$

The angle between the bottom of the cylinder head and the place of the entrance to the port is α. To achieve the smallest local resistance factor, α should be 0 degrees meaning that the entrance to the port is perpendicular to the bottom of the cylinder head.

According to [3], In the intake port, there is two types of cross-sectional variation. These are called shrink and expansion. To calculate the local resistance factors at these two cross sections, the follow equations can be used.

$$\zeta = \left(\frac{A_2}{A_1} - 1\right)^2 f\ (\Theta)$$

$$\zeta = \ f\ (\Theta) f\left(\frac{A_2}{A_1}\right)$$

A_1= Cross sectional area upstream

A_2= Cross sectional area downstream

θ = Angle of cross-sectional variation between downstream and upstream

Looking at the two equations above it is possible to determine that by effectively optimising cross sectional area throughout the port, the flow capacity through the port can be improved.

Finally, the local resistance factor of the bending part of the port can be found by using:

$$\zeta = \left[0.131 + 0.163 \left(\frac{d}{R}\right)^{3.5}\right] \frac{2\,\alpha}{\pi}$$

d = Diameter of bent port

R = Bending Radius

α = Angle of between cross-sections from downstream and upstream bending

The equation shows that the port bend angle directly corelates to the local resistance. To Achieve a small local resistance, the bend angle should be as small as possible. The image below is taken from the study reference [3]. It shows the structural parameters of an inlet port.

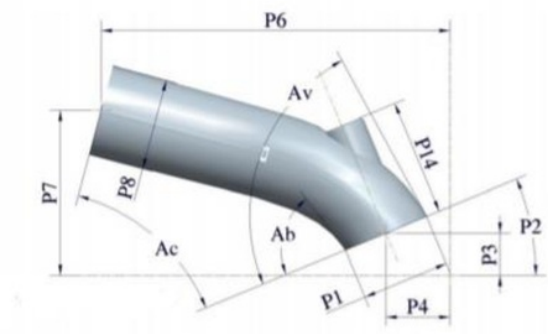


FIGURE 6: [3] STRUCTURAL PARAMETERS OF AN INLET PORT

Parameter	Description	Unit
P1	Diameter of intake port outlet	mm
P2	Angle between cylinder head bottom and outlet plane	Deg
P3	Distance between cylinder head bottom and outlet centre	mm
P4	Distance between axis of the cylinder and outlet centre	mm

P5	Distance between symmetry plane of inlet port and the outlet centre	mm
P6	Distance between axis of the cylinder and entrance centre	mm
P7	Distance between cylinder head bottom and centre of port entrance	mm
P8	Height of the port entrance	mm
P9	Width of the port entrance (not shown)	mm
Av	Angle between outlet plane and upper wall	Deg
Ab	Angle between outlet plane and lower wall	Deg
Ar	Ratio between outlet area and entrance are	
Ac	Angle between outlet plane and entrance plane	Deg

TABLE 1: TABLE OF PORT PARAMETERS

By changing these different parameters of the port, flow can be reduced or improved.

David Vizzard's book 'how to port and flow test cylinder heads' [5] also gives an insight into how air flow can be improved into the combustion chamber. Previous test conducted by David has concluded that at low pressures the air flow tends to stay more attached to the port floor, meaning that air passes over the whole circumference of the valve. As the velocity of air increases through the port. The air flow detaches from the floor (short turn radius), passes over the valve, and tries to join the air already exiting at the long side radius.

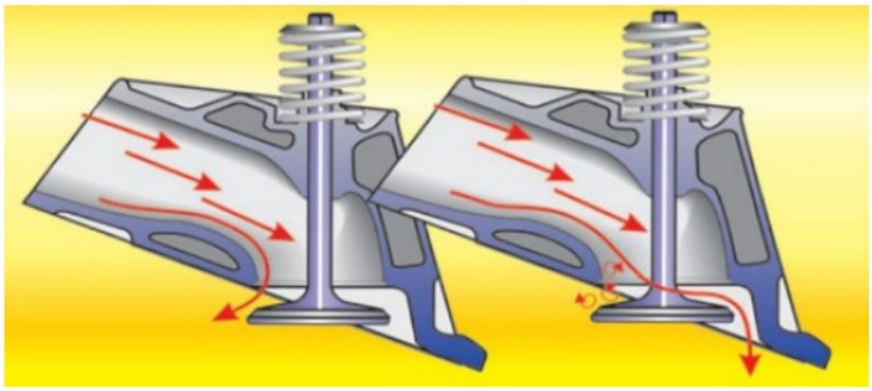


FIGURE 7: [5] AIR PASSING OVER SHORT AND LONG TURN RADIUS

The shapes down and upstream of high flow areas in the port are what causes the high velocities. Figure 7 shows that the area at the short turn needs to be increased so that more air is able to travel along a higher efficiency path. This be done by increasing the height of the roof. Unlike previous study [4] where the

largest area will create the best flow, he exclaims that to attach more airflow at lower velocity's, material should be added to the point at which the lowest flow velocities occur. This will decrease the cross-sectional area. Much like the previous work he emphasises the importance of cross-sectional areas and velocities in the port. One of the biggest improvements that can be made to increase flow through the port is to raise the port floor, just after the short turn radius. In turn, increasing the short turn radius, however this decreases the cross-sectional area inside the port. To combat this the port should be made wider to restore the same cross-sectional area. This cross-sectional area should be made to be around 77%-80% of the intake valve area. By making the area (port) bigger than this, velocity and flow can be compromised. Larger ports only show small gains in situations of high valve lifts, and greatly reduce the flow and low valve lifts.

The bend inside the port is where the biggest influence on flow is found. A bend is needed to house the valve guide and stem. A poor and unblended turn into the valve area, creates a smaller orifice for the air to flow through. By increasing the angle of the port, the orifice in which air is allowed to travel becomes greater, and the valve curtain area can become more utilised. The short turn radius is where the greatest obstacle in good flow is found. Engines in formula one use a large short turn radius, with a small port angle.

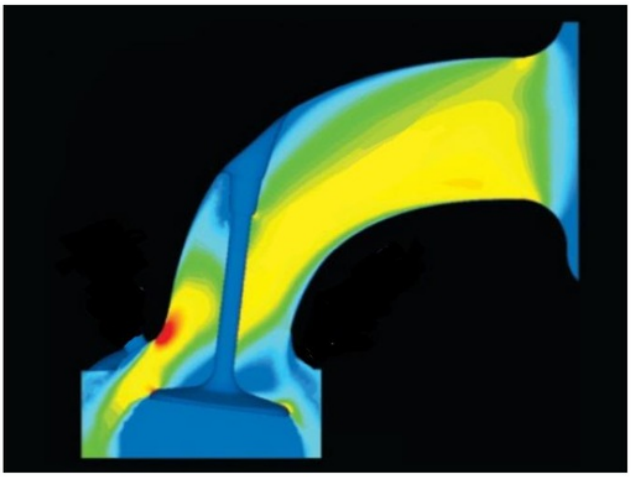


FIGURE 8: [5] CFD IMAGE OF AIR FLOW THROUGH INLET PORT

The above image shows a CFD analysis taken from Vizards book but conducted by Rick Roberts [5] looking at the flow we can see that the flow does not stay attached to the port wall. This means a smaller port area can be used here to optimise the stream of the flow and to increase its velocity. Redundancies in the port are where there is little or no flow, this results in low torque throughout the rev range. These areas should have material added so the velocities over them can be increased.

As well as the port shape. Seat configuration plays a vital roll in air flow into the cylinder. The study of velocities involved in a flow test show that seat composition is the most important factor in flow, up until just over half of the valve's maximum lift.

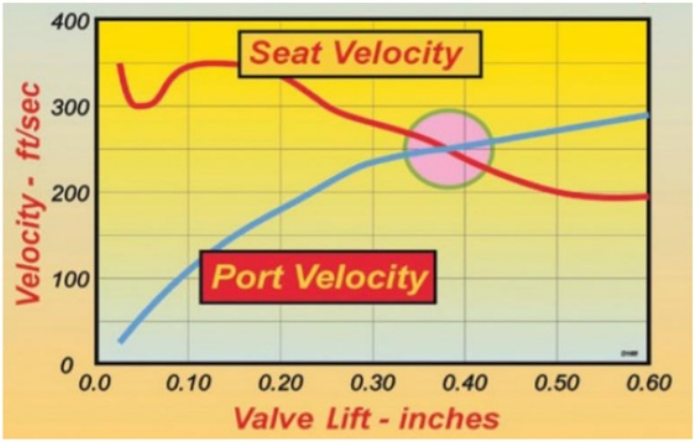


FIGURE 9: [5] SEAT AND PORT VELOCITY AS VALVE LIFT INCREASES

The graph above shows how seat velocity reduces and port velocity increases as valve lift increases. According to M. Taufik Bin Abd Kadir. [6] dimensions of the vale head, seat, stem and valve lift, all correspond to the valve flow area. There are three stages that occur as the lift of the valve increases.

The first stage is at small valve lift. The flow area or curtain area, is described as a circular cone, between valve face and its seat.

The area can be worked out using the equation below

$$A_m = \pi L_v \cos\beta \left(D_v - 2w + \left(\frac{L_V}{2}\right)\sin 2\beta\right)$$

β= Valve Seat Angle
L_v = Valve Lift
D_v = Diameter of valve head
w = Width of seat

The second stage at around roughly half the valve lift, the minimum area can be worked out using

$$A_m = \pi D_m ((L_v - w\tan\beta)^2 + w^2)^{0.5}$$

D_m= $D_v - w$ = Mean seat diameter

At a large valve lift, the minimum flow area is worked out using

$$A_m = \frac{\pi}{4}\left(D_p^2 - D_s^2\right)$$

D_P = Diameter of port

D_S = Diameter of valve stem

By making a more streamline valve seat, air can flow better around the valve, especially at low lifts. The image below shows how the flow efficiency of the seat improves as steps are taken towards improving the air flow into the seat and out of it.

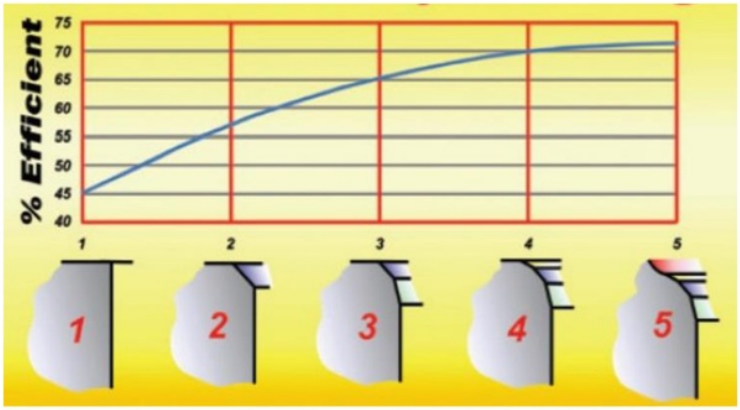


FIGURE 10: [5] FLOW EFFICIENCY INCREASE AS VALVE SEAT CURVATURE INCREASES

At each stage another cut is made to the seat, adding a more curved radius to it. The cuts and dimensions used are taken from experiments conducted by Vizard [5] and are found to be the optimum angles and lengths of cuts for most cylinder heads.

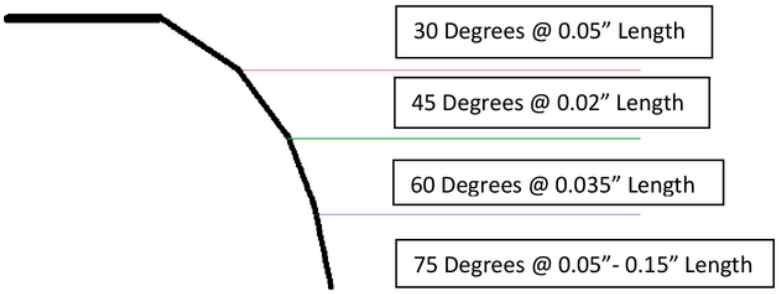


FIGURE 11: SEAT CUT ANGLES AND LENGTHS

Closely relating to seat design is the effect of valve shrouding. If a head is described to have bad valve shrouding, it means that the combustion chamber walls are too close to the edge of the valve. Limiting the amount of flow out around that particular valve edge.

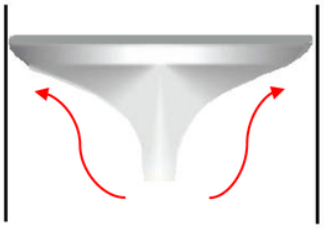


FIGURE 12: SIMPLIFIED EXAMPLE OF POOR VALVE SHROUDING

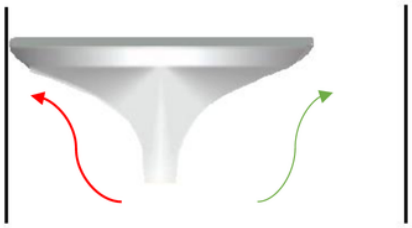


FIGURE 13: SIMPLIFIED VERSION OF ONE SIDED VALVE SHROUDING



FIGURE 14: SIMPLIFIED VERSION OF NO VALVE SHROUDING

By removing material from the combustion chamber walls, the flow exiting around the circumference the of the valve can be increased, this is due to air being able to pass freely without coming into contact with the walls. Precautions need to be taken so that material isn't removed from the circumference of the cylinder bore. Previous work by Vizard has shown that the A series cylinder head suffers from poor inlet valve shrouding. What was once regarded as well-designed cylinder head has been proved that infect it suffers from poor inlet flow.

If minimal flow is exiting a portion of the valve, there is no need to 'deshroud' it, as in fact it could make the flow into the chamber even worse.

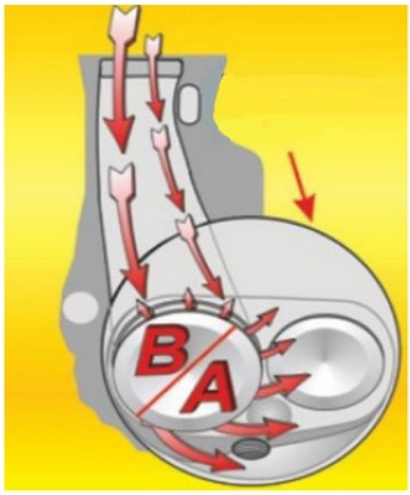


FIGURE 15: [5] HOW AIR FLOW EXITS DIFFERENT SECTIONS OF THE VALVE

Figure 15 shows how air does not evenly enter the cylinder around the intake valve. Over 60% of the flow enters the cylinder through Part A of the valve, with the rest entering over part B. Part B suffers from slight shrouding but material does not need to be removed as it does not greatly affect the inlet flow

1.5 WHAT IS CFM?

Cubic feet per minute or CFM is a measure of the amount of air a system can flow. It refers to the rate of which a volume of air can move through a system over a time period of a minute. Using the application not 'determining CFM in cubic FT/Min [7] the following process can be used. To calculate the cfm of an object (In this case a cylinder head), the flow velocity and the cross-sectional area of the orifice that is pulling the air through. Both of these measurements require a flow bench to be used. For this example, we can say that the diameter of the orifice is 150mm or 5.9".

The area of circle is found using

$$A = \pi r^2$$

$$A = \pi \times (5.9)^{\,2}$$

$$A = 2.9Ft^2$$

Next the flow velocity can be found using the equation below

$$V = 4005 \times \sqrt{\Delta P}$$

ΔP = Velocity pressure measured by sensor

As an example, we can say the velocity pressure was measured at 0.25"

$$V = 4005 \times \sqrt{0.25}$$

$$V = 2.002\ FT\ /min$$

Cfm is then calculated by using:

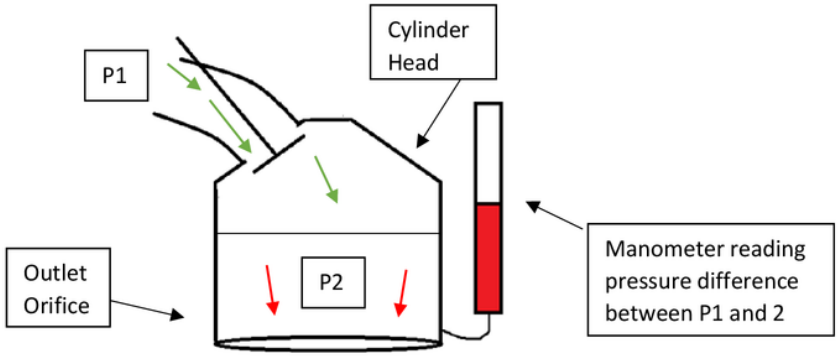
$$CFM = Flow\ Velocity \times Cross\ Sectional\ Area$$

$$CFM = 2.9 \times 2.002$$

$$CFM = 5.8$$

1.6 FLOW COEFFICIENT

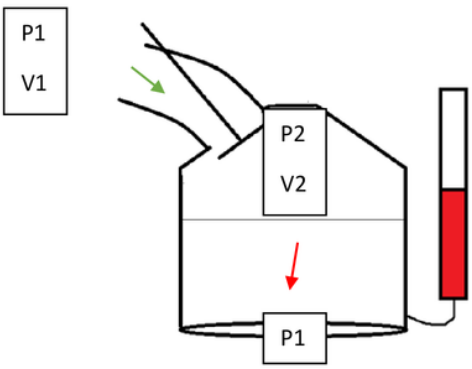
The CFM of the cylinder head can be found using a flow bench. Once the CFM has been found, the flow coefficient can be then calculated. The flow coefficient is the term used to describe the amount of flow restriction within the port.



$$\Delta P = 25" \, of \, water$$

$$\Delta P = P1 - P2$$

The difference in the pressure between P1 and P2 creates a suction. This can be adjusted. Due to the relatively large orifice, the pressure drops within the port. The flow rate is adjusted to the manometer shows 25" pressure drop. For 25" of water the perfect flow is 138 CFM/in^2. Per inch squared refers to the area of the inlet valve and port.



P2 Refers to the pressure and the end of the inlet port. V2 is larger than V1. P1 Is atmospheric pressure.

As an example, we can say that P1 = 1 Bar, and that V1= 0 m/s. The pressure drop accelerates the air entering the port from 0 m/s (V1) to Vmax (V2). This is the velocity of the air when it enters the cylinder.

Looking at Bernoulli's equation:

$$P_1 + \frac{1}{2}\rho V_1^2 = P_2 + \frac{1}{2}\rho V_2^2$$

In the example above V1 = 0, so:

$$P_1 = P_2 + \frac{1}{2}\rho V_2^2$$

Therefore

$$P_1 - P_2 = \frac{1}{2}\rho V_2^2$$

This equals the change in pressure. Bernoulli's equation is used to described the conservation of energy, where energy can not be destroyed or created but can only be transformed.

Pressure = Potential energy of 1m^3
$\frac{1}{2}\rho V_1^2$= Kinetic Energy of 1 m^3

$\Delta P = 25" \, of \, water$

1 BAR = 10^5 Pa
ρ of air at 20 Degrees = 1.2 kg / m^3

$$P_1 - P_2 = \frac{1}{2}\rho V_2^2$$

$$Weight = m.g$$

$$m = A.h.\rho.g$$

$$\rho = \frac{A.h.\rho.g}{A} = h\,\rho\,g\ (N/m^2)$$

$$25" \; of \; water \; = \; \frac{25 \; \times 25.4}{1000} \; = \; 0.635m \; of \; water$$

Density of water = 1000kg/m^3

Therefore:

$$P = 0.635 \; \times 1000 \; \times 9.81 = 6229.35 \; Pa$$

$$6229.35 \; = 6.23 \; KPa$$

$$V2 \; at \; 25" \; = \; \sqrt{\frac{\Delta \, P}{0.5. \rho}}$$

$$V2at \; 25" = \; \sqrt{\frac{6229.35}{0.5 \times \; 1.2}} = 101 \; m/s$$

$$25" \; of \; water \; perfect \; flow \; = 101 \; \times \; \frac{25 \times 25.4}{10000000} \; = \; 0.065m^3/s \; = \text{0r 138 CFM}$$

To obtain the flow efficiency along the port the equation below is needed

$$\frac{CFM}{Vavle \; area} = CFM/ \; Sq. In$$

Lastly the flow coefficient can be found using:

$$\frac{Measured \; CFM/ \; Sq. In}{Perfect \; CFM/ \; Sq. In}$$

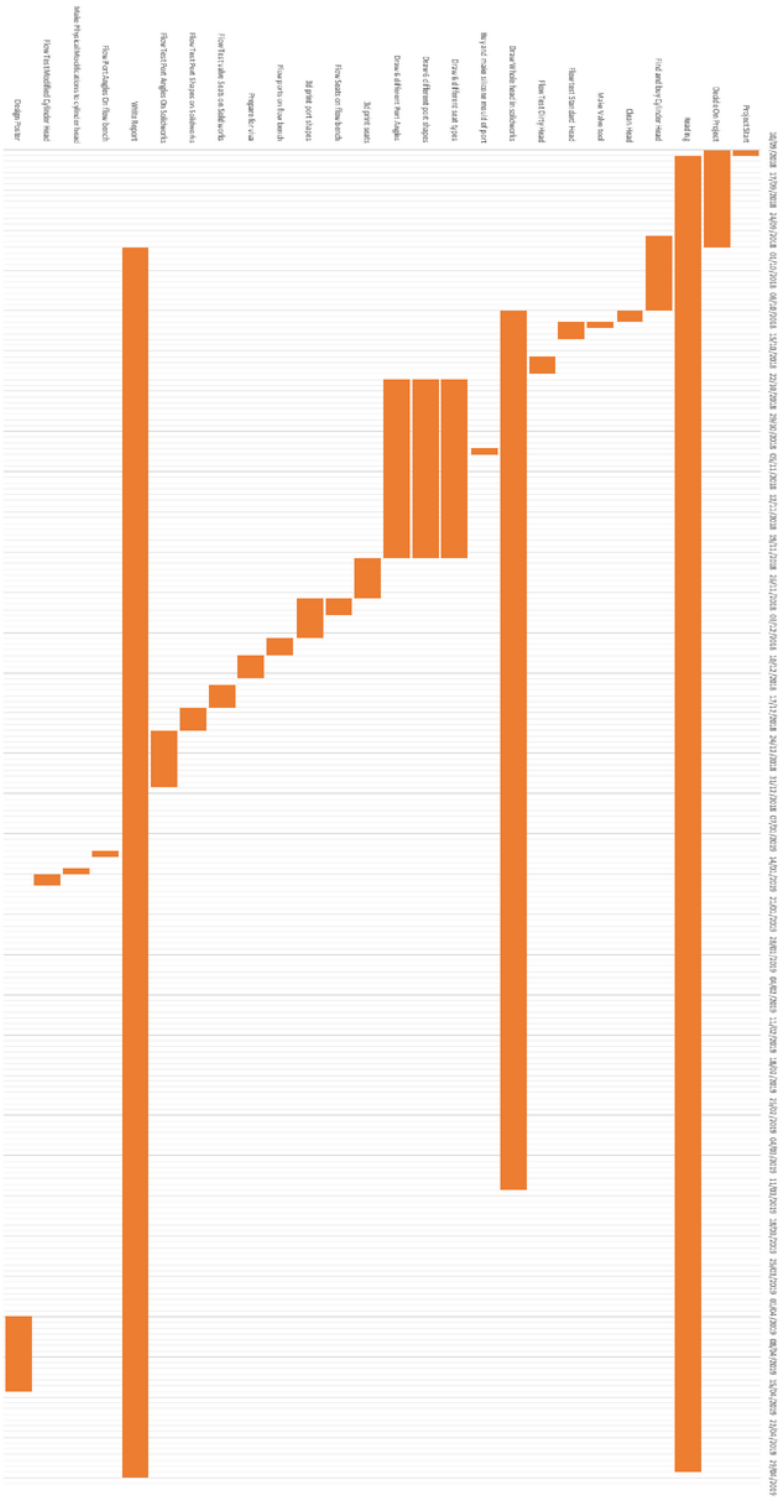
1.7 AIMS

After reviewing previous work in similar subject areas, some objectives for the project can be determined. At high valve lifts port design is key in flow entering the combustion chamber. A study into whether a re-design of mini inlet port can improve flow will be conducted. Exploring the potential for flow improvement at low valve lifts will also be part of this investigation. As previous papers have concluded each element in the design only makes up a portion of the inlet flow. To improve the overall flow throughout the whole entire valve lift range all individual elements will need to be looked at. Finally, as studies suggest, A series cylinder heads suffer from poor inlet valve shrouding, by removing unnecessary material from around the inlet valve circumference, a potential improvement to the flow could be made. Previous work made by other authors have only discussed these elements individually. This study will look at how changing these individual parameters can improve flow separately, but also what happens to the results, when they are modified together.

1.8 METHODOLOGY

- Purchase Compatible cylinder head for A series engine
- Conduct flow test and obtain results from standard cylinder head
- Accurately model 12G202 Inlet port by used of CAD
- Model 12g202 seat geometry in CAD
- Model 12g202 Combustion chamber by CAD
- 3D Print modelled parts
- Flow test modelled parts and compare to original
- Flow test modelled parts through sue of CFD and compare to original
- Compare results and verify drawings
- Make changes to modelled port deign by manipulating port floor and roof, long turn radius and short turn radius
- Make changes to modelled combustion chamber design by gradually removing valve shrouding
- Make changes to modelled seat design by adding multiple cuts to the seat
- Decide on best dimensions and component configurations to most increase flow
- Flow test all improved designs with each other
- Flow test all improved designs with each other with the use of CFD
- Validate real world flow testing with CFD test
- Conclude on best and worst design improvements to inlet port flow

1.9 GAANT CHART



1.10 REFERENCES

1 How Rah Engine Tuning. (N/A). *Cylinder Head.* Available:http://www.howrah.org/cylinder-head.html. Last accessed 12/1/19.

2 S.Belleghem. (2016). *How 3D printing is changing the customer relation.* Available: https://www.stevenvanbelleghem.com/blog/how-3d-printing-is-changing-the-customer-relation/. Last accessed 5/12/18.

3 L.Cui, T.Wang, Z. Lu, M Jia, Y. Sun. (2015). Full-Parameter Approach for the Intake Port Design of a Four-Valve Direct-Injection Gasoline Engine. *Journal of Engineering for Gas Turbines and Power.* Vol. 137 (N/A), 1-11.

4 Lu, Z. (2012). Parametric Design of the Tangential Intake Port in Diesel Engines, Proc. Inst. Mech. Eng., Part D, Vol 227 (3), 409–421.

5 D, Vizard (2012). How to port & Flow test cylinder heads . Minneapolis: Car Tech Inc . All.

6 M. TAUFIK BIN ABD KADIR. (2008). INTAKE PORT FLOW STUDY ON VARIOUS CYLINDER HEAD USING FLOWBENCH. *Faculty of Mechanical Engineering*. 1 (1), All .

7 Building Automation Products. (2015). *Determining Air Flow in Cubic Ft./Min.* Available: http://2avrmz2nom8p47cc28p2743e-wpengine.netdna-ssl.com/wp-content/uploads/2010/07/Determining-Air-Flow-in-CFM.pdf. Last accessed 1/11/19.

8 B Roy, R.D. M, K.M Pandey. (2016). Characterization of Shrouded Intake Valve in terms of Mean Flow Coefficient and Swirl Ratio. *International Journal of Applied Engineering Research*. 11 (1), 273-277.

9 M Krishna. J. M. Mallikarjuna. (2015). Experimental investigations of in-cylinder flows of Engine with Intake Shrouded Valve . *International Journal of Engineering Technology, Management and Applied Sciences*. 3 (1), 85-91.

10 S, Brown. (2005). *Comparing CFM Flow Numbers.* Available: http://www.flowspeed.com/cfm-numbers.htm. Last accessed 12/1/19

11 D.Oh , C Hoon Lee . (2015). Flow coefficient measurements for an engine cylinder head under transient flow conditions with continuous valve lift change. *International Journal of Engineering and Technology*. 7 (3), 1135 -1142.

12 V M Latheesh. (2018). Design and CFD analysis of intake port and exhaust port for a 4 valve cylinder head engine. *Materials Science and Engineering*. 1 (307), 1-11.

13 Niyaz H M and Dhekane A S 2014 Twin helical intake port design optimization and validation by using cfd analysis *International Journal of Emerging Technology and Advanced Engineering* **4**454-462

14 Kawashima Junichi, Hiroshi O and Yoshiyuki T 1998 Research on a variable swirl intake port for 4 valve high-speed di diesel engines *SAE Technical Paper* **107** 982680

15 Heywood John B 1988 *Internal Combustion Engine Fundamentals* (St. Louis, MO: McGraw-Hill Book Company) 230-245

16 Xia X L, Chen D L and Wang S L 2007 Evaluation methods to performance of intake port in internal combustion engine *Modern Vehicle Power* **2** 00

CHAPTER 2

2 MINI COOPER ENGINE

The engine found in the project mini cooper is the Austin 997 small bore A series engine, with the engine code 9F/Sa/H 101.



FIGURE 16: AUSTIN 9F/SA/H 101

Engine data for the A series 997 engine can be found in the table below

Engine Data	
Number of Cylinders	4
Bore	2.458in (62.43mm)
Stroke	3.20in (81.28mm)
Capacity	60.87 cu in (997cc)
Compression Ratio (H prefix)	9.1
Compression Ratio (L prefix)	8.3:1
BMEP (H prefix)	134 psi (9.42kg/cm2) at 3500rpm
BMEP (L prefix)	129 psi (9.07kg/cm2) at 3500rpm
Torque (H prefix)	54 lbft (7.46 kgm) at 3600rpm
Torque (L prefix)	53 lbft (7.32 kgm) at 3500rpm
Peak Power (claimed)	55 bhp
Crankshaft Data	
Main Bearing Material	Steel-backed copper-lead; thin wall
Main Bearing Length	1.0625in (26.99mm)
Main Bearing Running Clearance	0.001 to 0.0027 in (0.025 to 0.069mm)
Con Rods	
Big-end Bearing Material	Steel-backed copper-lead;thin wall
Big-end Bearing Length	0.875in (22.22mm)

Pistons	
Type	Solid skirt
Clearance (bottom of skirt - pressure face)	0.0016 to 0.0022in (0.041 to 0.056mm)
Piston Rings	
Top	Plain, chrome-faced
Second and third	Tapered
Width	0.0615 to 0.0625in (1.563 to 1.588mm)
Valves and Valve Gear	
Inlet Valve Diameter	1.156in (29.4mm)
Exhaust Valve Diameter	1.000in (25.4mm)
Inlet Throat Diameter	1.0312in (26.2mm)
Exhaust Throat Diameter	0.908in (23.06mm)

FIGURE 17: AUSTIN 9F/SA/H 101 ENGINE DATA

2.1 12G202 CYLINDER HEAD

As previously stated in chapter 1, the original mini engine still worked, and although the university project of exploring the port flow needed to be conducted on the cylinder head, the whole mini renovation project would have taken a few steps backwards therefore a donor cylinder head needed to be found. The donor head could then be modified, experimented on compared to the original still working head. Finding a cylinder head in budget, within a 50-mile radius and that was compatible with the 997 Engine proved to be a challenge but with a couple of weeks searching one was found and purchased for £18. The head is a 12G202 cylinder head that can be found on Morris 1100's. This is the same cylinder head as found on the the 9F/Sa/H 101 engine, with the only difference being square formed inlet ports instead of oval.



FIGURE 18: 12G202 COMBUSTION CHAMBERS



FIGURE 20: 12G202 PORTS AND CHAMBERS



FIGURE 19:TOP OF 12G202 CYLINDER HEAD

The head contains valves of the diameter 29.4mm for the inlet and 25.4mm for the exhaust.



FIGURE 22: INLET VALVE



FIGURE 21: EXHAUST VALVE

2.2 CLEANING THE HEAD

Looking at the cylinder head once it had arrived, it was obvious that it hadn't been used for a while, as grease, debris and surface rust had built up all over the head. Before any other work could take place the first thing needing to be done was to clean it. This task was undertaken using the bead blaster at the University. When first enquiry's into using the machine were made the machine hadn't actually been installed completely so progress was delayed by a couple of days. Once operational the blaster would a keep getting blocked (due to wet bead) this meant taking it apart, cleaning the gun out and putting it back together, after about 5 hours of standing at the blaster the head was clean enough to be worked with and used on the flow bench.



FIGURE 23: SAND BLASTING CABINET

2.3 MAKING A VALVE OPENING TOOL

In order to obtain results for different valves lifts whilst on the flow bench, a tool needs to be made to hold the valves down in the cylinder head. Unlike most common cylinder heads, that have threaded holes either side of the head that a plate can be bolted down onto, the mini head doesn't have these holes so a different approach and tool was needed.



FIGURE 24: IMAGE SHOWING LACK OF THREADED HOLES TO BOLT INTO HEAD

Looking at the top of the cylinder head, there is a few issues that need to be overcome. Firstly, there is no direct securing method for the tool to attach to the head, and secondly the surface in which the tool could sit is uneven due to identification marks and lips of the head.



FIGURE 25: TYPICAL VALVE OPENING TOOL

A preliminary sketch was drawn on solid works, with a view to making a metal final product if the sketch seemed viable and easy enough to create out of aluminium.

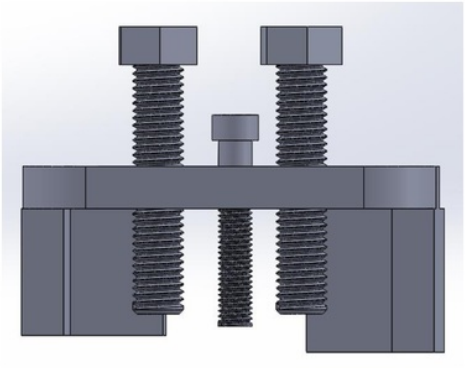


FIGURE 26: FRONT VIEW OF CAD VALVE OPENING TOOL

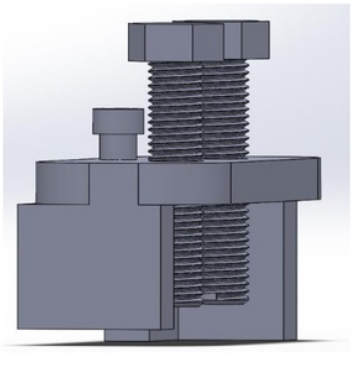


FIGURE 27: SIDE VIEW OF CAD VALVE OPENING TOOL

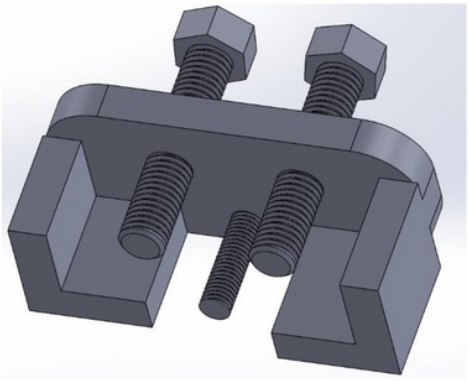


FIGURE 29: BOTTOM VIEW OF CAD VALVE OPENING TOOL

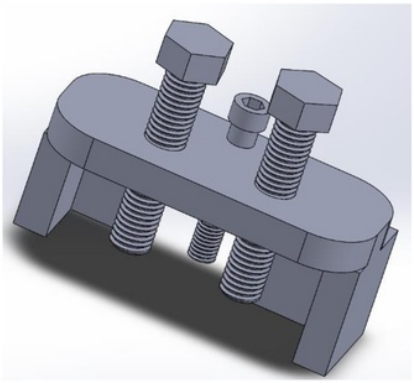


FIGURE 28: TOP VIEW OF CAD VALVE OPENING TOOL

The sketches show three 10mm plates with two 14mm threaded holes through the top plate for the valve bolts to wind through. The top plate is supported by one 30mm in height 90-degree section and another 34mm in height section (to compensate for the lip that it sits on). A 10mm Hex bolt goes through the top plate, and threads into a hole that is used for the rocker arm dowel. This bolt tightens the top plate down onto its supports and pushes the supports down onto the head keeping the valve tool secure. A sketch of the cylinder head is then made and the valve tool added to the assembly to check that the measurements and dimensions of the bolts are correct and will work with the real cylinder head.

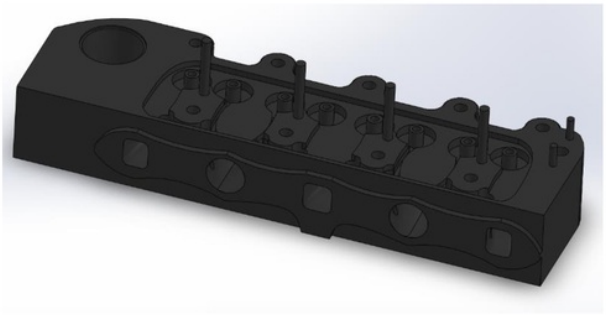


FIGURE 31: REAR VIEW OF 12G202 CYLINDER HEAD

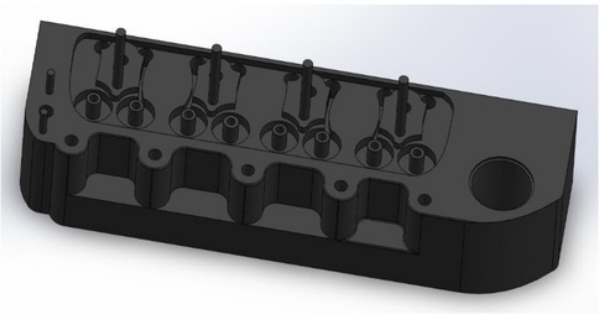


FIGURE 30: FRONT VIEW OF CAD OF 12G202 CYLINDER HEAD

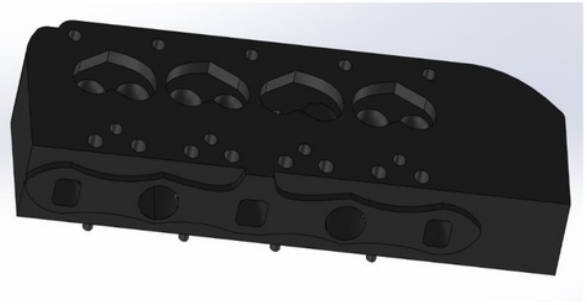


FIGURE 32: VIEW OF BOTTOM OF CAD CYLINDER HEAD

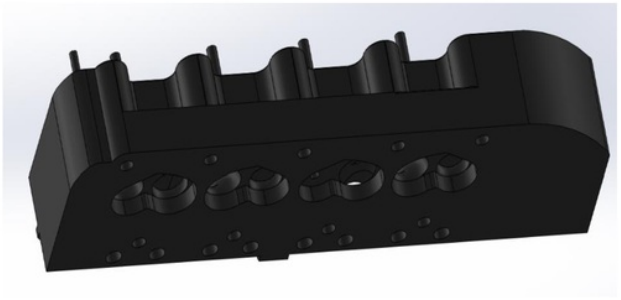


FIGURE 33: VIEW OF BOTTOM AND REAR OF CAD CYLINDER HEAD

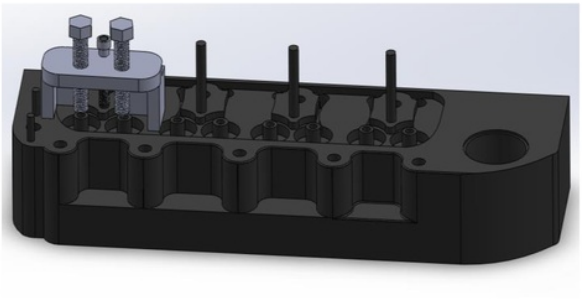


FIGURE 34: TOP, FRONT VIEW OF CAD CYLINDER HEAD WITH VALVE OPENING TOOL

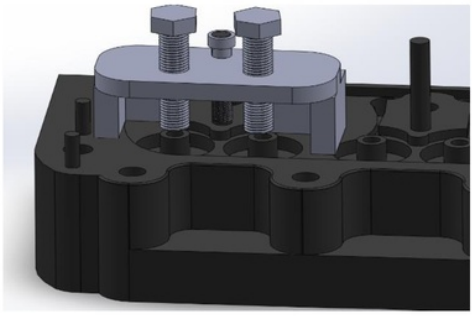


FIGURE 35 TOP FRONT VIEW OF CAD CYLINDER HEAD WITH ADDED VALVE OPENING TOOL

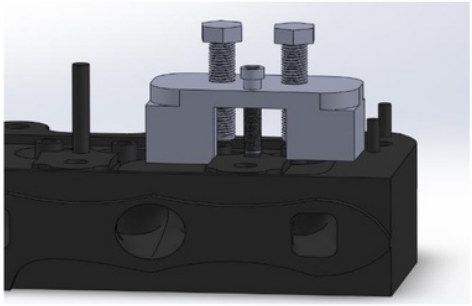


FIGURE 36: REAR VIEW OF CAD CYLINDER HEAD WITH ADDED VALVE OPENING TOOL

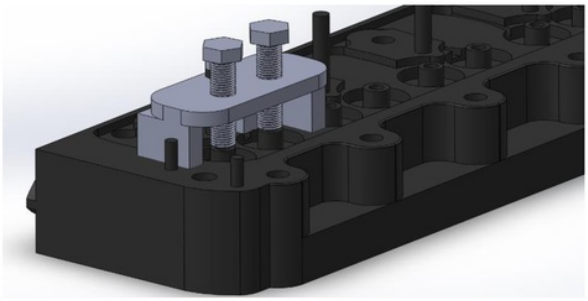


FIGURE 37: SIDE VIEW OF CAD CYLINDER HEAD WITH ADDED VALVE OPENING TOOL

Now that the tool fits and should work with the cylinder head, an aluminium version of the valve opener can be made.



FIGURE 38: ALUMINIUM LEGS FOR VALVE OPENING TOOL



FIGURE 39: TOP PLATE FOR VALVE OPENING TOOL



FIGURE 400: SECURING BOLT AND BOLTS USED TO PUSH DOWN VALVE



FIGURE 41: COMPLETE VALVE OPENING TOOL



FIGURE 41: VALVE TOOL ON TOP OF CYLINDER HEAD

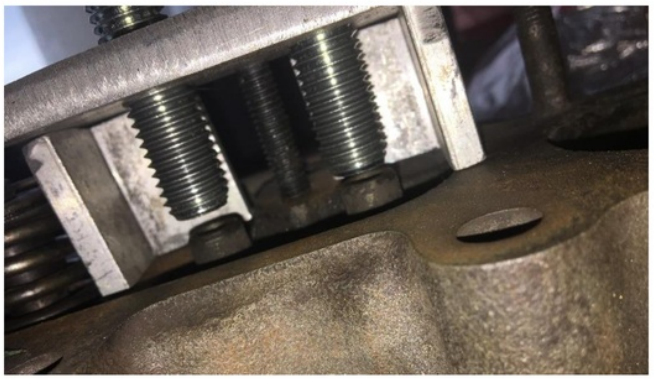


FIGURE 42: VALVE TOOL SAT ON TOP OF VALVE GUIDES

2.4 SETTING UP FLOW BENCH WITH THE 12G202 HEAD

Once the valve tool had been made, flow testing the standard cylinder head could begin. The flow bench is used to measure the resistance of the air flow through intake manifolds, velocity stacks and cylinder heads. For intake testing the cylinder head Is placed on top of the bench and sealed. An air pump pulls air through the cylinder head and through the flow bench at a constant pressure. The amount of air pulled through the head and bench is changed by a flow control knob. The air being pulled through the system creates a pressure drop in the test plenum.

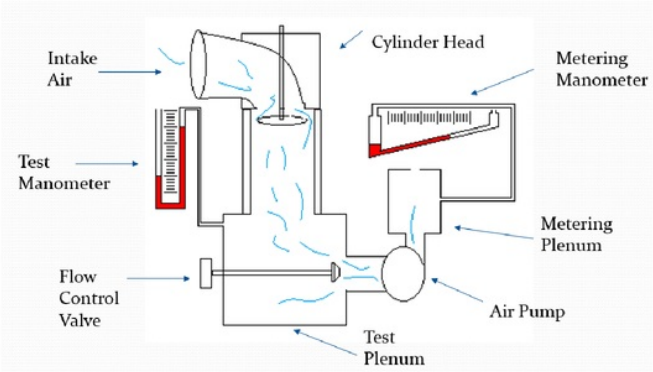


FIGURE 43: SIMPLIFIED DRAWING OF A FLOW BENCH

The flow bench used for the project is the SF-110 this uses a pressure drop controlled by the dia of 10" (25.4cm) of water. The manometer in the metering plenum then shows a percentage of the air that is flowing through the system. The manometer measures the difference of pressures across 5 orifices at the top of the bench. The percentage of flow reads from 0% to 100%. The percentage given by the flow meter then needs to be used and converted to CFM (Cubic Feet per Minute), using the graph below.

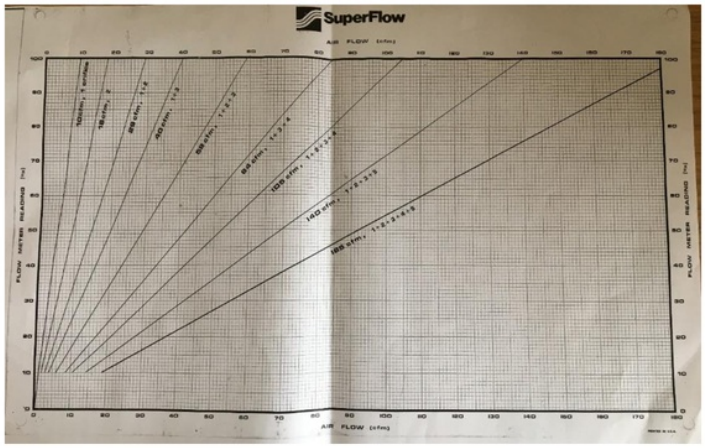


FIGURE 44: SUPERFLOW CFM CONVERSION CHART

To mount the cylinder head to the flow bench, an adaptor plate is used. The adaptor is a tube of 100cm in length and the diameter of the engines bore. In this case for the mini the diameter is 62.4mm at either end of the adaptor is a flange. The lower end of the flange is bolted to the flow bench and the other end is attached to the cylinder head. Both ends of the flange need to be tightly sealed using a gasket or blue tack so that air cannot leak past. A dial test indicator gauge can then be placed on the top of the valve opener. This can accurately show the amount that the valve has been opened.

According to the Superflow manual [8] the perfect flow at 10” is 87.1 CFM



FIGURE 45: CREATING A SEAL ON THE CYLINDER HEAD



FIGURE 46: CYLINDER HEAD AND CLAMP

First blue tack is added around the bottom flange of the adaptor plate and then bolted down onto the flow bench. Next blue tack is added around the combustion chamber of the cylinder head. The head is then clamped down onto the plate using G clamps.



FIGURE 48: SITTING THE HEAD ON THE ADAPTOR PLATE



FIGURE 47: CLAMPING THE CYLINDER HEAD DOWN

Next the valve opening tool can be bolted down onto the cylinder head and the dial test indicators can be added to the setup.



FIGURE 49: BOLTING ON VALVE OPENING TOOL



FIGURE 50: VALVE OPENING TOOL FROM THE SIDE



FIGURE 52: ADDING THE DTI GAUGE



FIGURE 51: CLOSE UP OF DTI GAUGE

For this test, the air flow will be measured at every 0.5 mm of valve lift



FIGURE 53: DTI WITH VALVE CLOSED



FIGURE 54: DTI WITH VALVE OPEN 0.5MM



FIGURE 56: FINAL SETUP OF TEST EQUIPMENT



FIGURE 55: FINAL SETUP OF TEST EQUIPMENT

2.5 FLOW TESTING STANDARD HEAD

The standard cylinder head was tested three times over three different days so that different ambient temperatures and pressures could be accounted for. The results were then averaged. The test results are below.

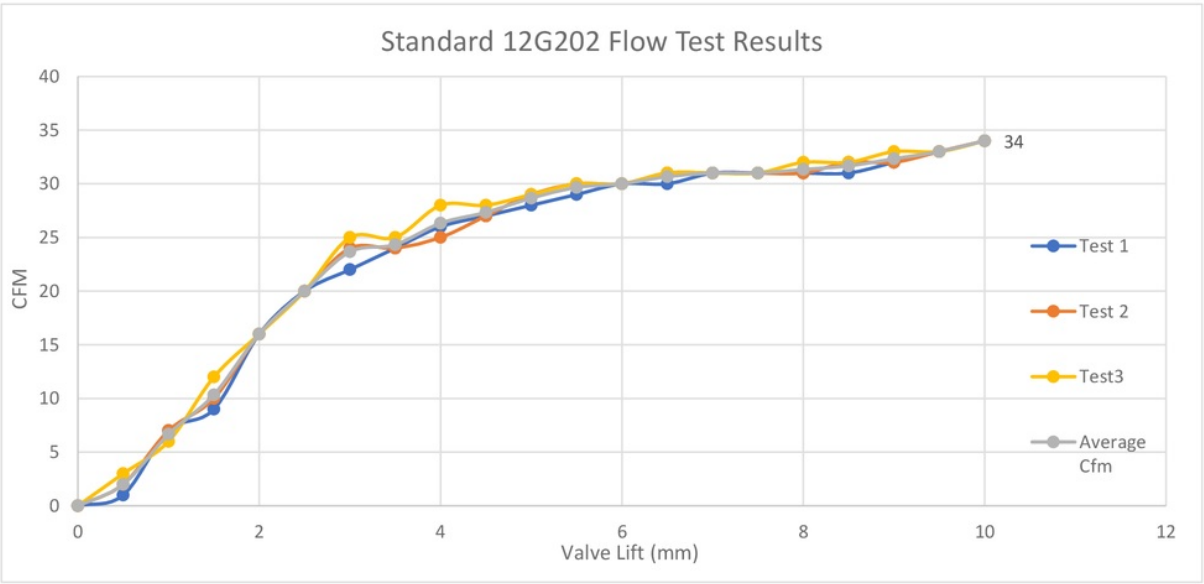


FIGURE 57: STANDARD FLOW TEST RESULTS

As you can see the trend of the results are what you would expect, with the cfm increasing as the valve lift increases. The flow starts to stagnate at around 6mm lift, as above this lift the flow only increases by only

8cfm over nearly half of the valve lift. The max average flow from all three tests was 34 cfm with the flow at around 32 cfm at the valve lift of ¼ of the valve diameter.

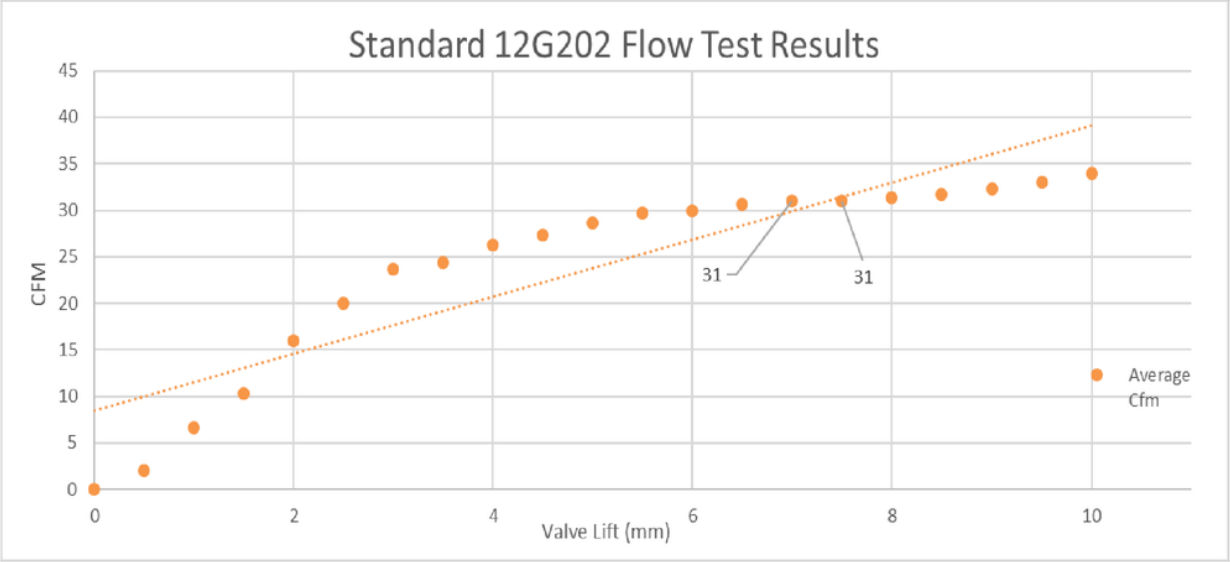


FIGURE 58: AVERAGE STANDARD FLOW TEST RESULTS

To find the flow coefficient the cfm of each result is divided by the diameter of the valve in inches squared. This value is then divided by the perfect flow at 10" (87.1) giving the flow coefficient of water is turned to create a pressure drop of 10" of water. The maximum flow coefficient for the standard head was 0.36.

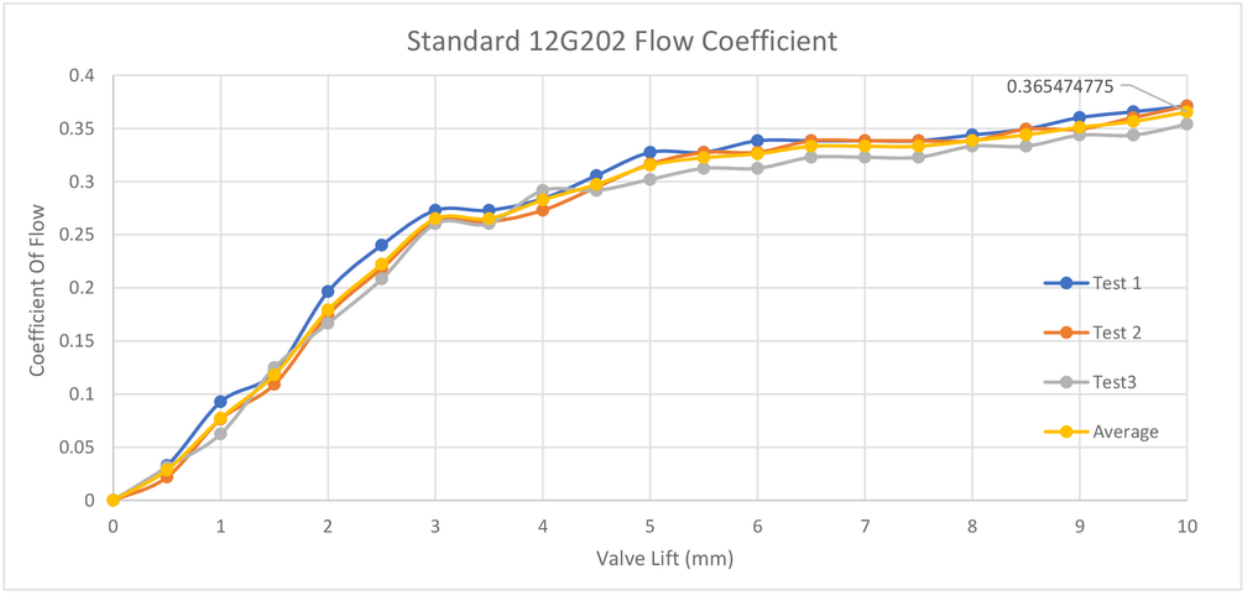


FIGURE 59: STANDARD FLOW TEST COEFFICIENT RESULTS

2.6 EFFECT OF CARBON BUILD UP ON THE VALVE

The next test was not planned however after inspecting the cylinder head when it arrived there seemed to be some carbon build up on the back of a couple of the inlet valves. This build up gives the effect of a reduced curtain area as the amount of space the air has to flow through has been reduced. Once again, the test was conducted three times over different days. The results of the first test was interesting, as you can see the flow was vastly increased throughout the whole test.

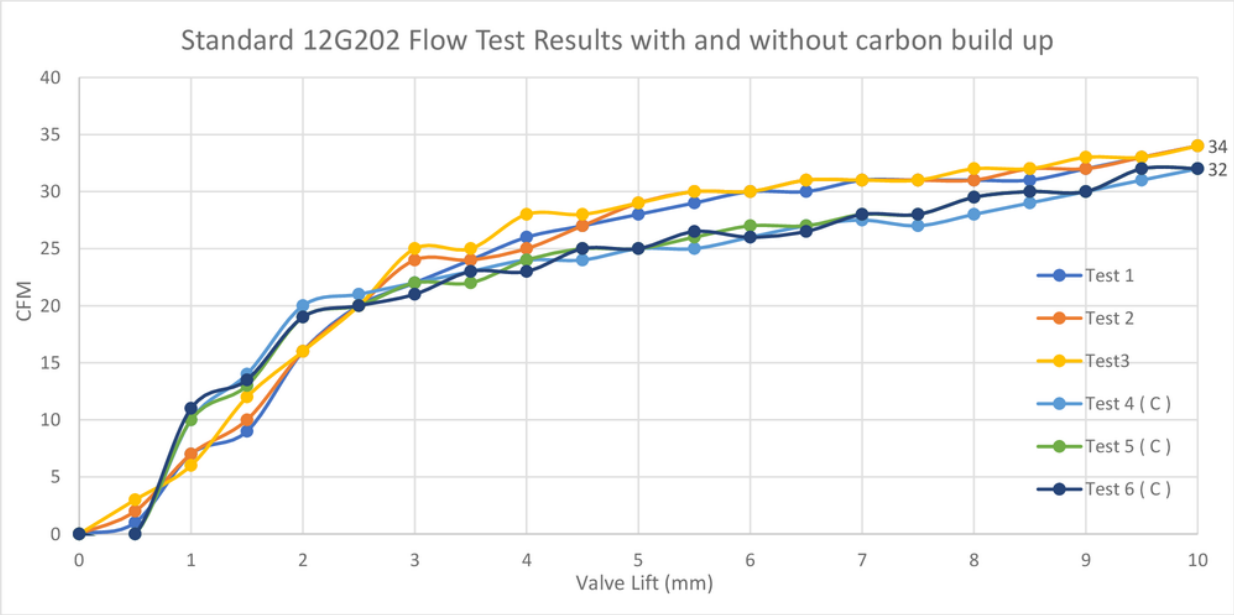


FIGURE 60: STANDARD FLOW TEST RESULTS WITH CARBON BUILD UP

The results are more what we would expect when there is a restriction to the curtain area. Looking at the compared results the first carbon valve test results are way out in comparison to the rest of the test. Looking at test 5 we can see that the carbon valve flows the same CFM until 1mm of lift when it then starts to flow a lot less than in comparison to a clean valve. The flow then becomes the same at around 6mm of lift. These results make sense as the smaller curtain area is the restriction of the flow until a higher lift where then the port then becomes the restriction, so to see the carbon valve flowing less up until this point is what I'd expect to see.

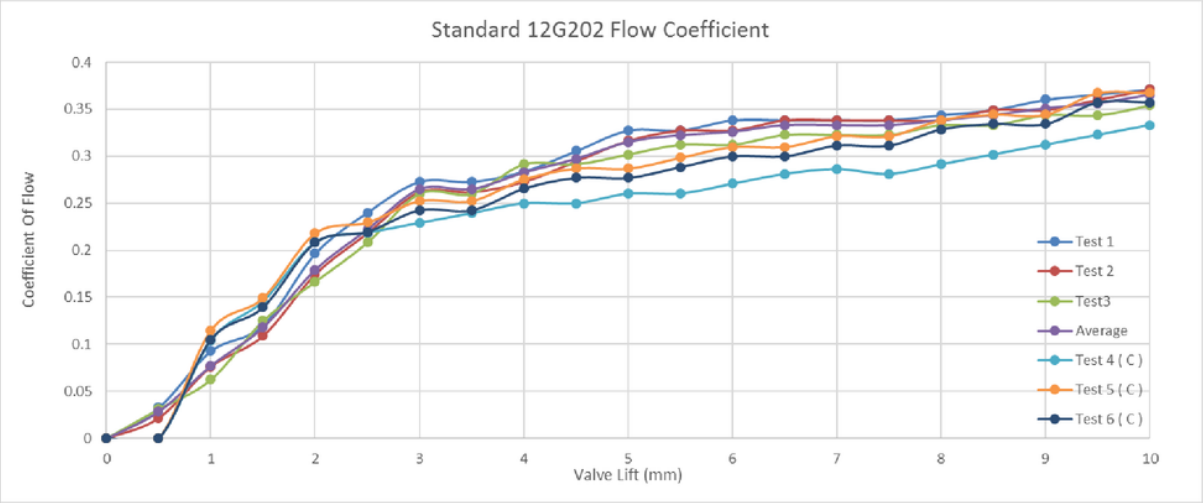


FIGURE 61: STANDARD FLOW COEFFICIENT RESULTS WITH CARBON BUILD UP

The results above show that the standard head has a maximum flow capacity of 34 and a flow coefficient of 0.37

2.7 CHAPTER 2 REFERENCES

1 Trad4u. (N/A). *Air sand blaster*. Available: https://www.manomano.co.uk/air-sand-blaster-3201?model_id=1667903&g=1&referer_id=537135&ach=c7480&achsqrt=c4a77&gclid=EAIaIQobChMIprjzlJfx4QIVrLztCh0KJQSJEAQYBCABEgJzS_D_BwE. Last accessed 2/3/19

2 Performance Trends, Inc.. (NA). *Manual Valve Opener for Flow Bench Testing*. Available: http://www.performancetrends.com/Valve_Opener_Actuator_Manual_Flow_Bench%20Testing.htm. Last accessed 5/3/19.

3 Mini Mani . (2017). *Identifying Minis by Engine/Power Unit*. Available: https://www.minimania.com/Mini_Identification__Identifying_Minis_by_Engine-Power_Unit. Last accessed 29/12/18.

4 Superflow Corperation (N/A). *SF-110 Flowbench Operators Manual*. Colorado: Superflow Corperation. 1 - 44.

5 L. Porter (1998). *Mini Restoration Manual*. Yeoville: Haynes Publishing Group. All .

CHAPTER 3

3 CREATING A CAD MODEL OF THE PORT PHASE 1

Now that the results from the standard cylinder head flow bench test have been obtained, work could start towards making a CAD drawing of the port. After Sufficient drawings had been created on Solid works, the sketches could then be turned into physical components by the use of a 3d printer. The first plan was to use Vernier callipers to measure all the dimensions and to make educated guesses towards the internal diameters of the port. The first sketches of the mini port are below.

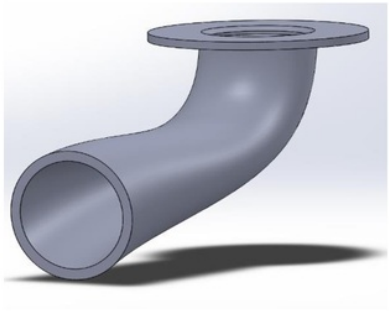


FIGURE 62: FRONT VIEW OF FIRST DESIGN

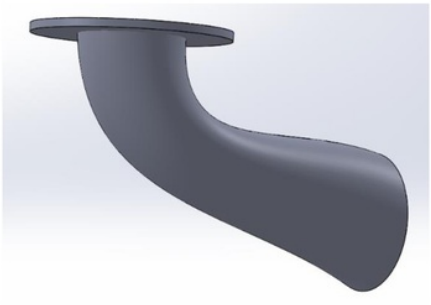


FIGURE 63: REAR VIEW OF FIRST DESIGN

After an evaluation of the first designs it was decided that the ports needed to be drawn more accurately, the combustion chamber needed to be drawn as well. At first, the idea was to draw different ports, with extreme port dimensions to prove that raised floors and roofs etc did have a substantial impact the amount of flow that came through the port.

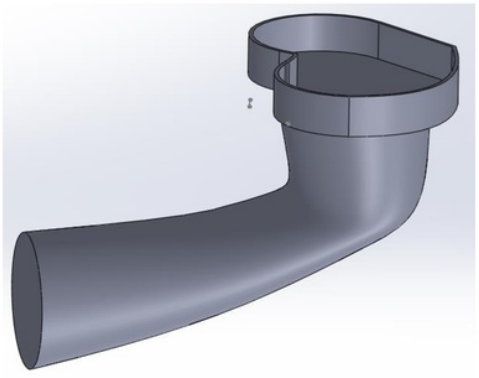


FIGURE 64: MINI PORT WITHOUT SHORT SIDE RADIUS

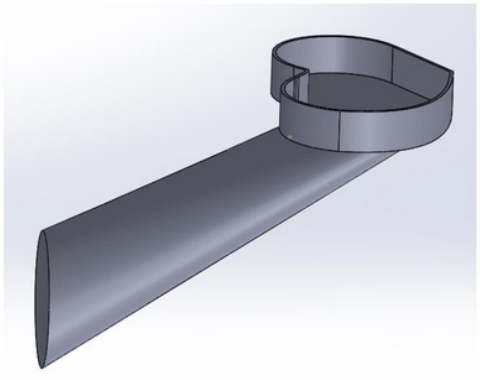


FIGURE 65: MINI PORT WITHOUT SHORT AND LONG SIDE RADIUS

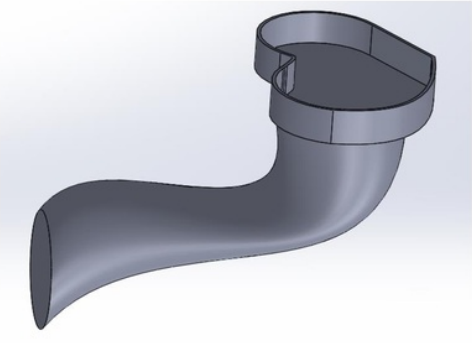


FIGURE 67: MINI PORT WITH CURVED FLOOR AND CEILING

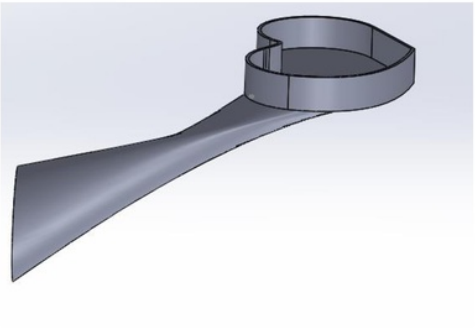


FIGURE 66: MINI PORT WITH INCREASE FLOOR HEIGHT AND REDUCED CEILING

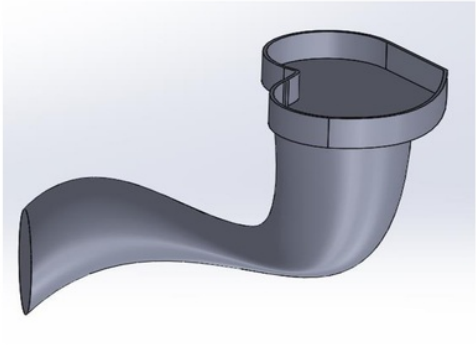


FIGURE 68: MINI PORT WITH EXTREME CURVED FLOOR AND CEILING

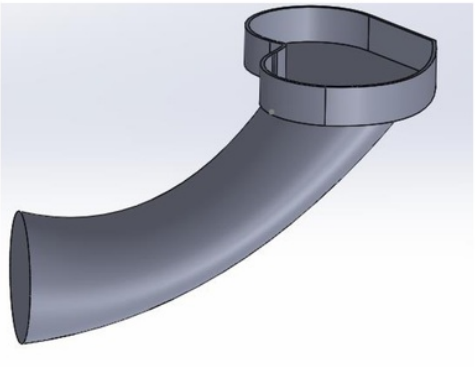


FIGURE 69: MINI PORT WITH INCREASED SHORT AND LONG SIDE RADIUS

Separate to the port designs were the drawings for the valve seats. To see what affect valve seats had on flow, the first preliminary designs were created below. The idea was to have 5 separate straight ports that housed a valve through the middle. They could then be tested on the flow bench and at different valves lifts and the results between them could be compared.

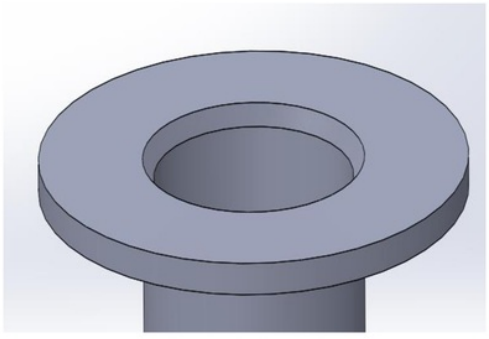


FIGURE 71: 1 ANGLE SEAT

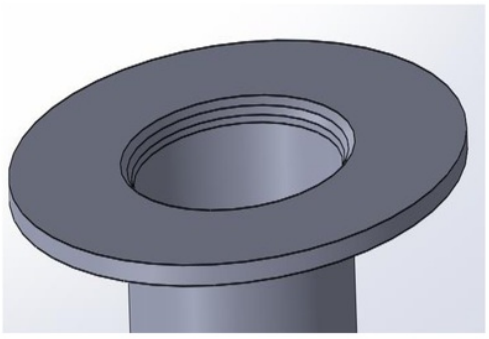


FIGURE 70: 3 ANGLE SEAT

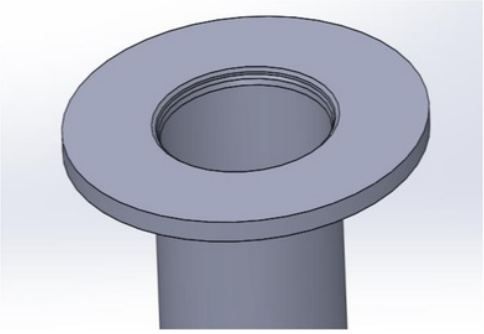


FIGURE 73: 4 ANGLE SEAT

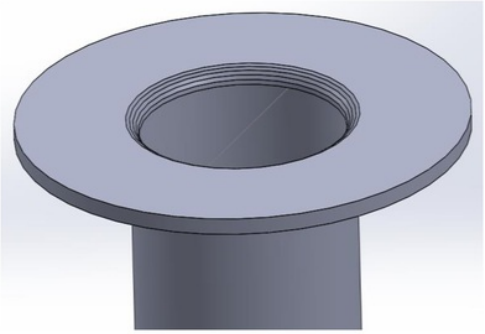


FIGURE 72: 5 ANGLE SEAT

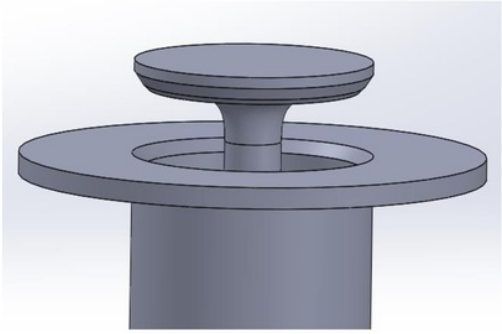


FIGURE 75 : SEAT AND VALVE

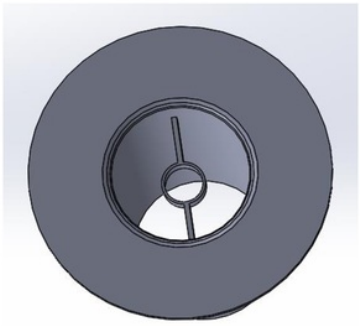


FIGURE 74: VALVE GUIDE

Reviewing the aims for the project, the objective was to see whether the flow through the mini port could be improved by the use of port geometry manipulation and seat configuration changes. The previous seat designs were not related in any way to the mini cylinder head, and the preliminary sketches of the port were not accurate or relevant enough. The extremities of their designs were to unrealistic to provide real viable data in accordance to improving the flow through the mini. A design re think was needed.

3.1 CREATING A CAD MODEL OF THE PORT PHASE 2

So that the components could be tested in the same way as the cylinder head, they needed to be able to attach to the flow bench, this is something that the first phase of designs did not consider. A large flat-bottomed square was fitted around the combustion chamber so that it could be sealed down onto the flow bench. As well as this a more accurate design of the port was drawn.

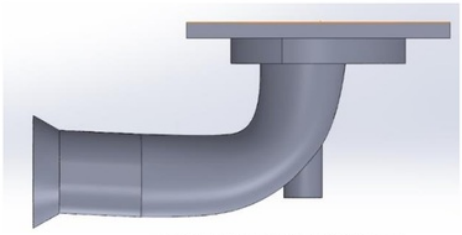


FIGURE 77 SIDE VIEW OF MINI PORT

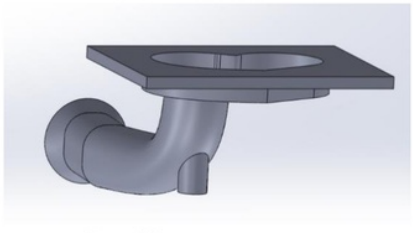


FIGURE 76: REAR VIEW OF MINI PORT

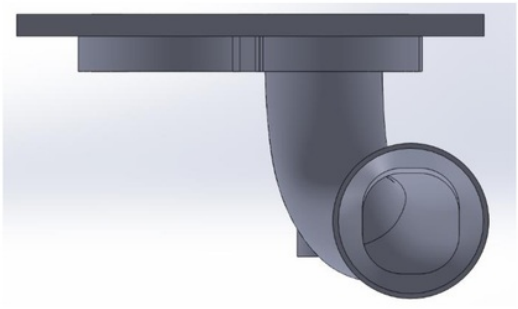


FIGURE 78: FRONT VIEW OF MINI PORT

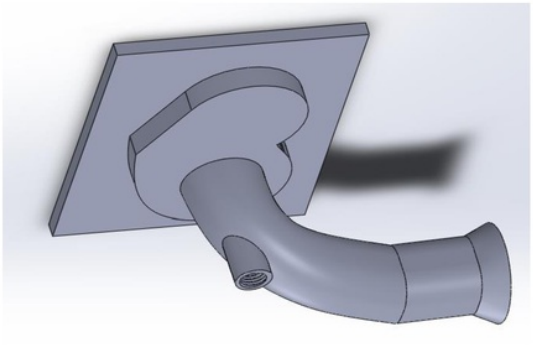


FIGURE 79: BOTTOM VIEW OF MINI PORT

In a cylinder head, the valves are held shut by springs and pushed open by a camshaft. As previous development work has shown in this project, testing a cylinder head on the flow bench, needs some type of device involved where valves can be held open at different lifts. To be able to recreate the same tests on the printed ports the valves will need to be moved and secured by some other method. There are two issues that need to be overcome with this problem. The first being that the suction from the flow bench would pull the valve into the bench if not secured properly, and the second being that the valve needs to be able to be moved and held at different heights throughout the test. The answer to this was to cut a thread through the valve guide, and to extrude a thread onto the valve stem. This way the valve could be turned until the desired valve lift was required and could be held at that height as well.



FIGURE 80: CAD OF MINI INLET VALVE



FIGURE 81: CAD OF MINI INLET VALVE WITH THREAD

The plan for testing was to print the design seen in figure [76-79] for each different port seat and chamber configuration. (A total of 160 prints) The first print would consist of a reduced shrouding, a raised roof, and a one angle seat. The next one would have the same shrouding, the same roof and a two-angle seat. This would be the same up to 5 angles. They could all be flow tested and the results could be compared.

After that, a second stage of shrouding could be implemented on the combustion chamber, and the 5 different angle seat designs, could be drawn and printed separately again.

3.2 SETTING UP THE 3D PRINTER

In order to flow test the CAD designs and obtain real world test results, the 3d printer was to be used. Rather than carrying out time consuming and 'un-doable' porting work on the cylinder head, designs could be drawn, quickly printed and tested to see whether they had an advantage or disadvantage on the flow. At the start of the project the idea was to use the 3D printer provided by the university as it was already setup and running. After trying to arrange a time to print the first component it was clear that due to the substantial amount of designs planned for the project, that it was going to be difficult to able to book in sessions on the printer t get them completed. The decision was made to source a personal 3d printer so that the designs could constantly be printing without the need to liaise with a third party.

After searching for a few weeks for a well recommended printer within budget, a Creatility Ender 3 was purchased. It arrived as a kit and required building before the first print could be completed. The assembly guide below was provided and followed to complete the build.

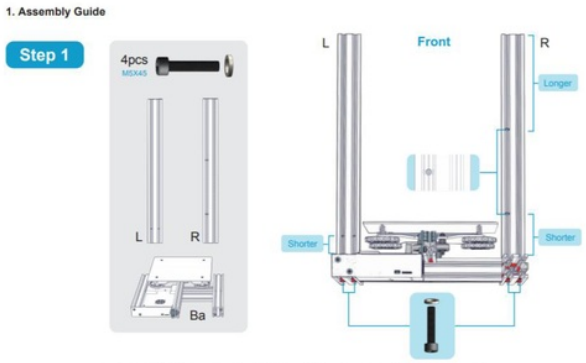


FIGURE 82: CREATILITY ENDER 3 ASSEMBLY GUIDE PART 1

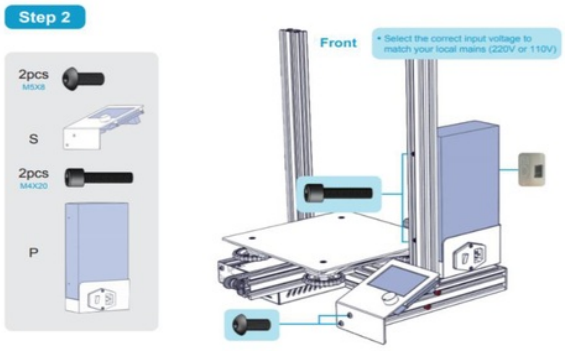


FIGURE 83: CREATILITY ENDER 3 ASSEMBLY GUIDE PART 2

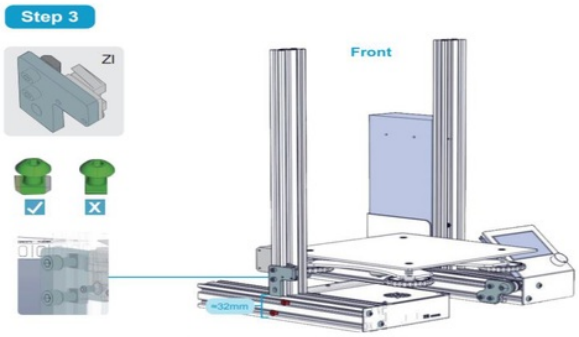


FIGURE 84: CREATILITY ENDER 3 ASSEMBLY GUIDE PART 3

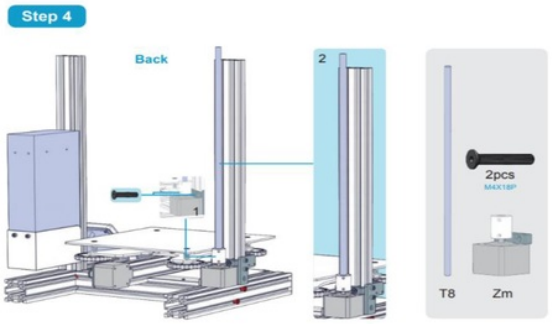


FIGURE 85: CREATILTY ENDER 3 ASSEMBLY GUIDE PART 4

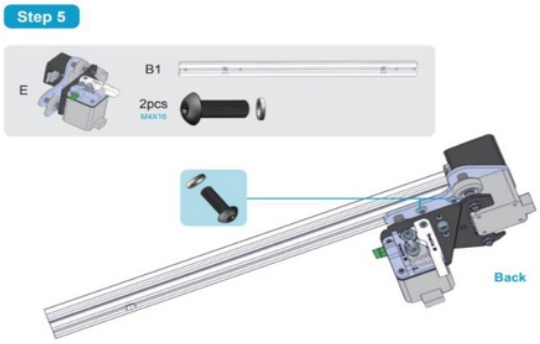


FIGURE 86: CREATILTY ENDER 3 ASSEMBLY GUIDE PART 5

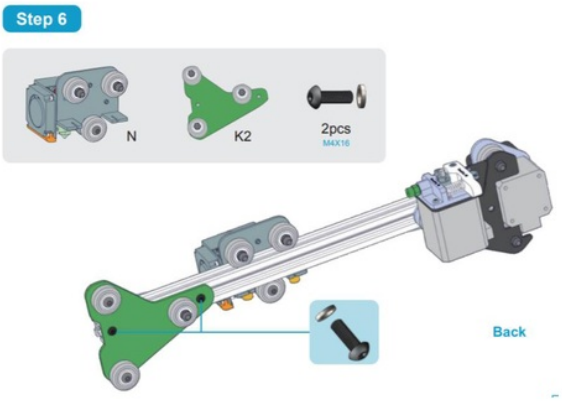


FIGURE 87: CREATILTY ENDER 3 ASSEMBLY GUIDE PART 6

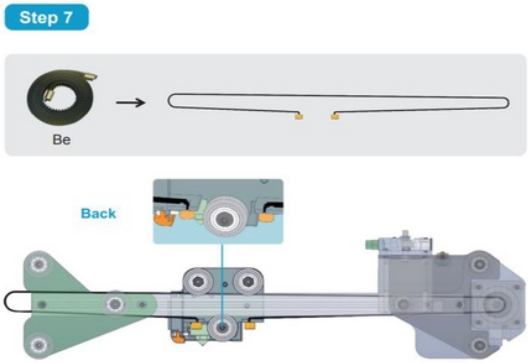


FIGURE 88: CREATILTY ENDER 3 ASSEMBLY GUIDE PART 7

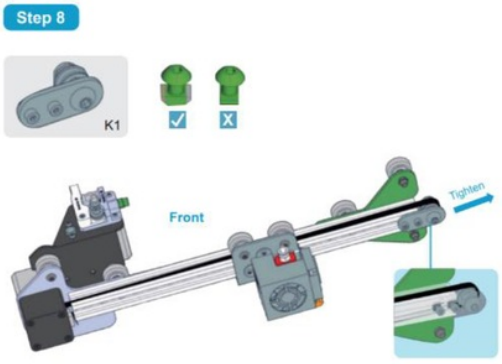


FIGURE 89: CREATILTY ENDER 3 ASSEMBLY GUIDE PART 8

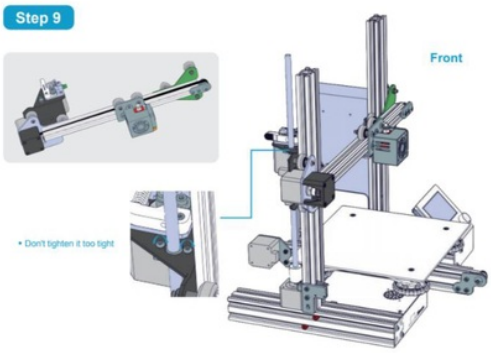


FIGURE 90: CREATILTY ENDER 3 ASSEMBLY GUIDE PART 9

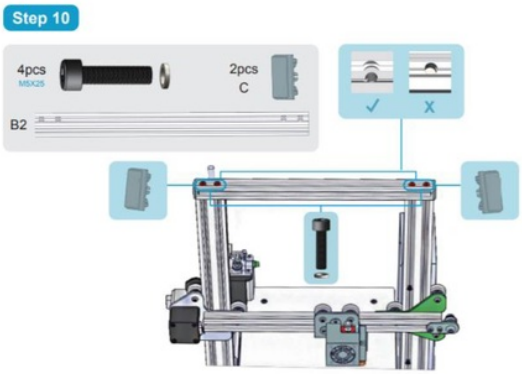


FIGURE 91: CREATILTY ENDER 3 ASSEMBLY GUIDE PART 10

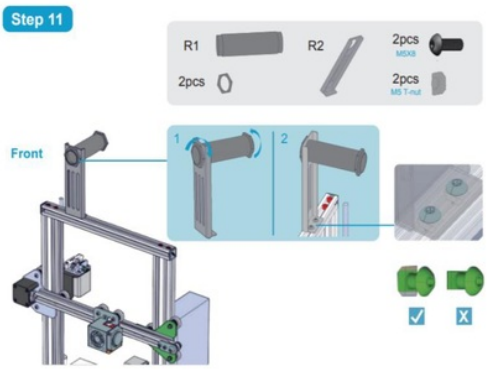


FIGURE 92: CREATILTY ENDER 3 ASSEMBLY GUIDE PART 11

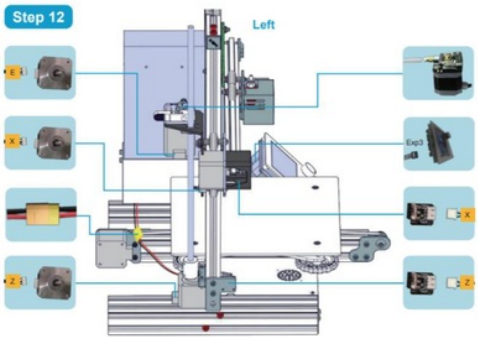


FIGURE 93: CREATILTY ENDER 3 ASSEMBLY GUIDE PART 12

Sainsmart. (N/A). *Ender 3D Printer User manual.* Available: https://images-na.ssl-images-amazon.com/images/I/D1N3oS2crrS.pdf. Last accessed 5/3/19.

After following the guide the printer was ready to use and try a test print



FIGURE 95: COMPLETED FRONT VIEW OF PRINTER

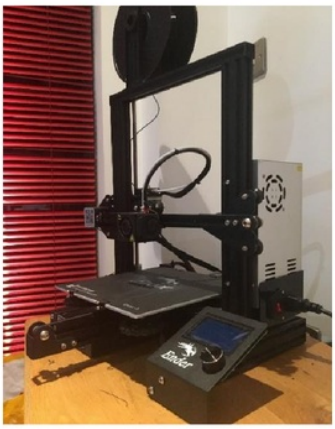


FIGURE 94: COMPLETED SIDE VIEW OF PRINTER



FIGURE 96: COMPLETED TOP VIEW OF PRINTER



FIGURE 97: FIRST TEST PRINT

The test print printed well, so now it was time to move onto the project components.

3.3 PRINTING THE CAD COMPONENTS

Once the printer had been setup, the process of printing the individual flow bench test pieces could begin. The first piece to be printed was below.



FIGURE 99: TOP VIEW OF FIRST 3D PRINT



FIGURE 98: BOTTOM VIEW OF FIRST 3D PRINT

The print itself was created as test to see how successfully the CAD drawings from sketches to physical objects. This print too around 4 hours. Looking at the images above it is possible to determine that the prints were relatively successful however, the component was printed combustion chamber side up, in order to create the right height in the print, supports were needed to build upon. These supports gave a poor finish and created small holes within the port. To combat this issue, the ports were rotated 180 degrees and printed again with the chamber facing up. This helped solve the issue of a poor finish quality and was the way in which all future prints should be conducted.



FIGURE 100: TOP VIEW OF SECOND 3D PRINT



FIGURE 101: TOP VIEW OF SECOND 3D PRINT

Now a print with the flange for the flow bench could be made.



FIGURE 103: TOP VIEW OF FLANGED PORT



FIGURE 102: BOTTOM VIEW OF FLANGED PORT

The print once again was made combustion chamber face down. The above example took around 5 hours to complete. After removing the component from the printer, it was clear to see that the method of using a Vernier calliper to measure the port was not accurate as the cylinder head port and the printer port design looked completely different. In order to obtain accurate results for the flow through a mini port a new way of obtaining the port measurements was needed.

3.4 USING SILICONE TO MODEL THE PORT GEOMETRY

A silicone moulding kit was purchased in order to help create a more detailed mini port CAD drawing. A silicone solution and a hardening agent are provided in the kit and need to be mixed before use. The mixture was then poured into the port and allowed to set for 24 hours. The results of this are below:



FIGURE 105: TOP VIEW OF SILICONE MOULD



FIGURE 104: BOTTOM VIEW OF SILICONE MOULD

The moulding process proved to be successful and dimensions of the port and combustion chamber could be measured and implemented into the CAD design.

3.5 CREATING A CAD MODEL OF THE PORT PHASE 3

After taking measurements of the silicone mould, the CAD looked like this. To help reduce print time a radius was taken away from the flange.

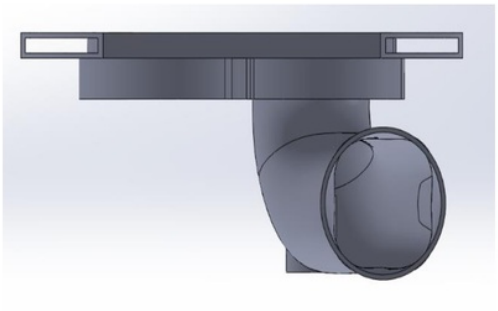


FIGURE 107: FRONT VIEW OF THE PHASE 3 PORT

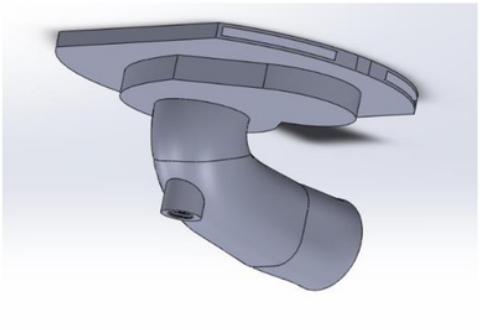


FIGURE 106: BOTTOM VIEW OF THE PHASE 3 PORT

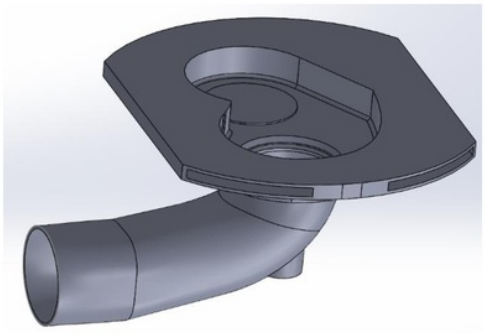


FIGURE 109: SIDE VIEW OF THE PHASE 3 PORT

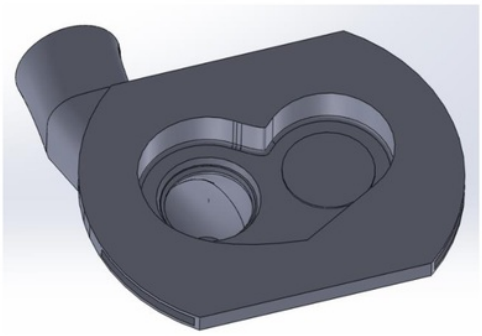


FIGURE 108: TOP VIEW OF THE PHASE 3 PORT

This new design was now ready to be printed. Each print individual print takes just under 6 hours

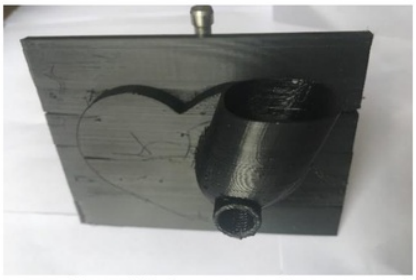


FIGURE 110: PRINT OF PHASE 3 DESIGN

With each print taking 6 hours to complete and 164 prints t be made, the amount of time needed was to great. A way of reducing the print time but still being able to compare components was needed.

3.6 CREATING A CAD MODEL OF THE PORT PHASE 4

By separating the port, the seat and the combustion chamber into separate components the print time could be reduced drastically. There would be 5 seat configurations, 4 combustion chambers and 8 ports designs. These are all separate components that could be clicked together, made into one single assembly and then tested on the flow bench.

Seat Design

The first components to be created were the valve seats. The seat that comes on the mini cylinder head standard mini head is 2.1mm wide with a seat of 45deg.

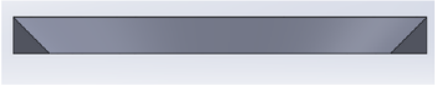


FIGURE 111: 1 ANGLE SEAT

Following the studies found in chapter 1, a two-angle seat has been made, with a 30 degree and 45 degree cut made in the seat.



FIGURE 112: 2 ANGLE SEAT

Then created another version but with 3 angle seats, was made this is a 30deg, a 45deg and a 65deg seat.

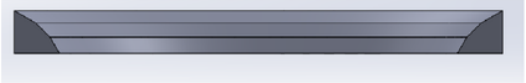


FIGURE 113: 3 ANGLE SEAT

This next design uses 4 angles in the seat 30,45,60,75.

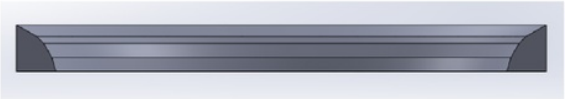


FIGURE 114: 4 ANGLE SEAT

Lastly the final design enquires into the need for a perfect curved radius for the air to follow into the combustion chamber. It has the same seat angles as before but with an added 80 degree cut to create an even more smoothed entry.



FIGURE 115: 5 ANGLE SEAT

Port Design

The next components to be created were the inlet ports. After measuring the dimensions of the silicone model, the design below could be created of the standard mini port.



FIGURE 116: PORT 1 MINI PORT

The next design to be made was a severely reduced port cross sectional area, this should show an increase in cfm at low lift due to a venturi effect, but a severe restriction at high lift.

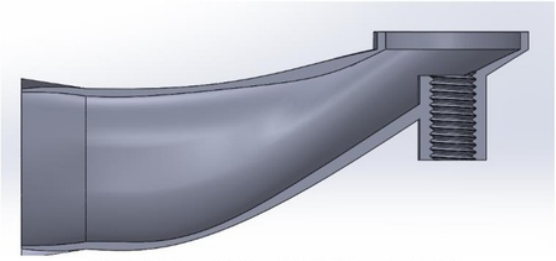


FIGURE 117: PORT 2 REDUCED CROSS SECTIONAL AREA

The third port design features a reduced long turn radius this should have a negative impact on the flow as it creates a restriction.



FIGURE 118: PORT 3 REDUCED LONG TURN RADIUS

The fourth design has a reduced short turn radius this should also have a negative impact on the flow, as it creates a sudden turn for air to travel into the cylinder.



FIGURE 119: PORT 4 REDUCED SHORT TURN RADIUS

The next port design has a smoothed valve guide this should improve flow as it allows air to stick to the long turn radius better.

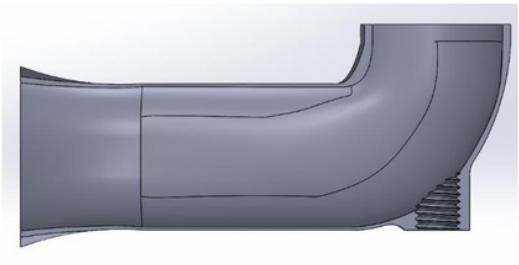


FIGURE 120: PORT 5 SMOOTHED VALVE GUIDE

The sixth design features an Increased short radius this should aid flow as it creates a fillet for air to stick to into the chamber.

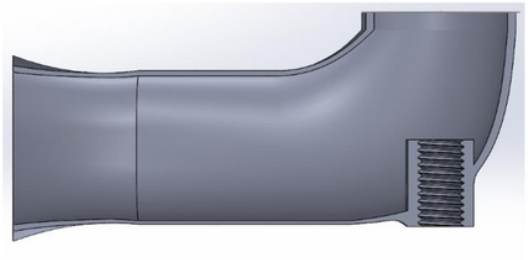


FIGURE 121: PORT 6 INCREASED SHORT TURN RADIUS

This design implements a Increased short radius, increased long turn radius help increase the flow.



FIGURE 122: PORT 7 INCREASED SHORT TURN RAD AND LONG TURN RADIUS

The last design has an Increased short radius, increased long turn radius and smoothed guide, this should be the best flowing design as it aids flow throughout the port and reduces restrictions.



FIGURE 123: PORT 8, INCREASED SHORT RAD, INCREASED LONG RAD AND SMOOTHED GUIDE

No increases in ceiling height or floor depth could be made, as the water jackets in the mini cylinder head prevent this, the only modifications that could be achieved are the ones mentioned above.

Combustion Chamber Design

The original Mini combustion chamber design has been created from the silicone model in the first CAD drawing, the three designs all take 0.5mm of the combustion chamber wall around the circumference of the inlet valve.

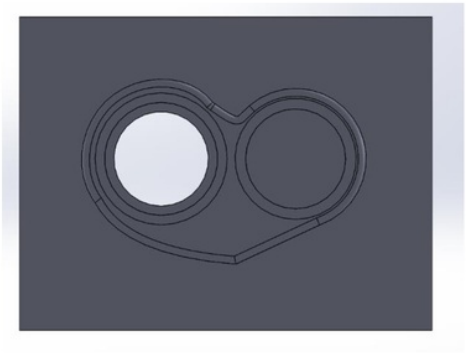


FIGURE 125: COMBUSTION CHAMBER 1

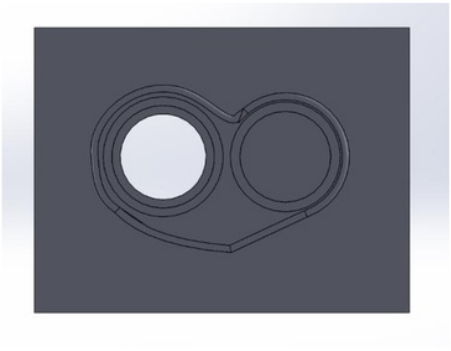


FIGURE 124: COMBUSTION CHAMBER 2 , REDUCED SHROUD 1

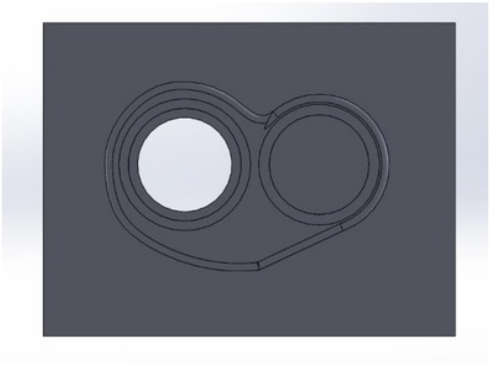


FIGURE 127: COMBUSTION CHAMBER 2 , REDUCED SHROUD 2

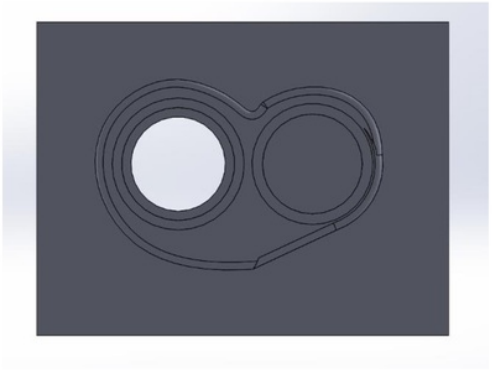


FIGURE 126: COMBUSTION CHAMBER 2 , REDUCED SHROUD 3

Now the designs have been drawn then can be printed.



FIGURE 129: PRINTED 1 ANGLE SEAT



FIGURE 128: PRINTED 2 ANGLE SEAT



FIGURE 131: PRINTED 3 ANGLE SEAT



FIGURE 130: PRINTED 4 ANGLE SEAT



FIGURE 132: PRINTED 5 ANGLE SEAT



FIGURE 134: PRINTED PORT 1



FIGURE 133: PRINTED PORT 2



FIGURE 135: PRINTED PORT 3



FIGURE 136: PRINTED PORT 4



FIGURE 137: PRINTED PORT 5



FIGURE 138: PRINTED PORT 6



FIGURE 139: PRINTED PORT 7



FIGURE 140: PRINTED PORT 8



FIGURE 142: PRINTED CHAMBER 1



FIGURE 141: PRINTED CHAMBER 2



FIGURE 143: PRINTED CHAMBER 3



FIGURE 144: PRINTED CHAMBER 4

Now the parts have been printed, they can be assembled and tested on the flow bench. Although they click together, each individual part still needs to sealed. This is done by using blue tack. A dti gauge can be placed on the valve to measure the amount of lift.



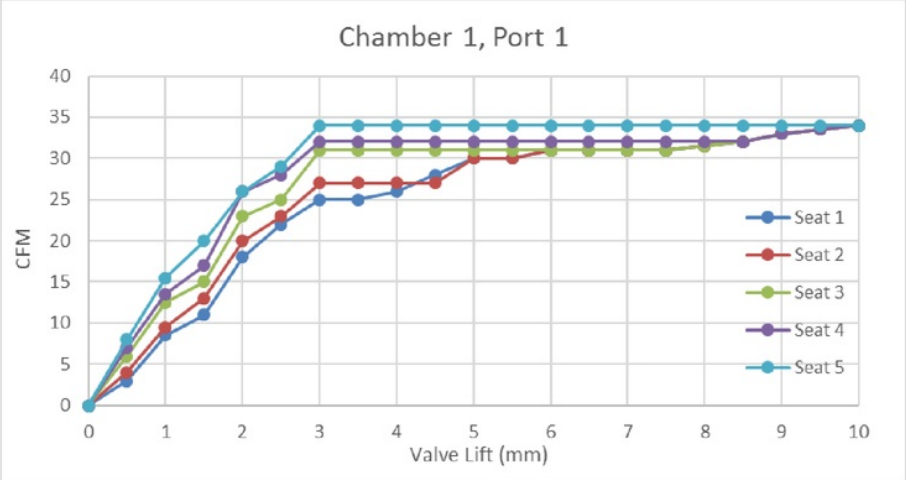
FIGURE 145: PRINTED PARTS BEING FLOW TESTED

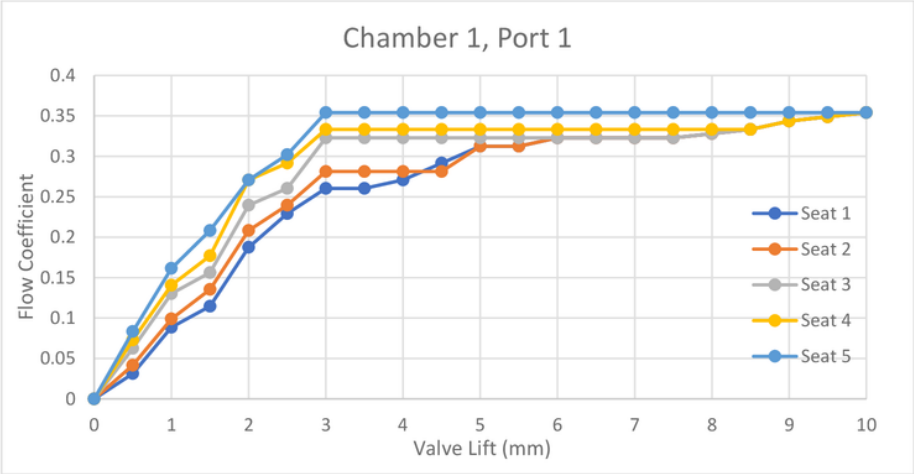


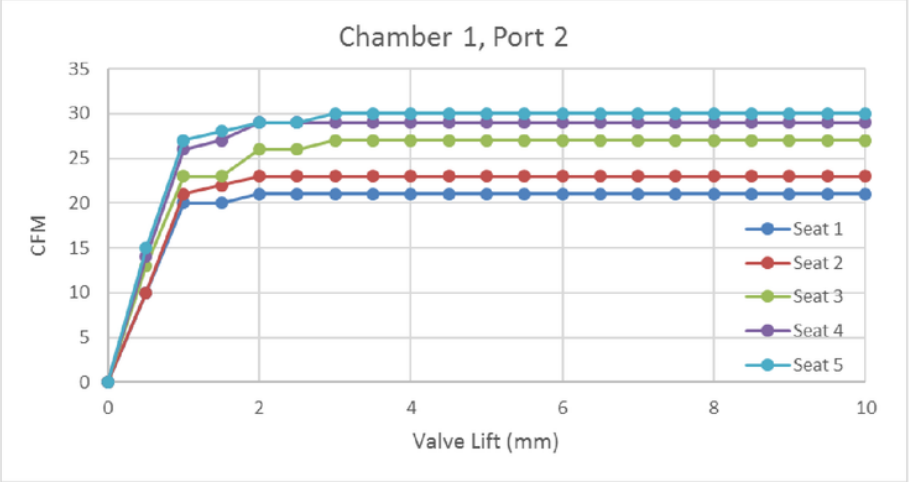
FIGURE 146: PRINTED PARTS BEING FLOW TESTED

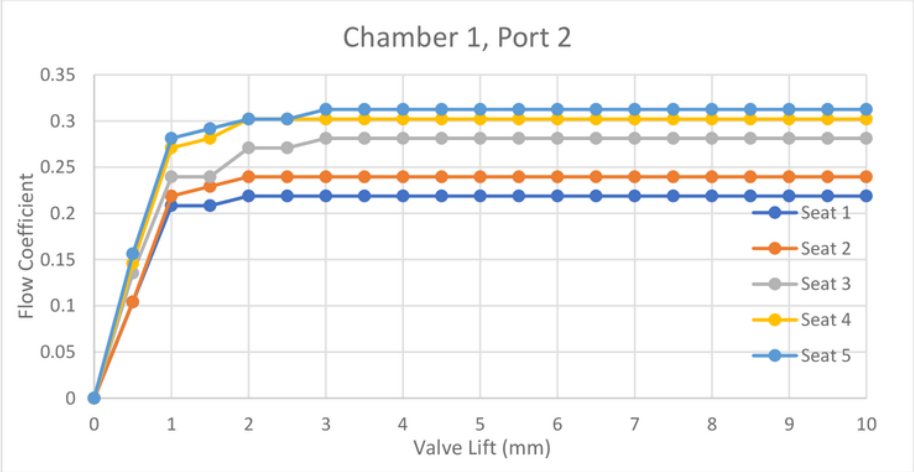
3.7 PRINTED PARTS FLOW TEST RESULTS

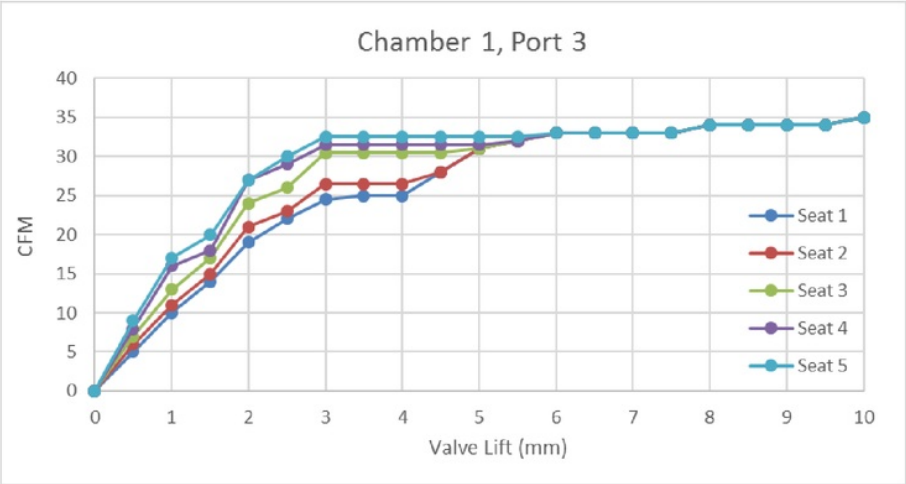
Below are the CFM and flow coefficient results for each intake port, seat and combustion chamber configuration.

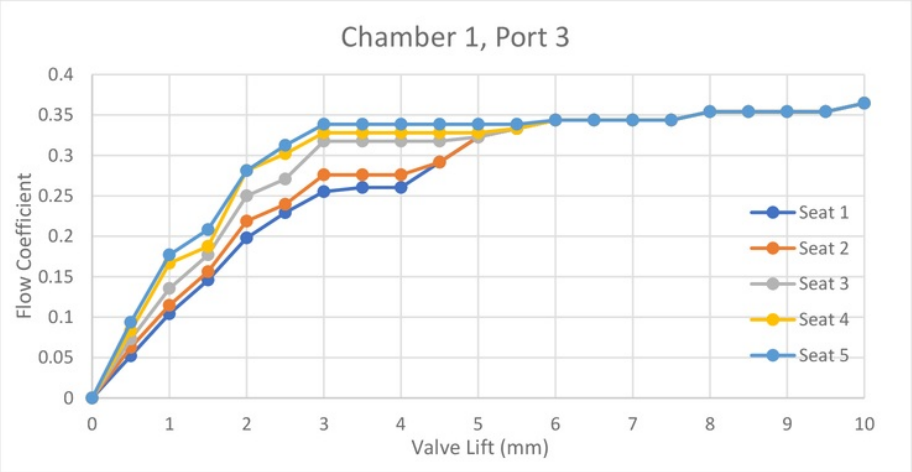


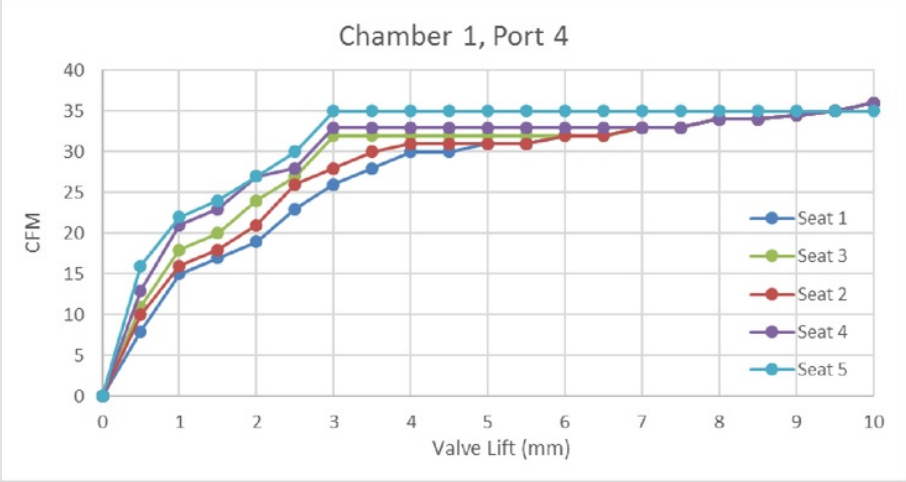

Chamber 1, Port 1
Flow Coefficient
0.4
0.35
0.3
0.25
0.2
0.15
0.1
0.05
0
0 1 2 3 4 5 6 7 8 9 10
Valve Lift (mm)
Seat 1
Seat 2
Seat 3
Seat 4
Seat 5

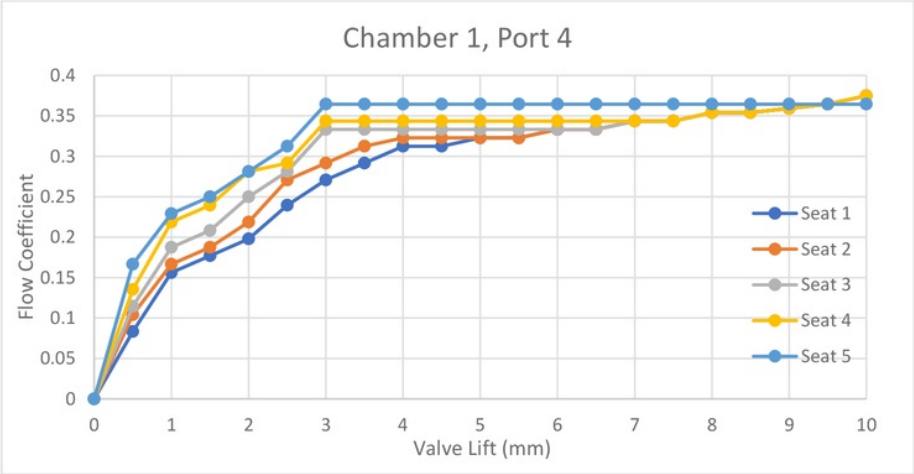

Chamber 1, Port 2
CFM
35
30
25
20
15
10
5
0
0 2 4 6 8 10
Valve Lift (mm)
Seat 1
Seat 2
Seat 3
Seat 4
Seat 5

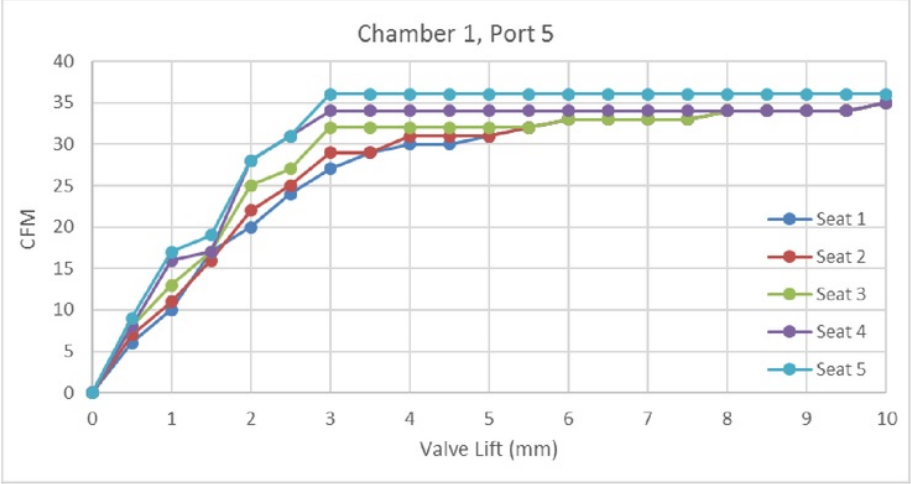

Chamber 1, Port 2
Flow Coefficient
0.35
0.3
0.25
0.2
0.15
0.1
0.05
0
0 1 2 3 4 5 6 7 8 9 10
Valve Lift (mm)
Seat 1
Seat 2
Seat 3
Seat 4
Seat 5

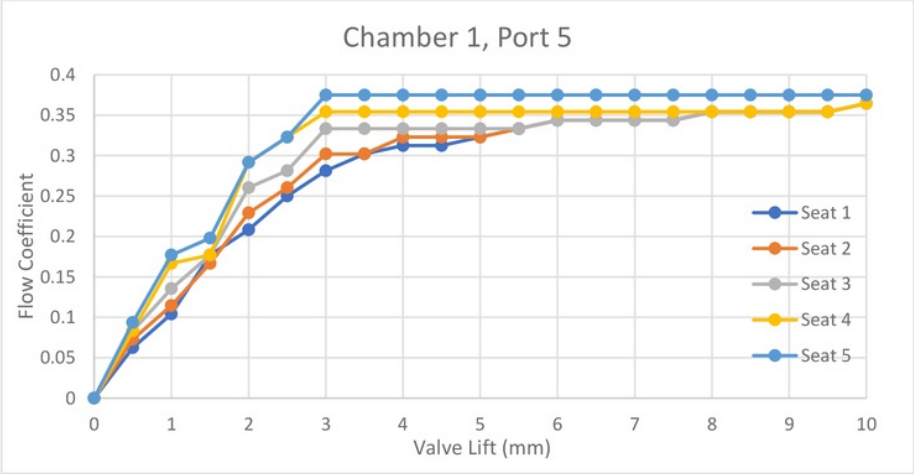

Chamber 1, Port 3
CFM
Valve Lift (mm)
Seat 1
Seat 2
Seat 3
Seat 4
Seat 5

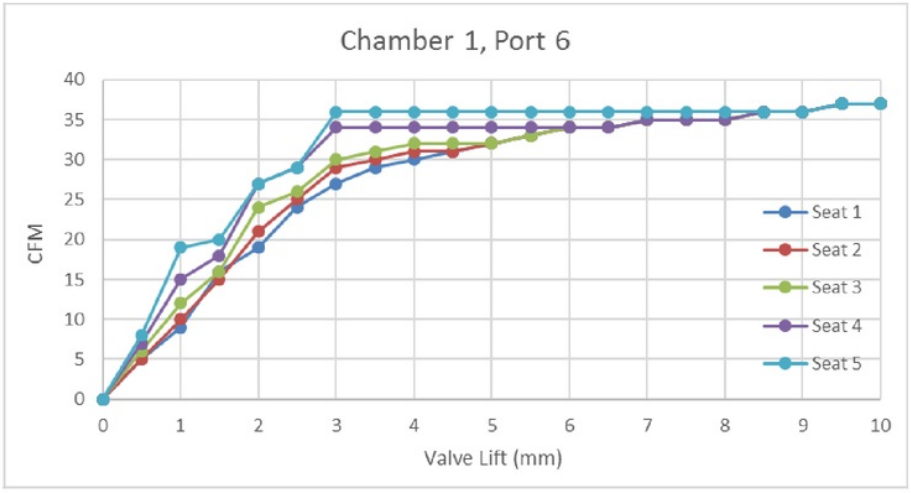

Chamber 1, Port 3
Flow Coefficient
Valve Lift (mm)
Seat 1
Seat 2
Seat 3
Seat 4
Seat 5

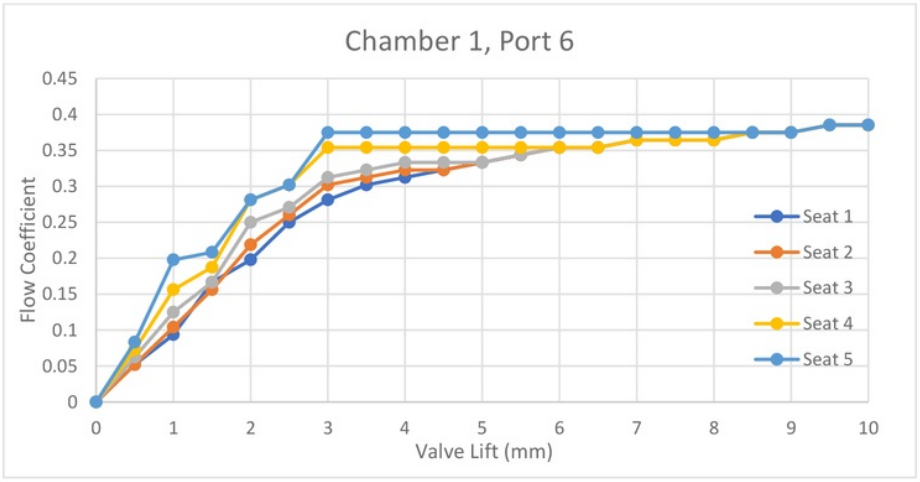

Chamber 1, Port 4
CFM
Valve Lift (mm)
Seat 1
Seat 3
Seat 2
Seat 4
Seat 5

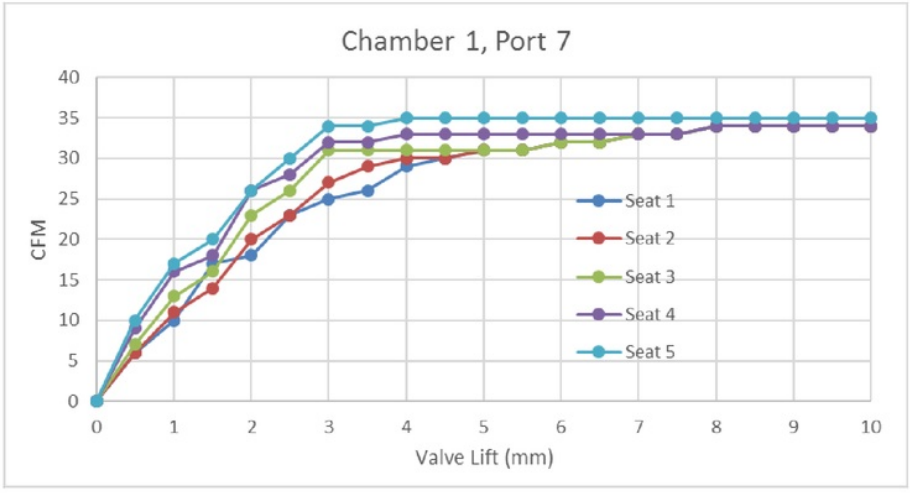

Chamber 1, Port 4
Flow Coefficient
0.4
0.35
0.3
0.25
0.2
0.15
0.1
0.05
0
0 1 2 3 4 5 6 7 8 9 10
Valve Lift (mm)
Seat 1
Seat 2
Seat 3
Seat 4
Seat 5

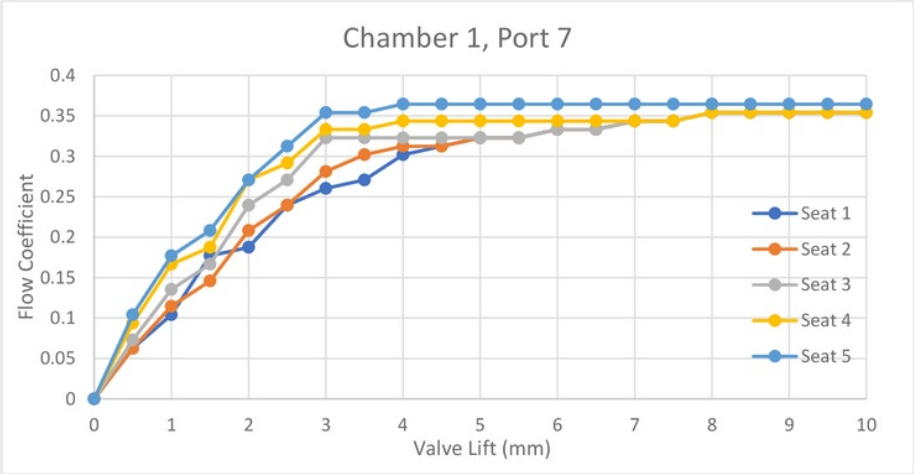

Chamber 1, Port 5
CFM
40
35
30
25
20
15
10
5
0
0 1 2 3 4 5 6 7 8 9 10
Valve Lift (mm)
Seat 1
Seat 2
Seat 3
Seat 4
Seat 5

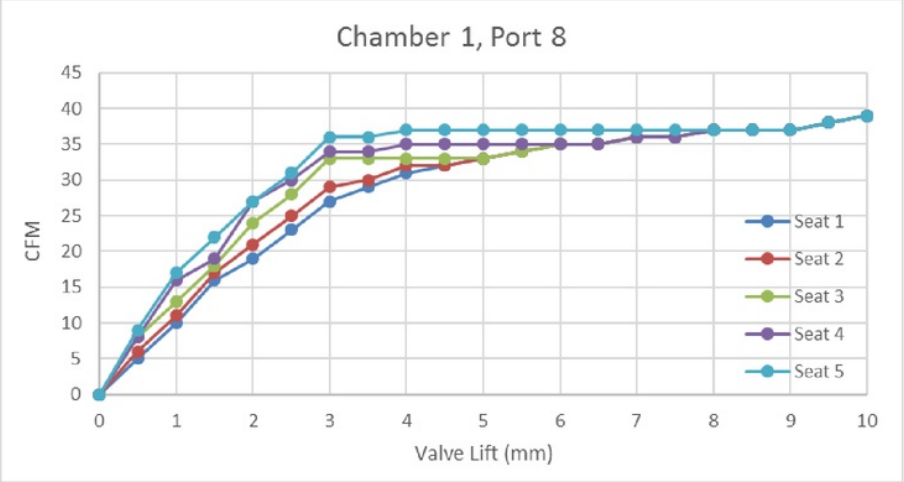

Chamber 1, Port 5
Flow Coefficient
0.4
0.35
0.3
0.25
0.2
0.15
0.1
0.05
0
0 1 2 3 4 5 6 7 8 9 10
Valve Lift (mm)
Seat 1
Seat 2
Seat 3
Seat 4
Seat 5

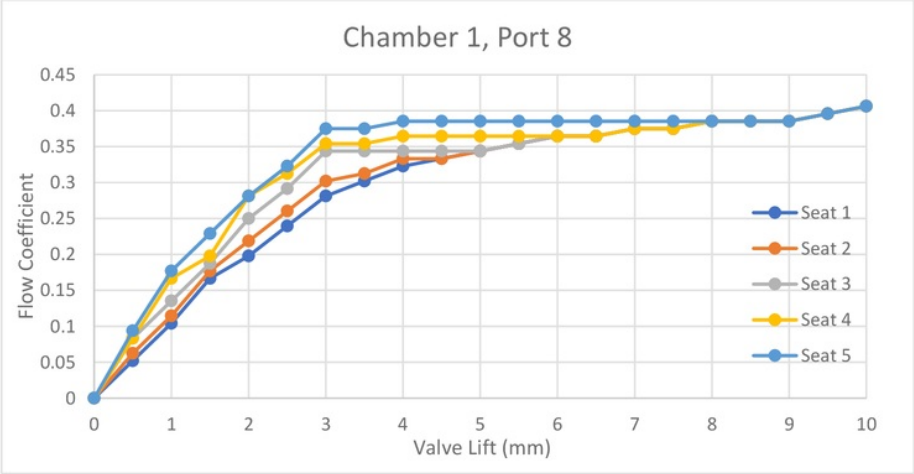

Chamber 1, Port 6
CFM
Valve Lift (mm)
Seat 1
Seat 2
Seat 3
Seat 4
Seat 5

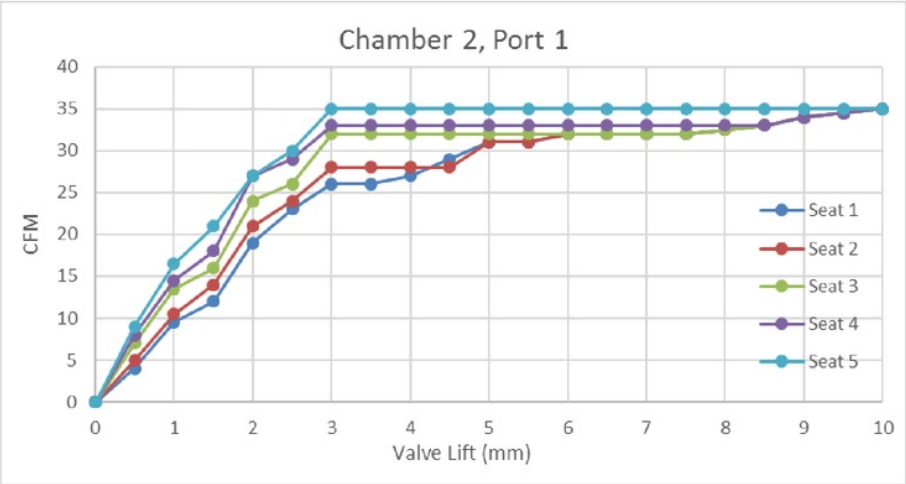

Chamber 1, Port 6
Flow Coefficient
Valve Lift (mm)
Seat 1
Seat 2
Seat 3
Seat 4
Seat 5

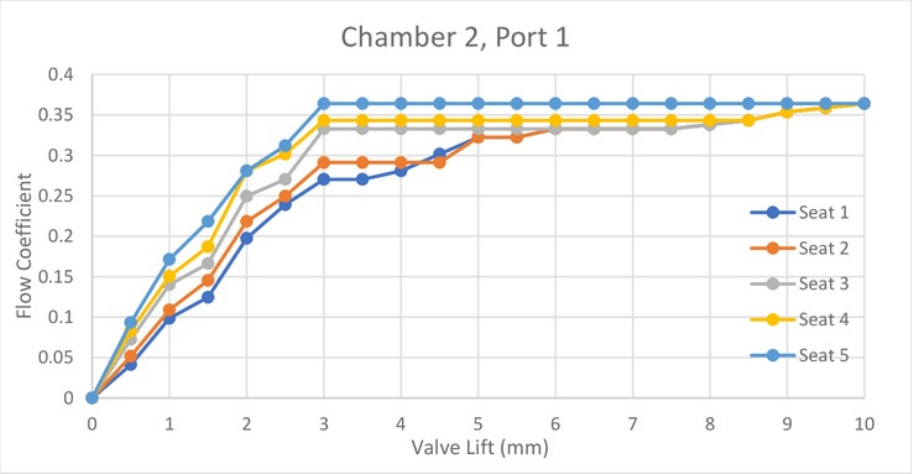

Chamber 1, Port 7
CFM
Valve Lift (mm)
Seat 1
Seat 2
Seat 3
Seat 4
Seat 5

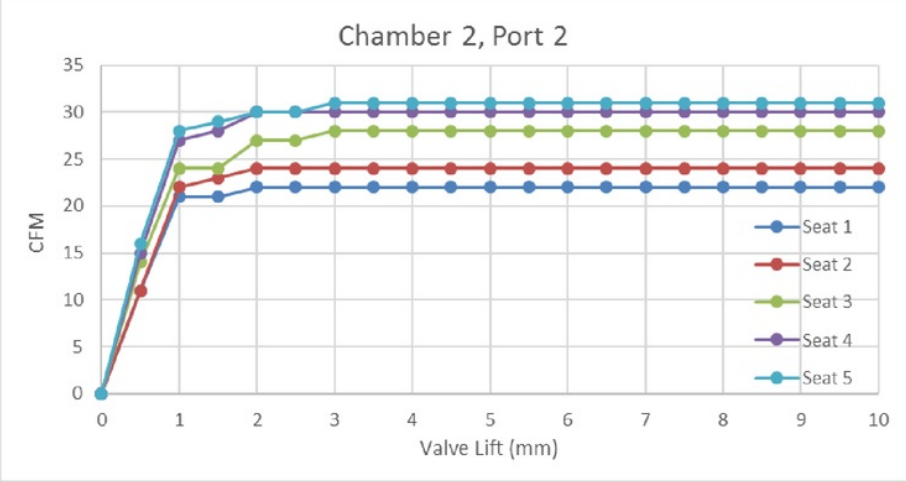

Chamber 1, Port 7
Flow Coefficient
0.4
0.35
0.3
0.25
0.2
0.15
0.1
0.05
0
0 1 2 3 4 5 6 7 8 9 10
Valve Lift (mm)
Seat 1
Seat 2
Seat 3
Seat 4
Seat 5

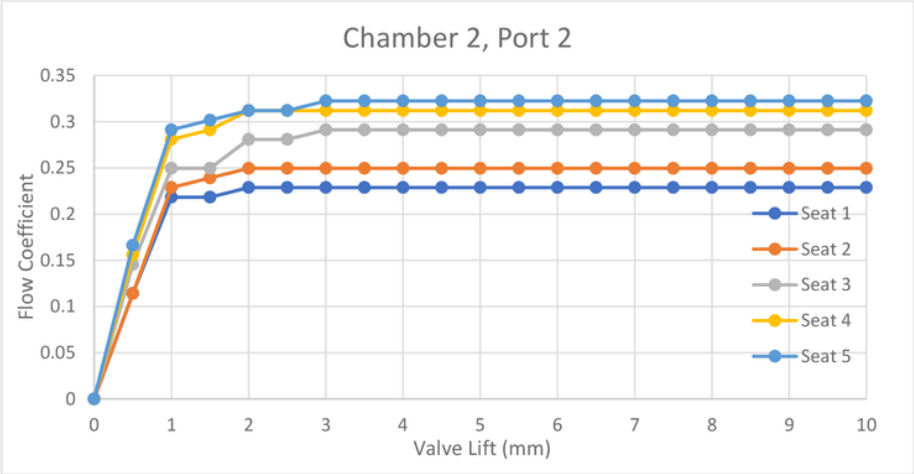

Chamber 1, Port 8
CFM
45
40
35
30
25
20
15
10
5
0
0 1 2 3 4 5 6 7 8 9 10
Valve Lift (mm)
Seat 1
Seat 2
Seat 3
Seat 4
Seat 5

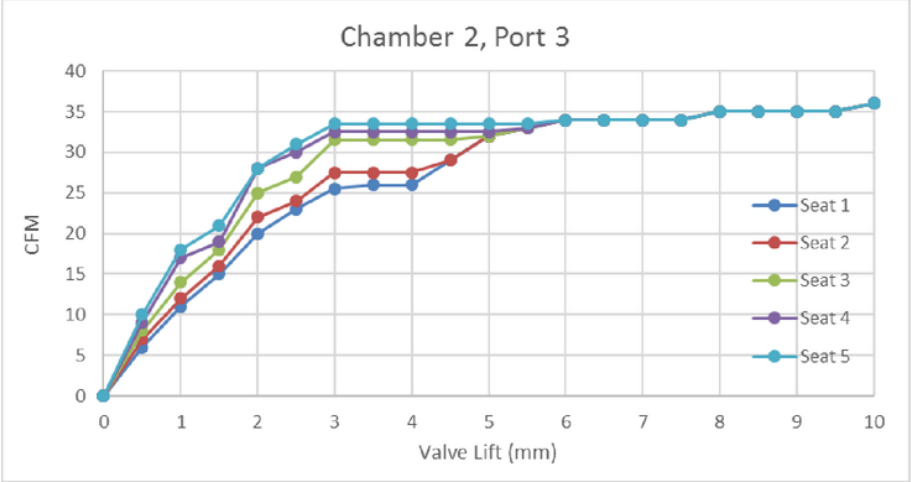

Chamber 1, Port 8
Flow Coefficient
0.45
0.4
0.35
0.3
0.25
0.2
0.15
0.1
0.05
0
0 1 2 3 4 5 6 7 8 9 10
Valve Lift (mm)
Seat 1
Seat 2
Seat 3
Seat 4
Seat 5

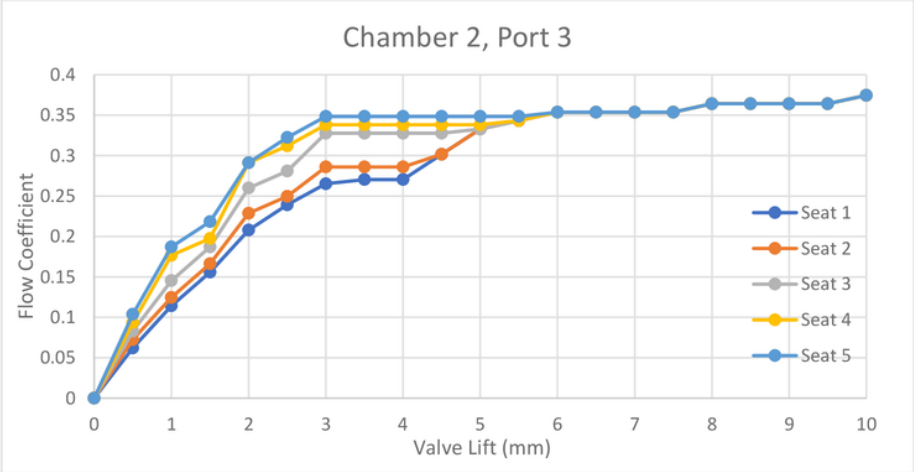

Chamber 2, Port 1
CFM
Valve Lift (mm)
Seat 1
Seat 2
Seat 3
Seat 4
Seat 5

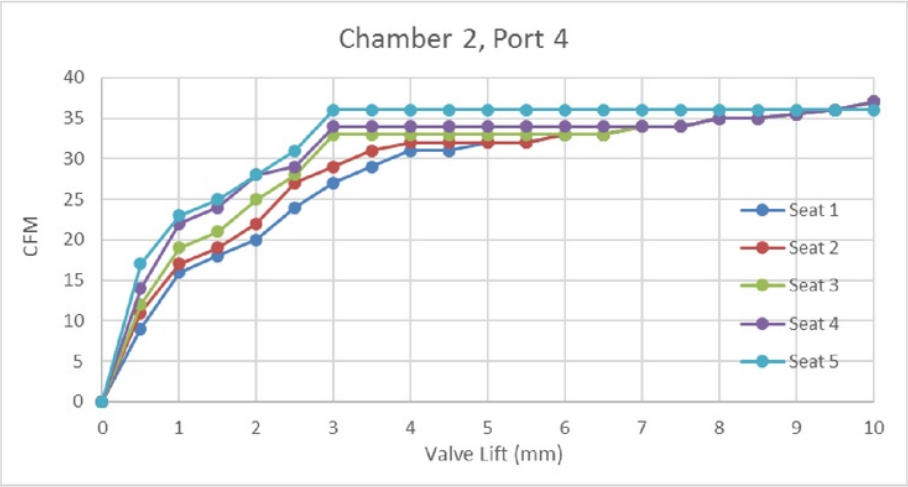

Chamber 2, Port 1
Flow Coefficient
Valve Lift (mm)
Seat 1
Seat 2
Seat 3
Seat 4
Seat 5

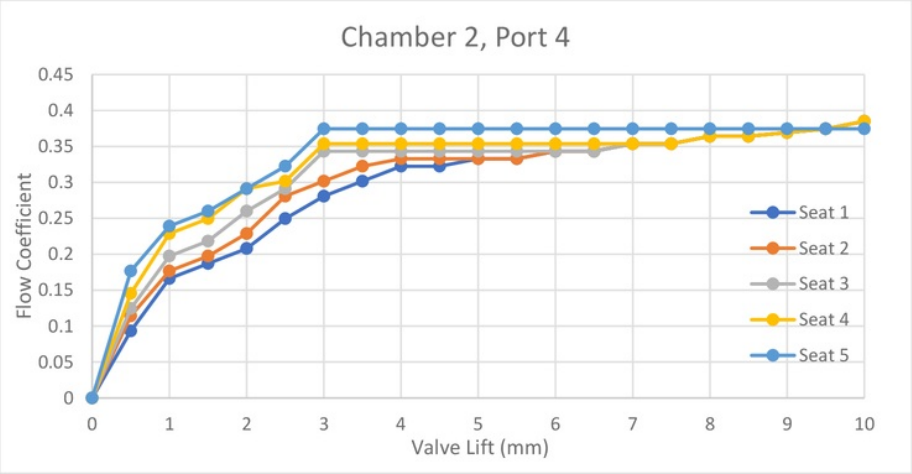

Chamber 2, Port 2
CFM
Valve Lift (mm)
Seat 1
Seat 2
Seat 3
Seat 4
Seat 5

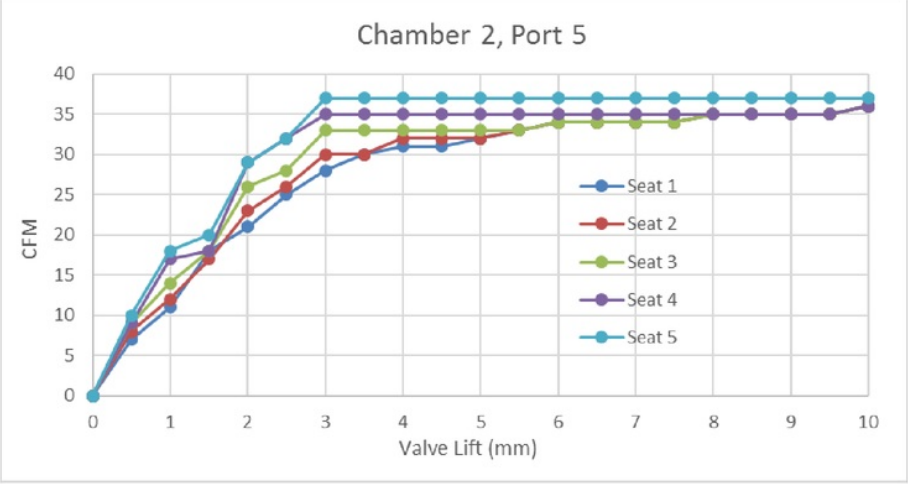

Chamber 2, Port 2
Flow Coefficient
0.35
0.3
0.25
0.2
0.15
0.1
0.05
0
0 1 2 3 4 5 6 7 8 9 10
Valve Lift (mm)
Seat 1
Seat 2
Seat 3
Seat 4
Seat 5

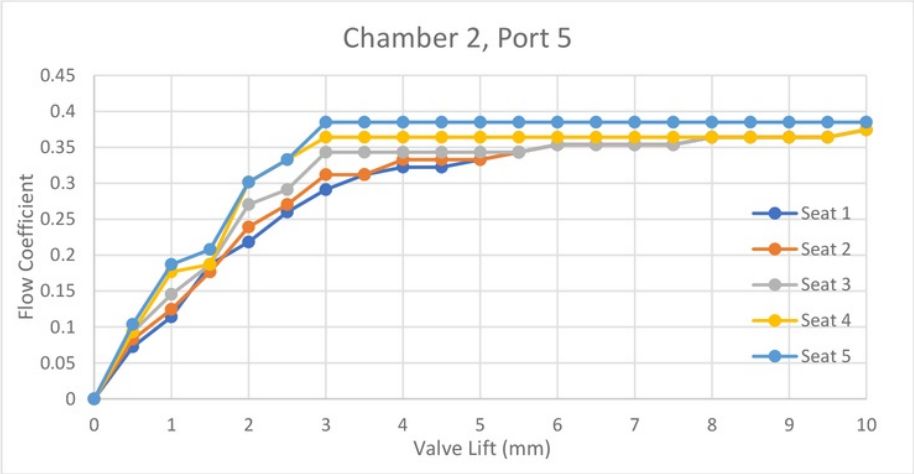

Chamber 2, Port 3
CFM
40
35
30
25
20
15
10
5
0
0 1 2 3 4 5 6 7 8 9 10
Valve Lift (mm)
Seat 1
Seat 2
Seat 3
Seat 4
Seat 5

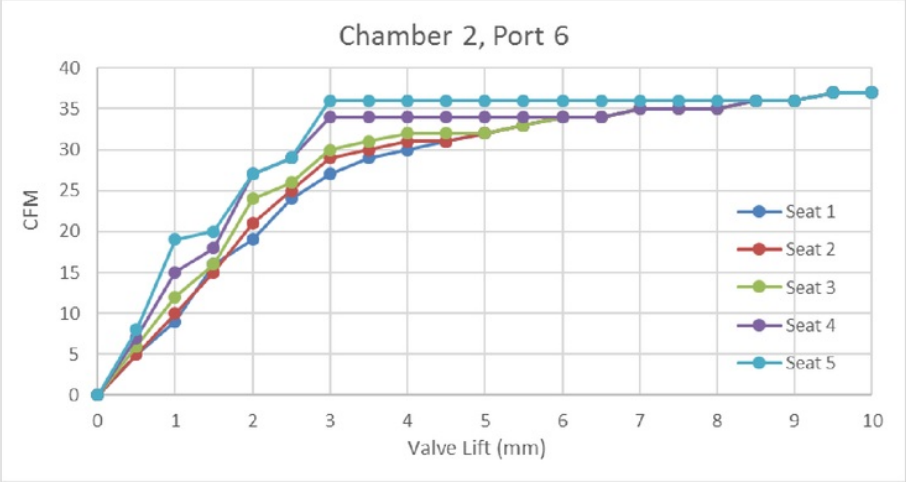

Chamber 2, Port 3
Flow Coefficient
0.4
0.35
0.3
0.25
0.2
0.15
0.1
0.05
0
0 1 2 3 4 5 6 7 8 9 10
Valve Lift (mm)
Seat 1
Seat 2
Seat 3
Seat 4
Seat 5

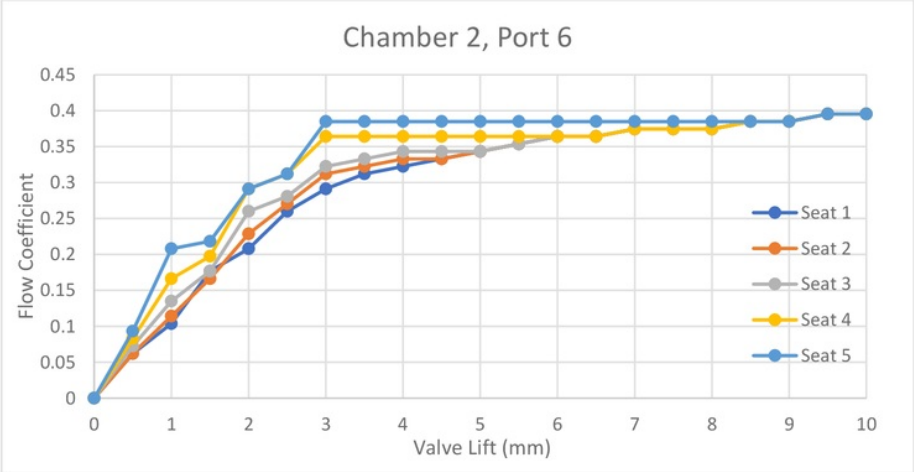

Chamber 2, Port 4
CFM
Valve Lift (mm)
Seat 1
Seat 2
Seat 3
Seat 4
Seat 5

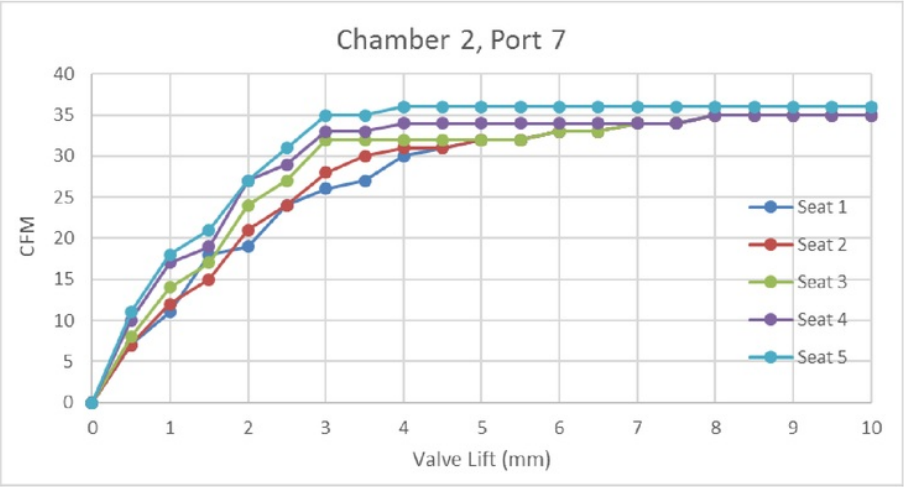

Chamber 2, Port 4
Flow Coefficient
Valve Lift (mm)
Seat 1
Seat 2
Seat 3
Seat 4
Seat 5

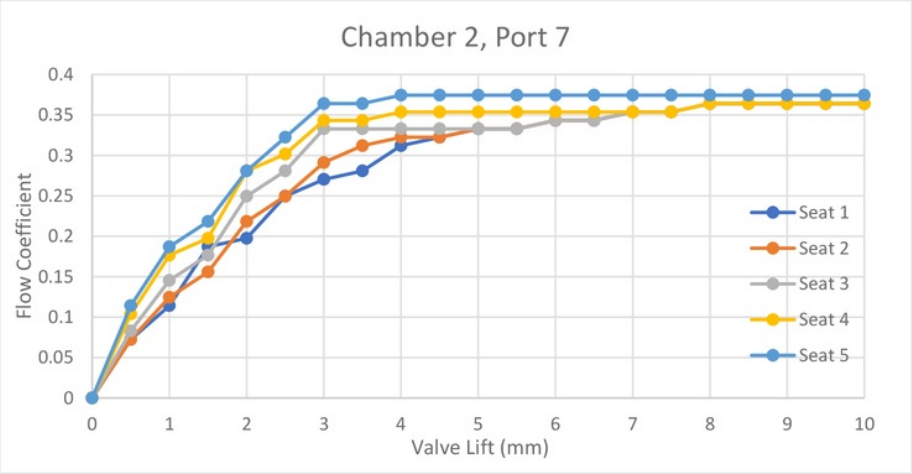

Chamber 2, Port 5
CFM
Valve Lift (mm)
Seat 1
Seat 2
Seat 3
Seat 4
Seat 5

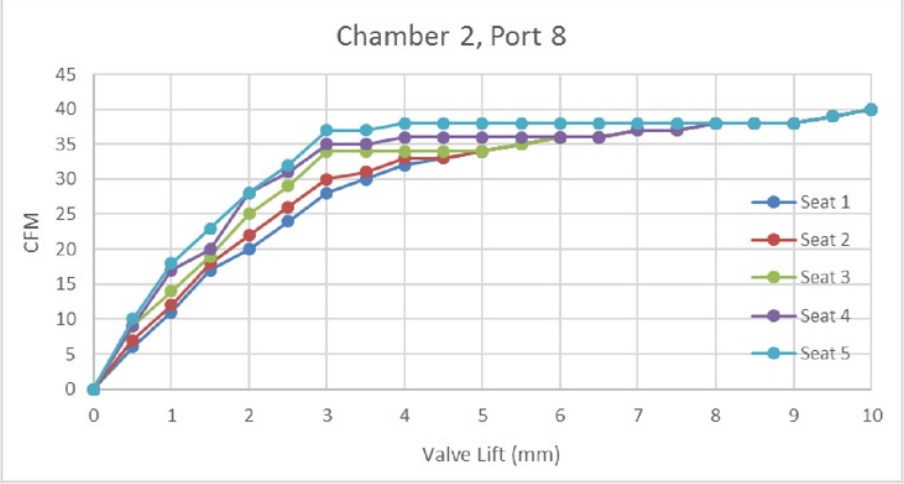

Chamber 2, Port 5
Flow Coefficient
0.45
0.4
0.35
0.3
0.25
0.2
0.15
0.1
0.05
0
0 1 2 3 4 5 6 7 8 9 10
Valve Lift (mm)
Seat 1
Seat 2
Seat 3
Seat 4
Seat 5

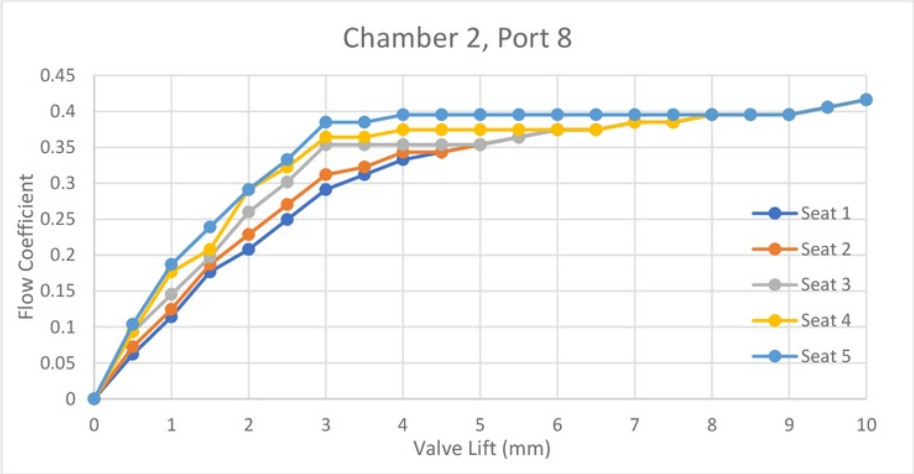

Chamber 2, Port 6
CFM
40
35
30
25
20
15
10
5
0
0 1 2 3 4 5 6 7 8 9 10
Valve Lift (mm)
Seat 1
Seat 2
Seat 3
Seat 4
Seat 5

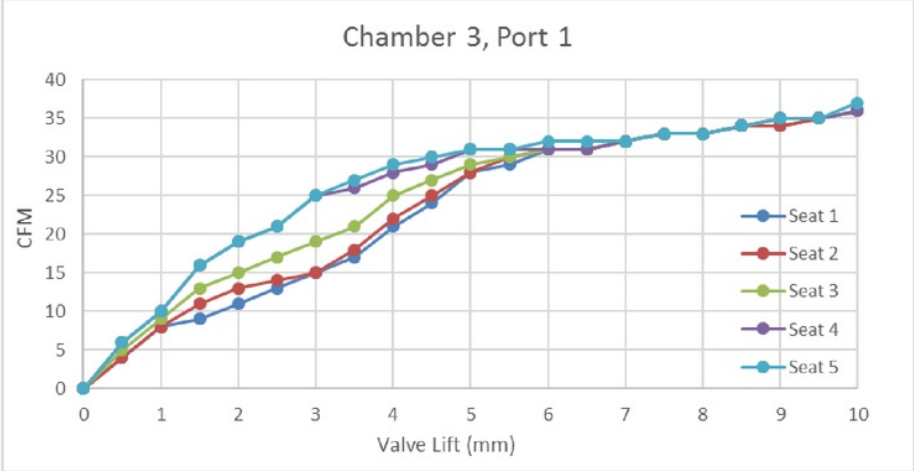

Chamber 2, Port 6
Flow Coefficient
0.45
0.4
0.35
0.3
0.25
0.2
0.15
0.1
0.05
0
0 1 2 3 4 5 6 7 8 9 10
Valve Lift (mm)
Seat 1
Seat 2
Seat 3
Seat 4
Seat 5

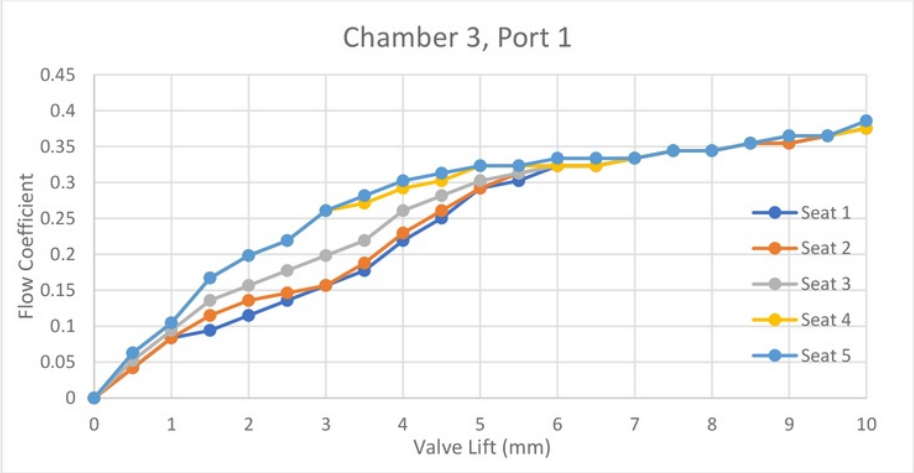

Chamber 2, Port 7
CFM
Valve Lift (mm)
Seat 1
Seat 2
Seat 3
Seat 4
Seat 5

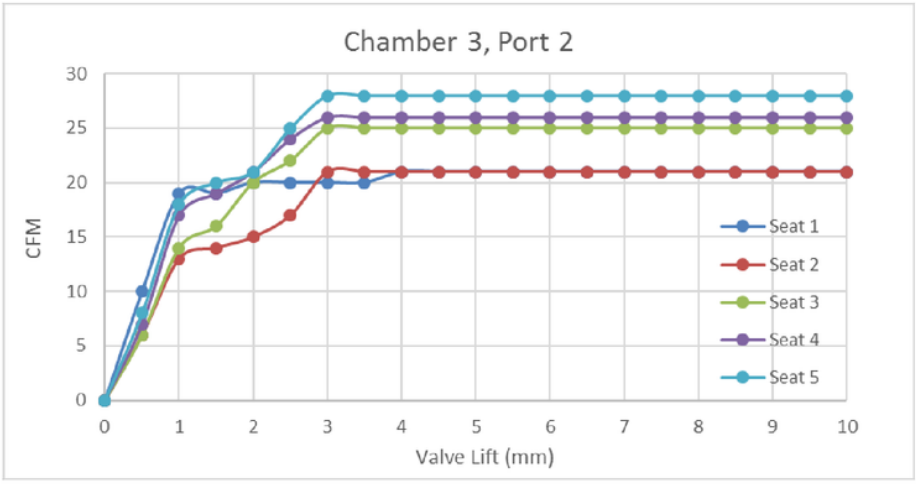

Chamber 2, Port 7
Flow Coefficient
Valve Lift (mm)
Seat 1
Seat 2
Seat 3
Seat 4
Seat 5

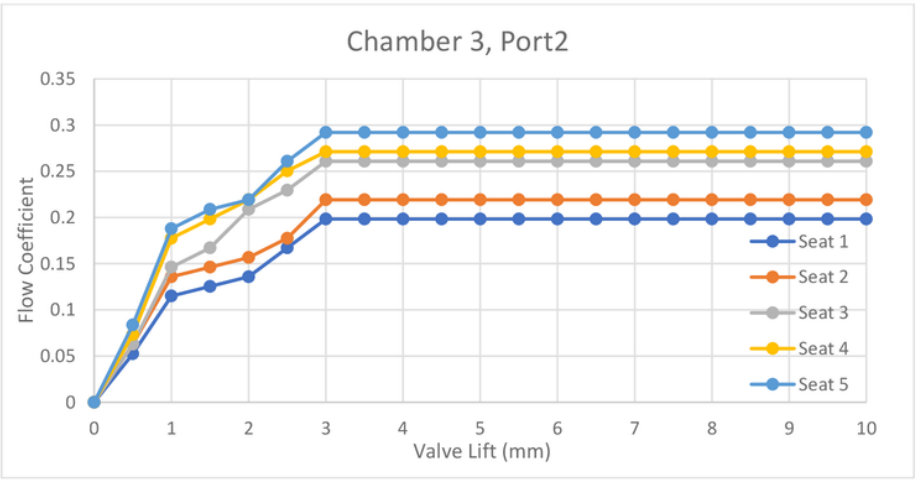

Chamber 2, Port 8
CFM
Valve Lift (mm)
Seat 1
Seat 2
Seat 3
Seat 4
Seat 5

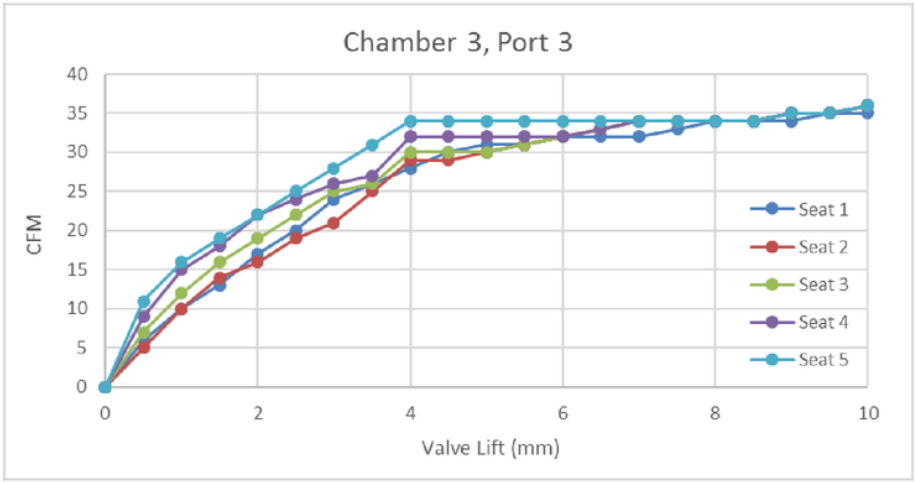

Chamber 2, Port 8
Flow Coefficient
0.45
0.4
0.35
0.3
0.25
0.2
0.15
0.1
0.05
0
0 1 2 3 4 5 6 7 8 9 10
Valve Lift (mm)
Seat 1
Seat 2
Seat 3
Seat 4
Seat 5

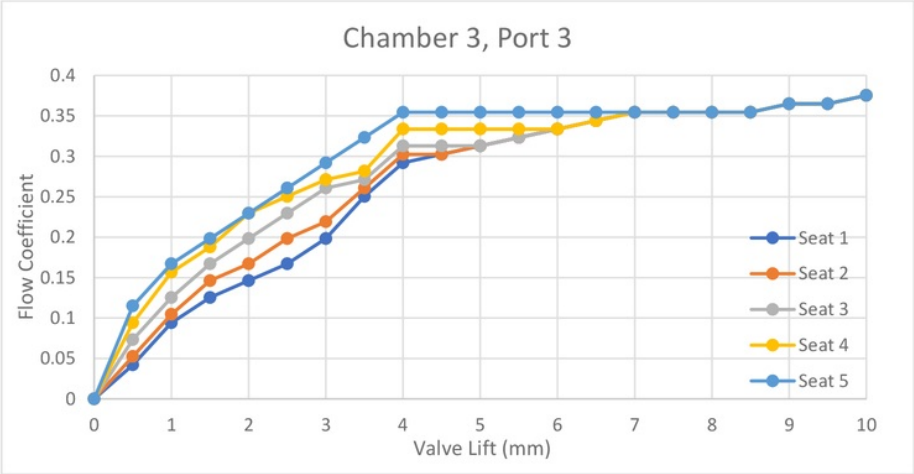

Chamber 3, Port 1
CFM
40
35
30
25
20
15
10
5
0
0 1 2 3 4 5 6 7 8 9 10
Valve Lift (mm)
Seat 1
Seat 2
Seat 3
Seat 4
Seat 5

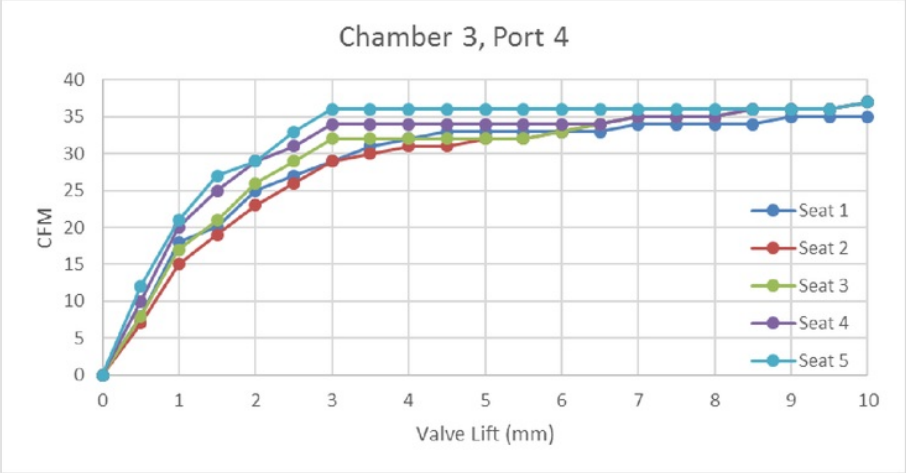

Chamber 3, Port 1
Flow Coefficient
0.45
0.4
0.35
0.3
0.25
0.2
0.15
0.1
0.05
0
0 1 2 3 4 5 6 7 8 9 10
Valve Lift (mm)
Seat 1
Seat 2
Seat 3
Seat 4
Seat 5

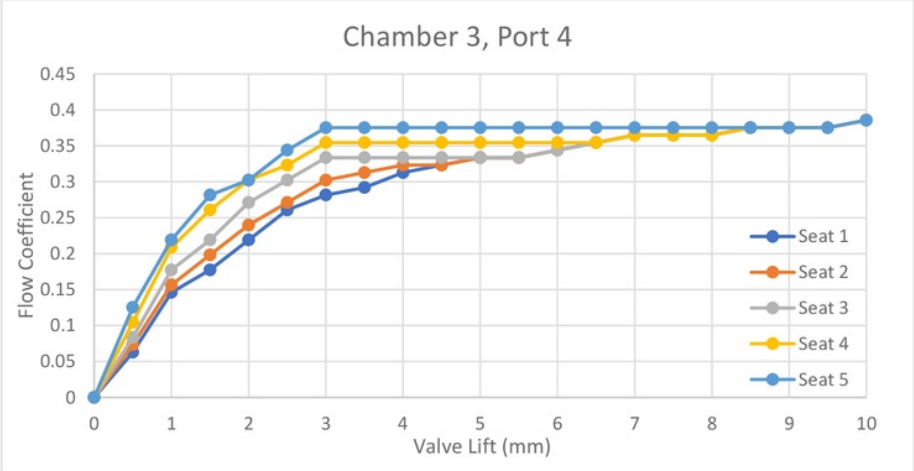

Chamber 3, Port 2
CFM
Valve Lift (mm)
Seat 1
Seat 2
Seat 3
Seat 4
Seat 5

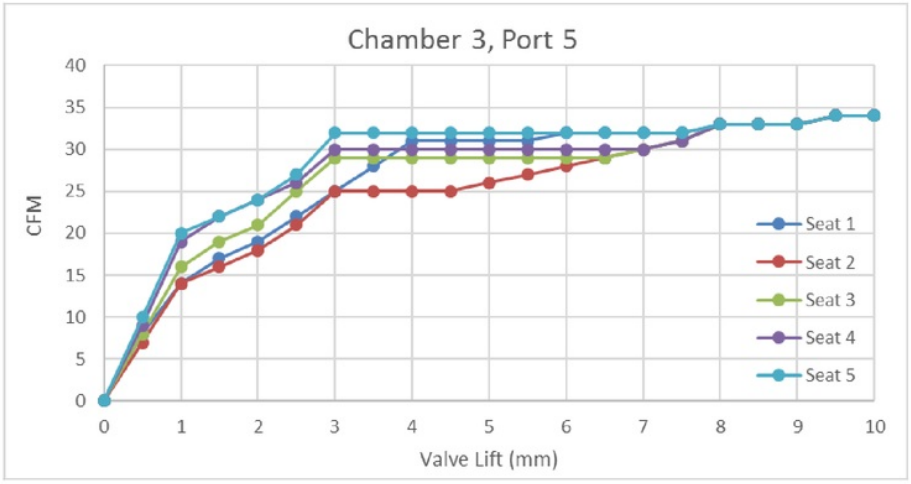

Chamber 3, Port2
Flow Coefficient
Valve Lift (mm)
Seat 1
Seat 2
Seat 3
Seat 4
Seat 5

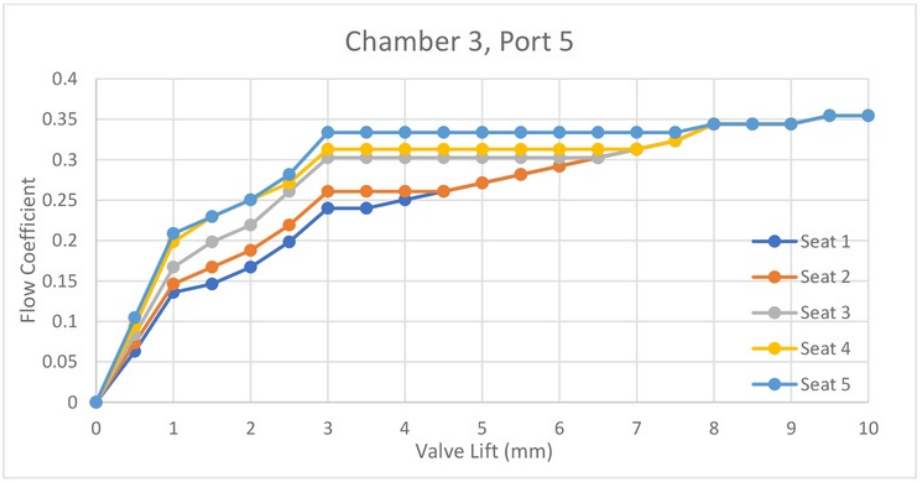

Chamber 3, Port 3
CFM
Valve Lift (mm)
Seat 1
Seat 2
Seat 3
Seat 4
Seat 5

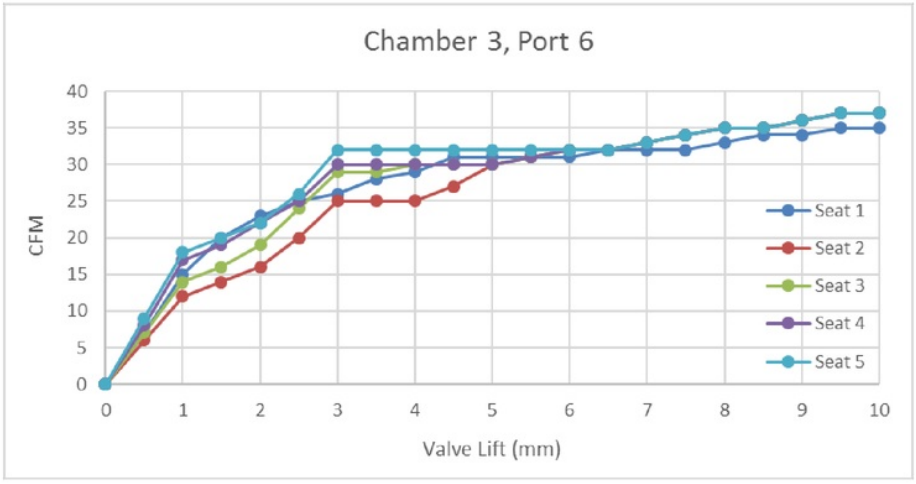

Chamber 3, Port 3
Flow Coefficient
0.4
0.35
0.3
0.25
0.2
0.15
0.1
0.05
0
0 1 2 3 4 5 6 7 8 9 10
Valve Lift (mm)
Seat 1
Seat 2
Seat 3
Seat 4
Seat 5

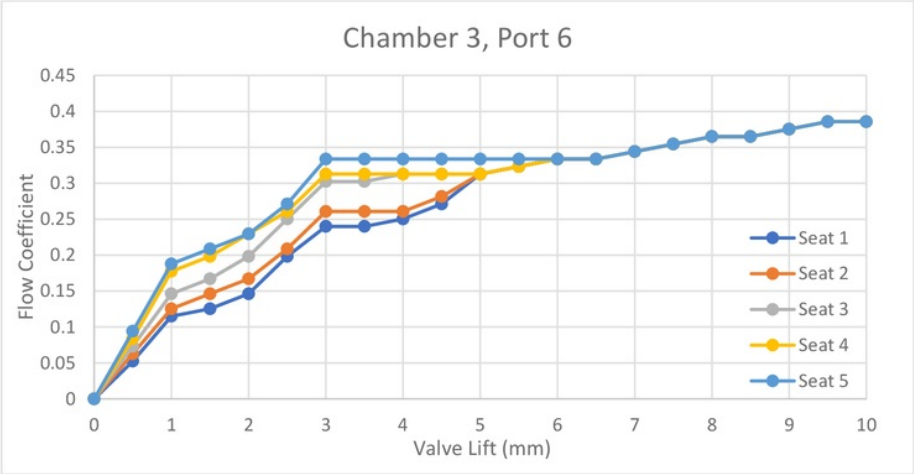

Chamber 3, Port 4
CFM
40
35
30
25
20
15
10
5
0
0 1 2 3 4 5 6 7 8 9 10
Valve Lift (mm)
Seat 1
Seat 2
Seat 3
Seat 4
Seat 5

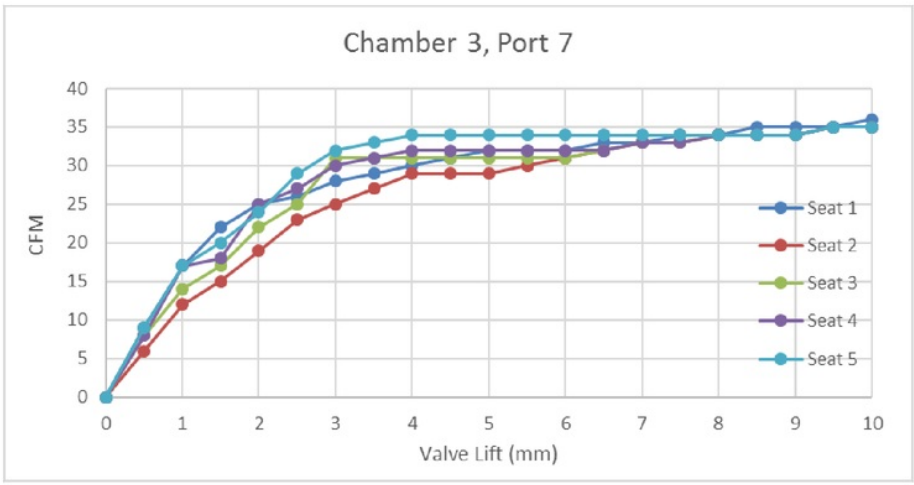

Chamber 3, Port 4
Flow Coefficient
0.45
0.4
0.35
0.3
0.25
0.2
0.15
0.1
0.05
0
0 1 2 3 4 5 6 7 8 9 10
Valve Lift (mm)
Seat 1
Seat 2
Seat 3
Seat 4
Seat 5

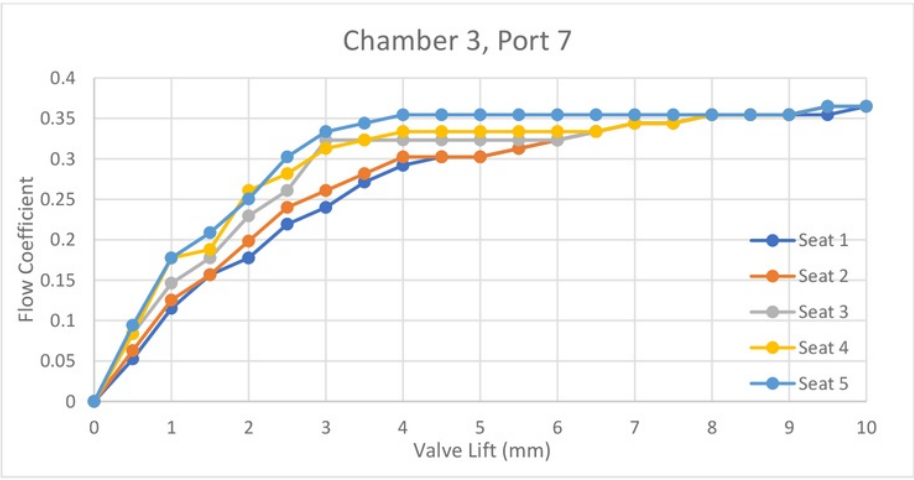

Chamber 3, Port 5
CFM
Valve Lift (mm)
Seat 1
Seat 2
Seat 3
Seat 4
Seat 5

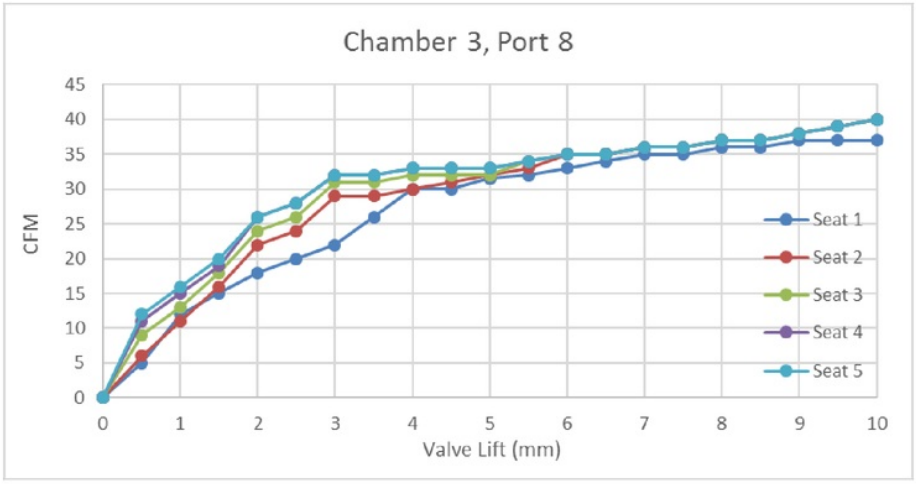

Chamber 3, Port 5
Flow Coefficient
Valve Lift (mm)
Seat 1
Seat 2
Seat 3
Seat 4
Seat 5

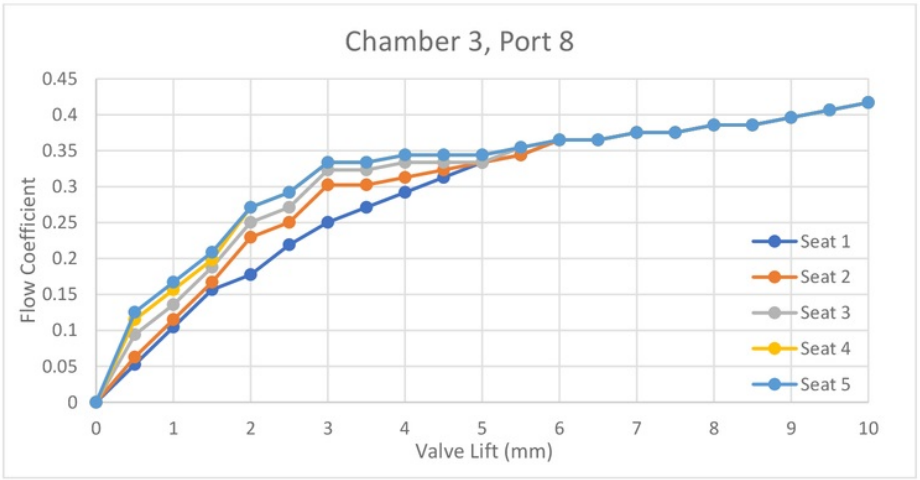

Chamber 3, Port 6
CFM
Valve Lift (mm)
Seat 1
Seat 2
Seat 3
Seat 4
Seat 5

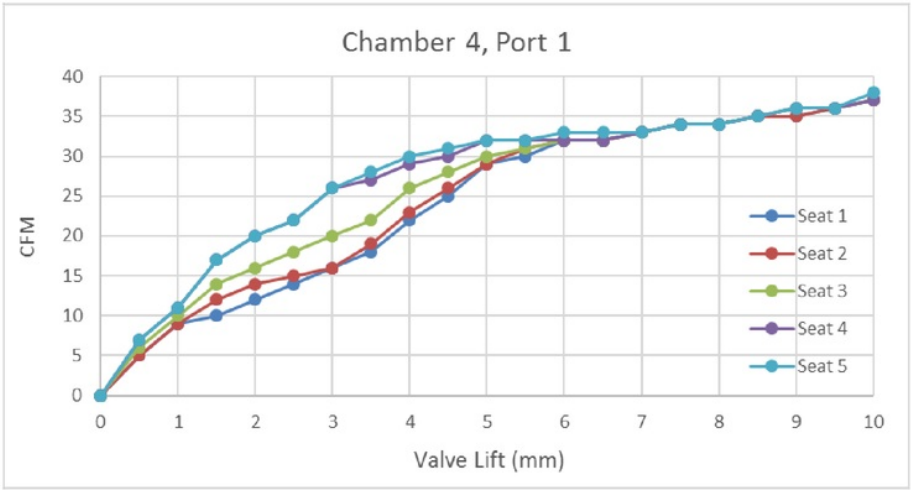

Chamber 3, Port 6
Flow Coefficient
0.45
0.4
0.35
0.3
0.25
0.2
0.15
0.1
0.05
0
0 1 2 3 4 5 6 7 8 9 10
Valve Lift (mm)
Seat 1
Seat 2
Seat 3
Seat 4
Seat 5

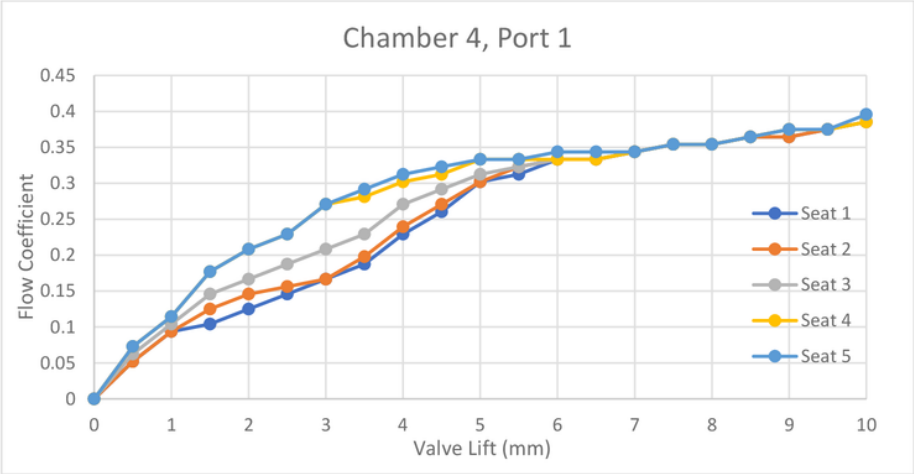

Chamber 3, Port 7
CFM
40
35
30
25
20
15
10
5
0
0 1 2 3 4 5 6 7 8 9 10
Valve Lift (mm)
Seat 1
Seat 2
Seat 3
Seat 4
Seat 5

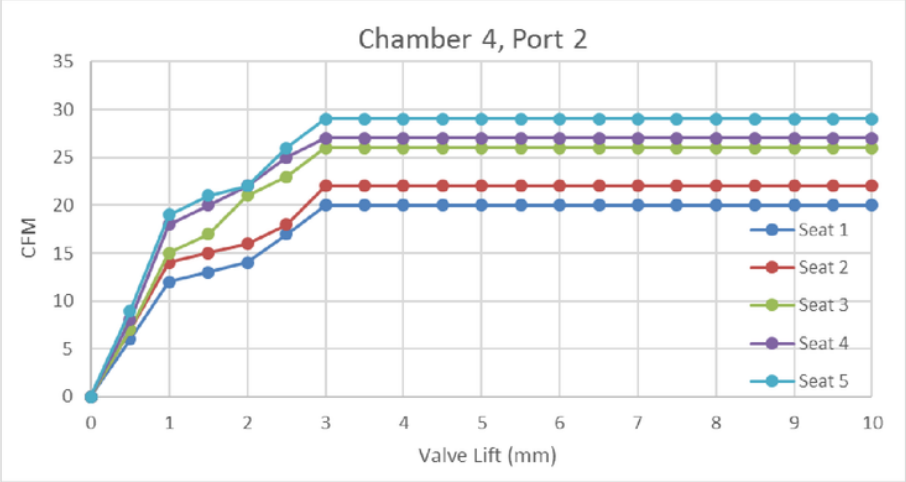

Chamber 3, Port 7
Flow Coefficient
0.4
0.35
0.3
0.25
0.2
0.15
0.1
0.05
0
0 1 2 3 4 5 6 7 8 9 10
Valve Lift (mm)
Seat 1
Seat 2
Seat 3
Seat 4
Seat 5

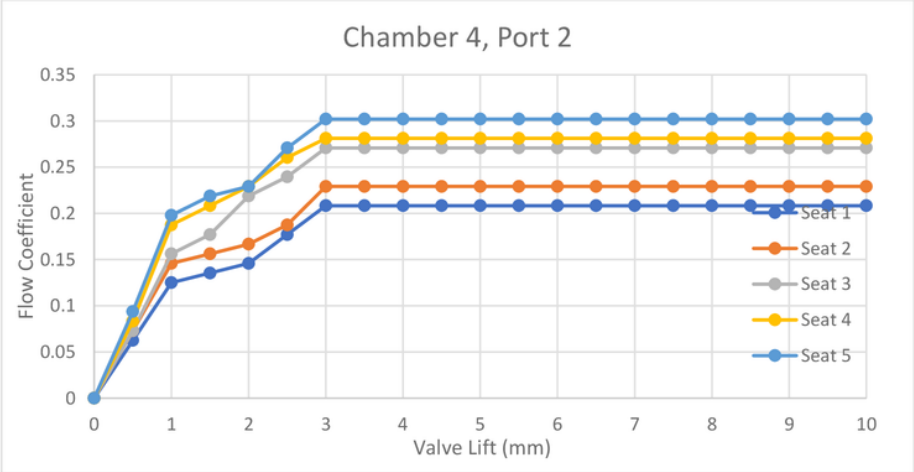

Chamber 3, Port 8
CFM
Valve Lift (mm)
Seat 1
Seat 2
Seat 3
Seat 4
Seat 5

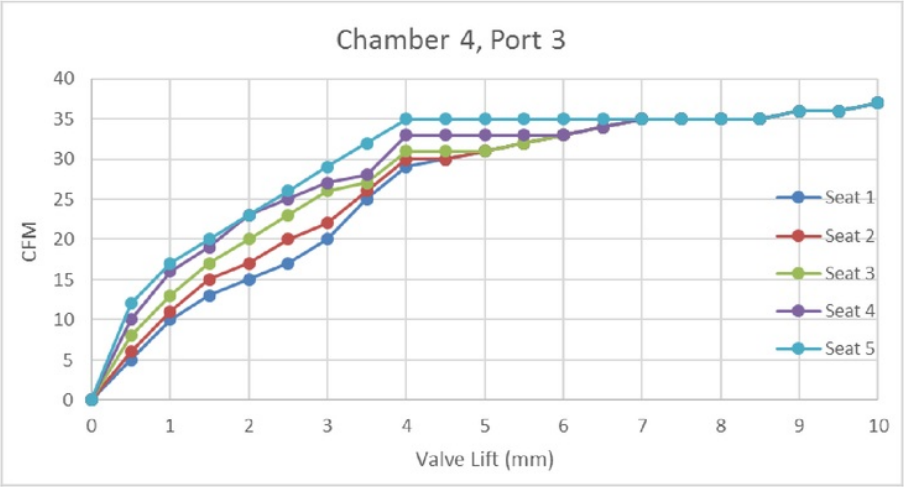

Chamber 3, Port 8
Flow Coefficient
Valve Lift (mm)
Seat 1
Seat 2
Seat 3
Seat 4
Seat 5

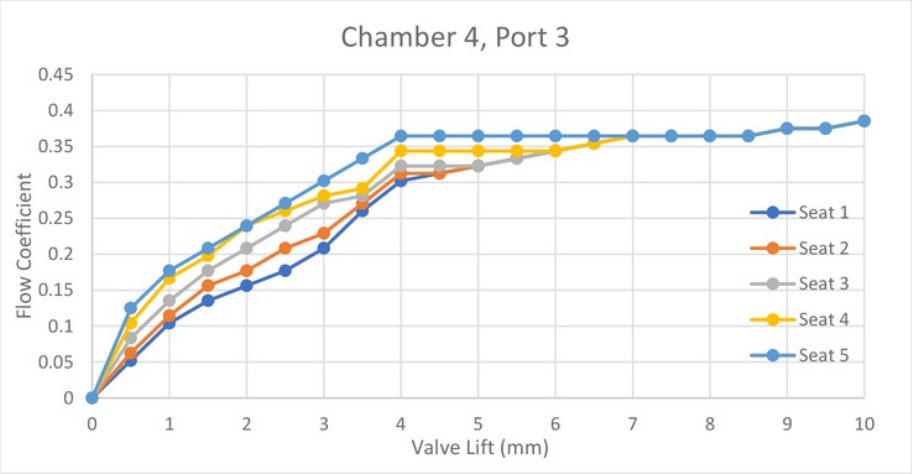

Chamber 4, Port 1
CFM
Valve Lift (mm)
Seat 1
Seat 2
Seat 3
Seat 4
Seat 5

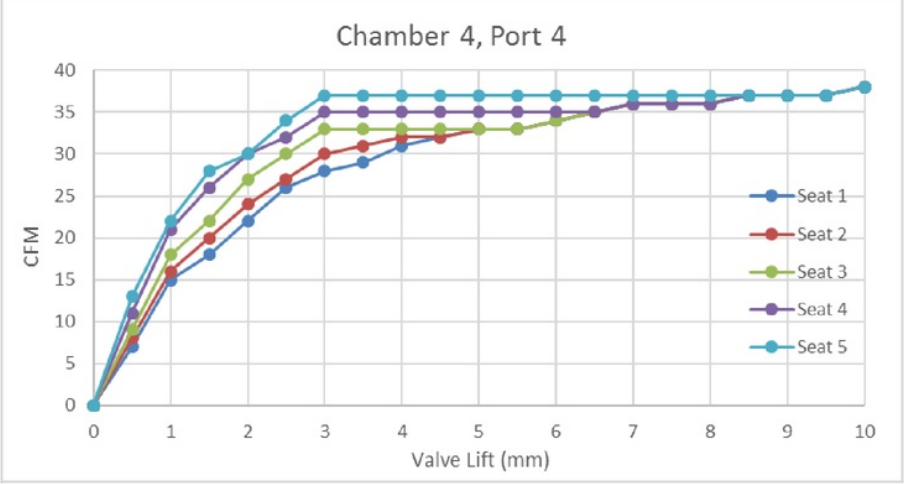

Chamber 4, Port 1
Flow Coefficient
0.45
0.4
0.35
0.3
0.25
0.2
0.15
0.1
0.05
0
0 1 2 3 4 5 6 7 8 9 10
Valve Lift (mm)
Seat 1
Seat 2
Seat 3
Seat 4
Seat 5

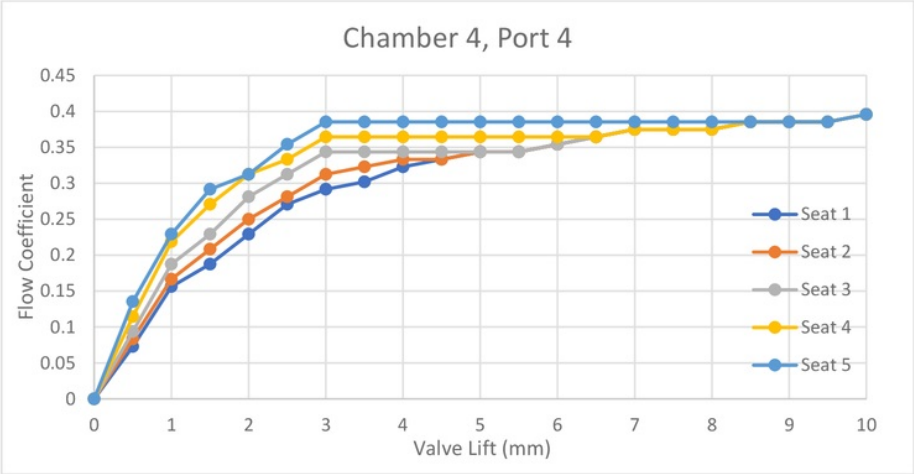

Chamber 4, Port 2
CFM
35
30
25
20
15
10
5
0
0 1 2 3 4 5 6 7 8 9 10
Valve Lift (mm)
Seat 1
Seat 2
Seat 3
Seat 4
Seat 5

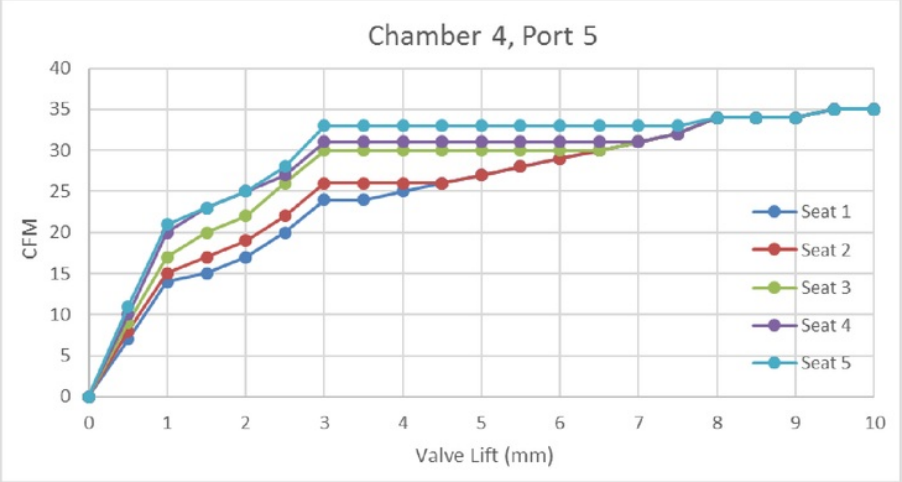

Chamber 4, Port 2
Flow Coefficient
0.35
0.3
0.25
0.2
0.15
0.1
0.05
0
0 1 2 3 4 5 6 7 8 9 10
Valve Lift (mm)
Seat 1
Seat 2
Seat 3
Seat 4
Seat 5

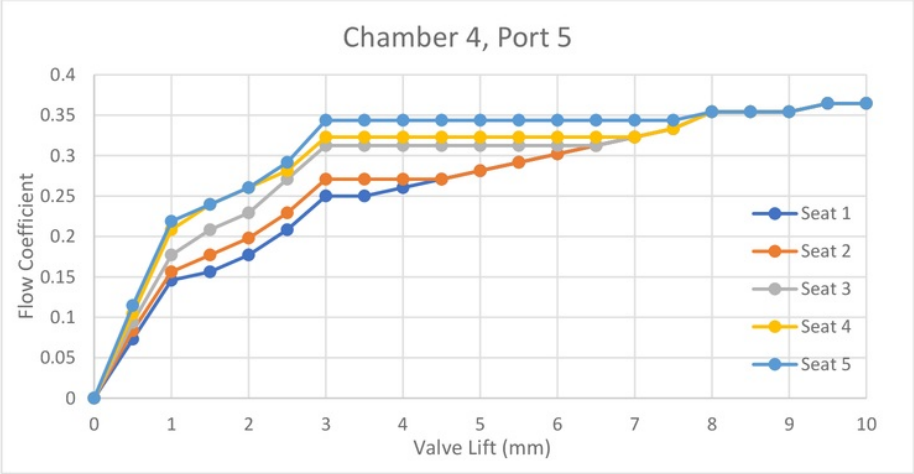

Chamber 4, Port 3
CFM
Valve Lift (mm)
Seat 1
Seat 2
Seat 3
Seat 4
Seat 5

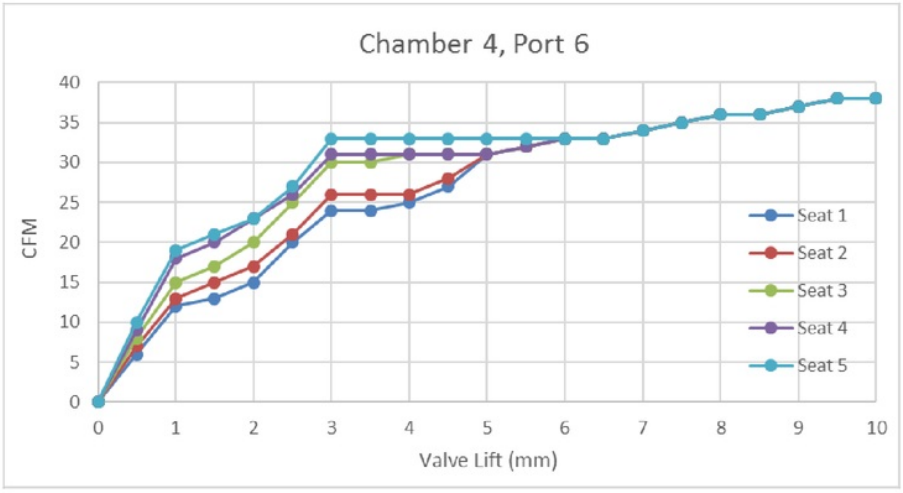

Chamber 4, Port 3
Flow Coefficient
Valve Lift (mm)
Seat 1
Seat 2
Seat 3
Seat 4
Seat 5

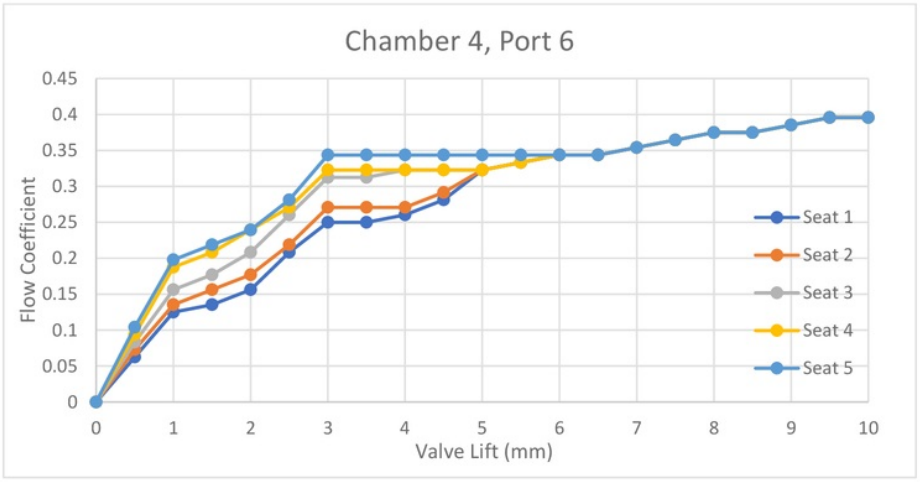

Chamber 4, Port 4
CFM
Valve Lift (mm)
Seat 1
Seat 2
Seat 3
Seat 4
Seat 5

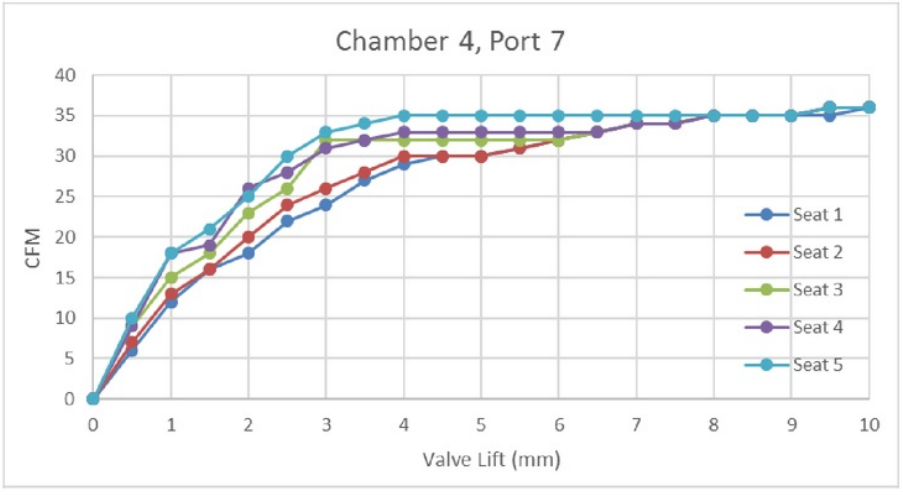

Chamber 4, Port 4
Flow Coefficient
0.45
0.4
0.35
0.3
0.25
0.2
0.15
0.1
0.05
0
0 1 2 3 4 5 6 7 8 9 10
Valve Lift (mm)
Seat 1
Seat 2
Seat 3
Seat 4
Seat 5

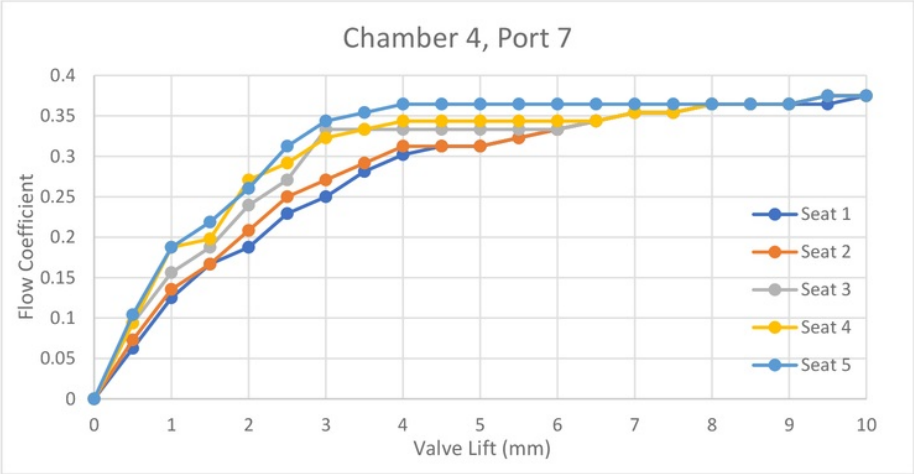

Chamber 4, Port 5
CFM
40
35
30
25
20
15
10
5
0
0 1 2 3 4 5 6 7 8 9 10
Valve Lift (mm)
Seat 1
Seat 2
Seat 3
Seat 4
Seat 5

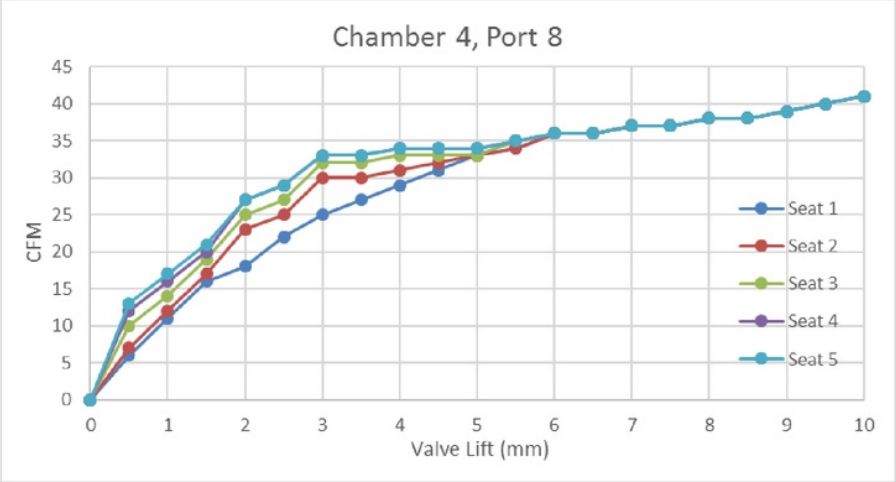

Chamber 4, Port 5
Flow Coefficient
0.4
0.35
0.3
0.25
0.2
0.15
0.1
0.05
0
0 1 2 3 4 5 6 7 8 9 10
Valve Lift (mm)
Seat 1
Seat 2
Seat 3
Seat 4
Seat 5

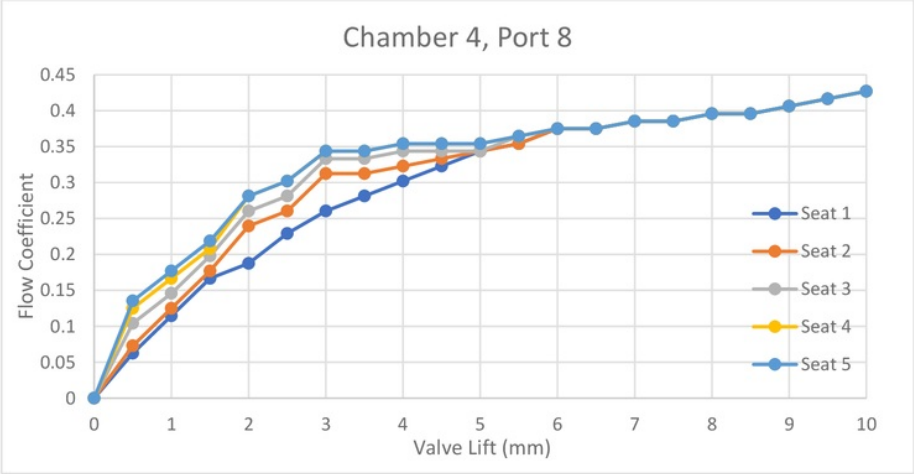

Chamber 4, Port 6
CFM
Valve Lift (mm)
Seat 1
Seat 2
Seat 3
Seat 4
Seat 5


Chamber 4, Port 6
Flow Coefficient
Valve Lift (mm)
Seat 1
Seat 2
Seat 3
Seat 4
Seat 5

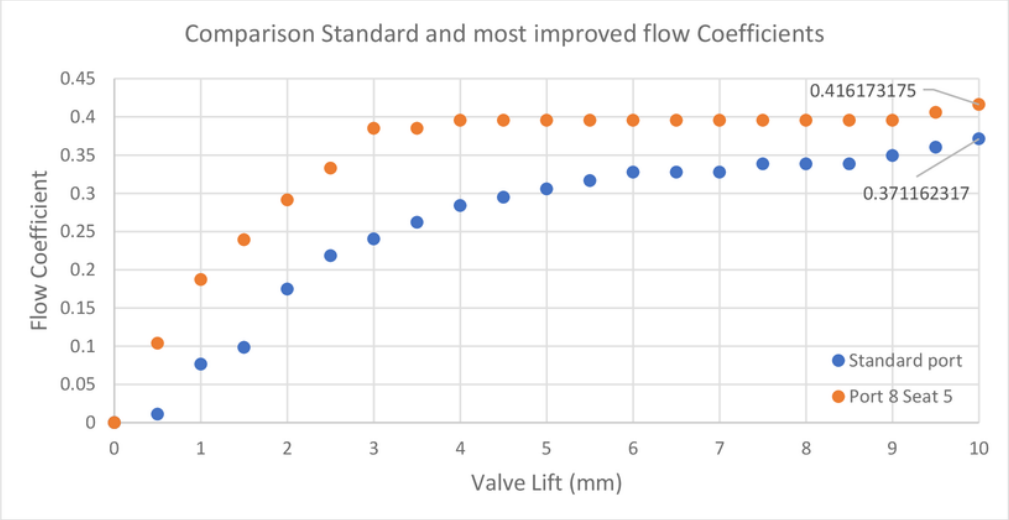

Chamber 4, Port 7
CFM
Valve Lift (mm)
Seat 1
Seat 2
Seat 3
Seat 4
Seat 5


Chamber 4, Port 7
Flow Coefficient
Valve Lift (mm)
Seat 1
Seat 2
Seat 3
Seat 4
Seat 5


Chamber 4, Port 8
CFM
Valve Lift (mm)
Seat 1
Seat 2
Seat 3
Seat 4
Seat 5


Chamber 4, Port 8
Flow Coefficient
Valve Lift (mm)
Seat 1
Seat 2
Seat 3
Seat 4
Seat 5

The results show that the biggest increase in flow can be seen with the increased short and long turn radius with the smoothed guide.



As the graph above shows, the best increase of flow was using the chamber with the biggest shrouding, the 5 angle seats and port 8. It showed significant increase in flow coefficient throughout the whole valve lift range.

As to be expected, by removing material away from the valve circumference the flow is increased. Every time 0.5mm of shrouding is removed, the flow rises.

By creating a smooth path for the air to flow along, the flow increases. As each cut was added to the valve seat, the flow increased especially at low valve lift, this confirms the back ground research in that valve seat configurations are the major player in flow in the port until roughly half of the valve lift range. Although 5 seats seemed to prove the most beneficial, implementing the type of seat in real life would be hard, and time consuming.

Benefits of creating a better path for air to flow along is clear to see. By making a larger short turn radius, the flow is allowed to stay attached longer to the wall. This is the same for increasing the long turn radius. By removing the valve guide a smaller restriction is left in the port and more air is allowed to flow freely past.

Port 2 shows some interesting results as the amount of flow at low valve lift is very high in comparison to the other ports. This is because the cross-sectional area is much smaller, and air is being dragged through. This causes an increase in velocity and flow. However, the flow stagnates towards half of vale lift and then it flows poorly compared to the rest of the ports.

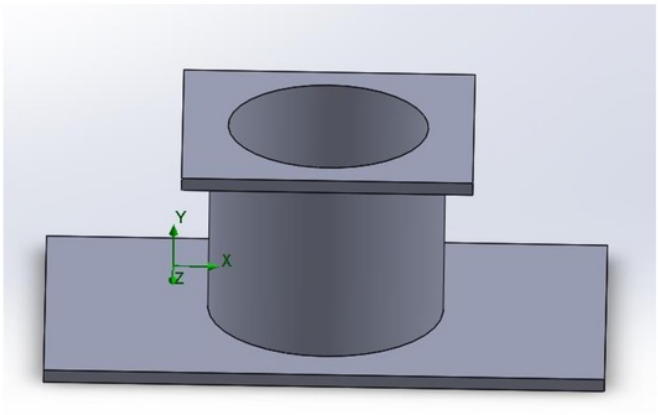
CHAPTER 4

4 FLOW TESTING USING COMPUTATION FLUID DYNAMICS

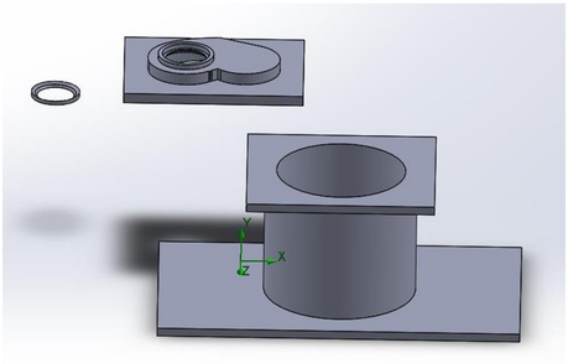
CFD or Computational fluid dynamics is a technology that has increased in popularity as computers have become have faster and more powerful. Liquid or gas flow, can be measured by using laws of conservation of energy, mass and momentum. In order to complete a CFD analysis, numerical algorithms have to be solved using flowing fluid situations. Boundary conditions are set for surfaces and calculations are made to simulate the interactions between the boundary's and the gas/liquid. Newtons second law of fluid motion, and the assumptions that fluids can have a stress in them, which Is calculated by the total of a pressure term and a viscous term is what is used to help calculate CFD simulations. The Navier Stokes Equations are used throughout CFD analysis and describe the correlation between temperature, pressure velocity and density.

What once took many hours of prototype building and physical testing, can now be done in a matter of minutes. These results can then be analysed, the design tweaked, and the new design tested again, without the need to have a physical object. This reduces the overall cost and time of the project and is one of the main reasons CFD has become so popular in design and engineering. In order to safely to produce accurate and reliable results between, computer testing and physical testing, a comparison and a degree of accuracy needs to be made between the two. The CFD analysis in this project is going to be undertaken using Solidworks 2019. An example setup procedure is shown below.

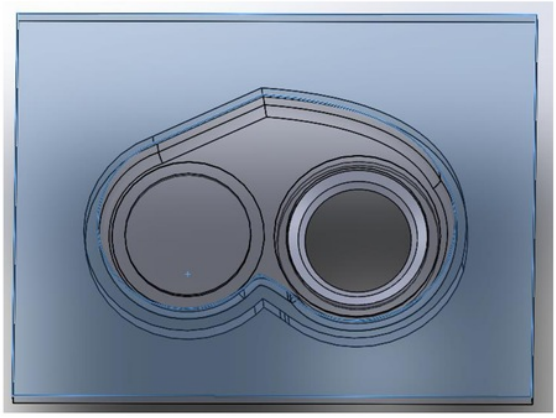
The first stage of setting up the CFD analysis is setting up the flow testing model. The model on solidworks needs to be as accurate and have the same dimensions as the real-life components. A solidworks assembly needs to be created with the first component added being the adaptor plate for the flow bench.



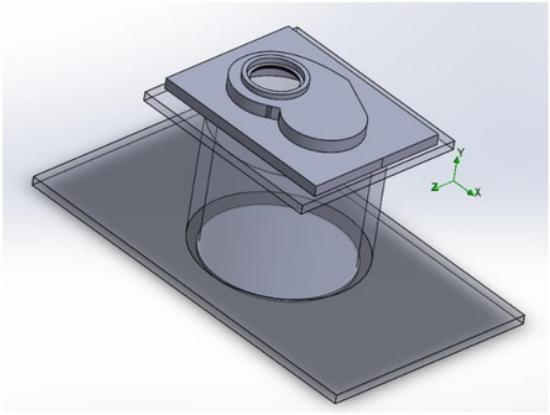
Next the selected combustion chamber can be added to the assembly with the desired seat configuration.



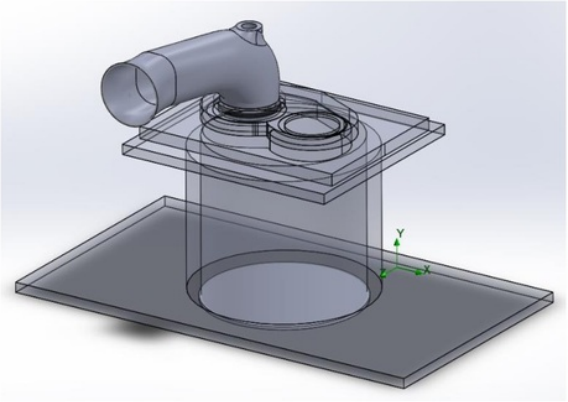
The seat can be mated to the inside of the combustion chamber using a concentric mate.



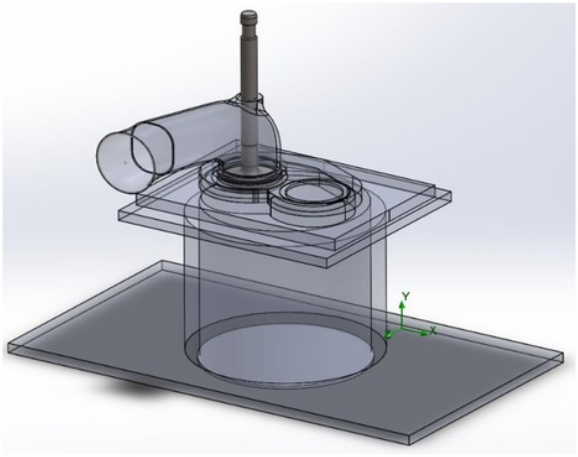
The combustion chamber can then be mated face down on top of the adaptor plate flange.



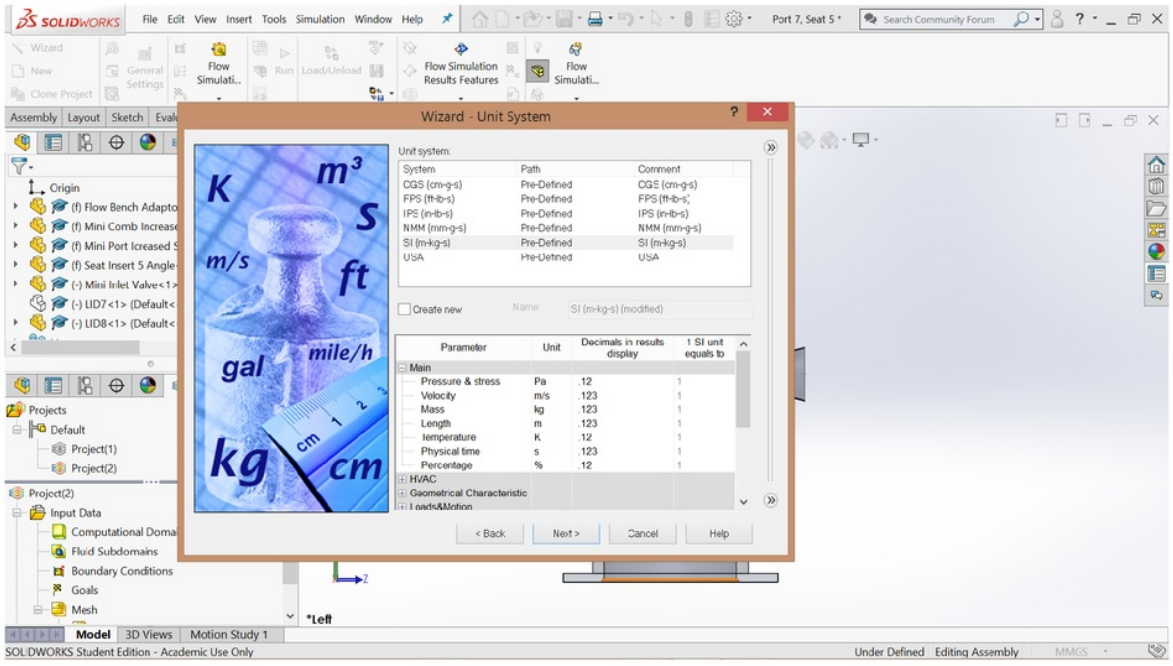
After that, the desired port shape can then be mated to the underside of the combustion chamber using a concentric mate.



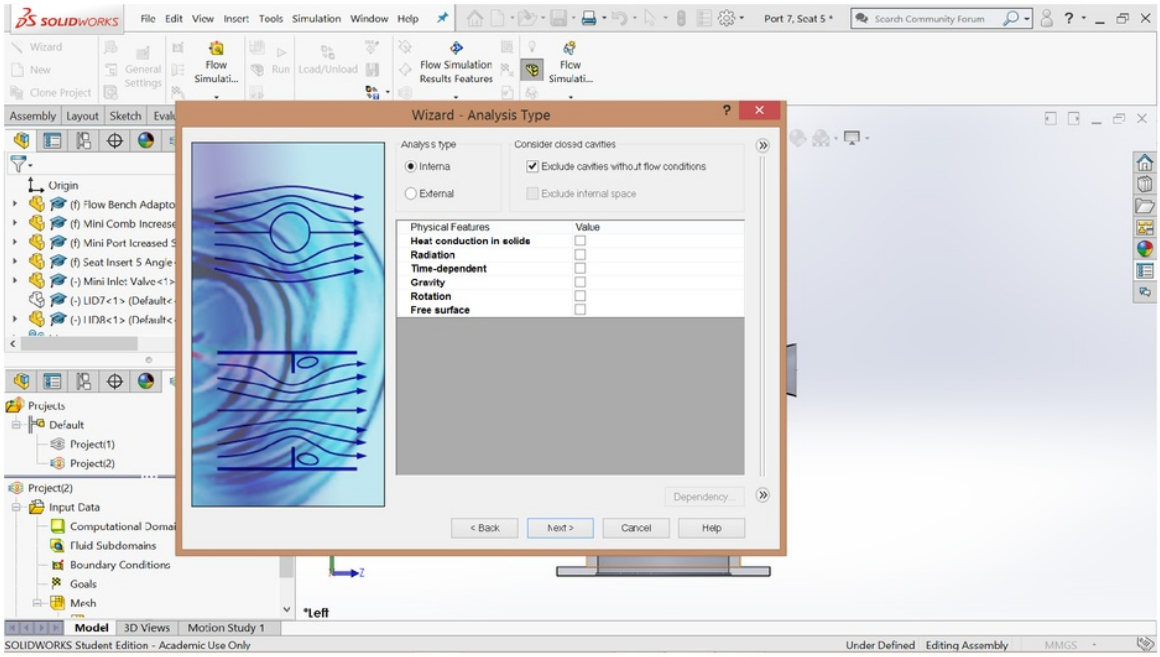
Lastly, the valve can be added to the assembly, using a concentric mate through the guide, and a minimum distance mate to the floor of the combustion chamber, this way the valve will not go through the chamber floor.



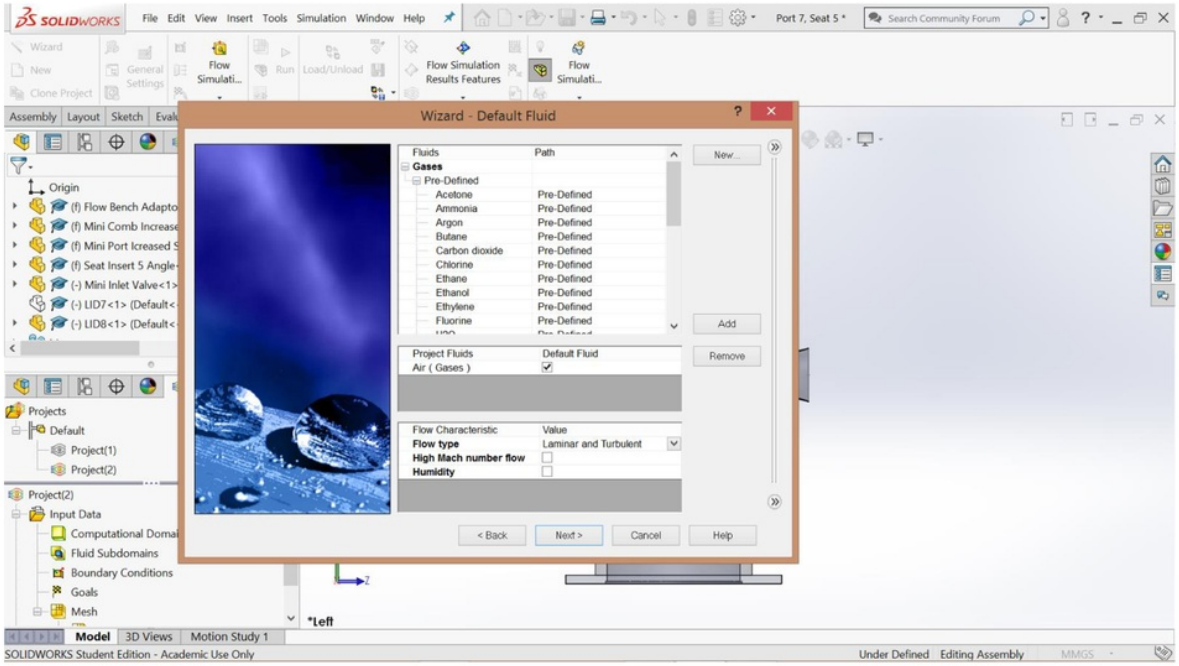
Next, the set up wizard for the CFD analysis can be followed. The first parameters needed to be setup are the type of SI units needed in the analysis.



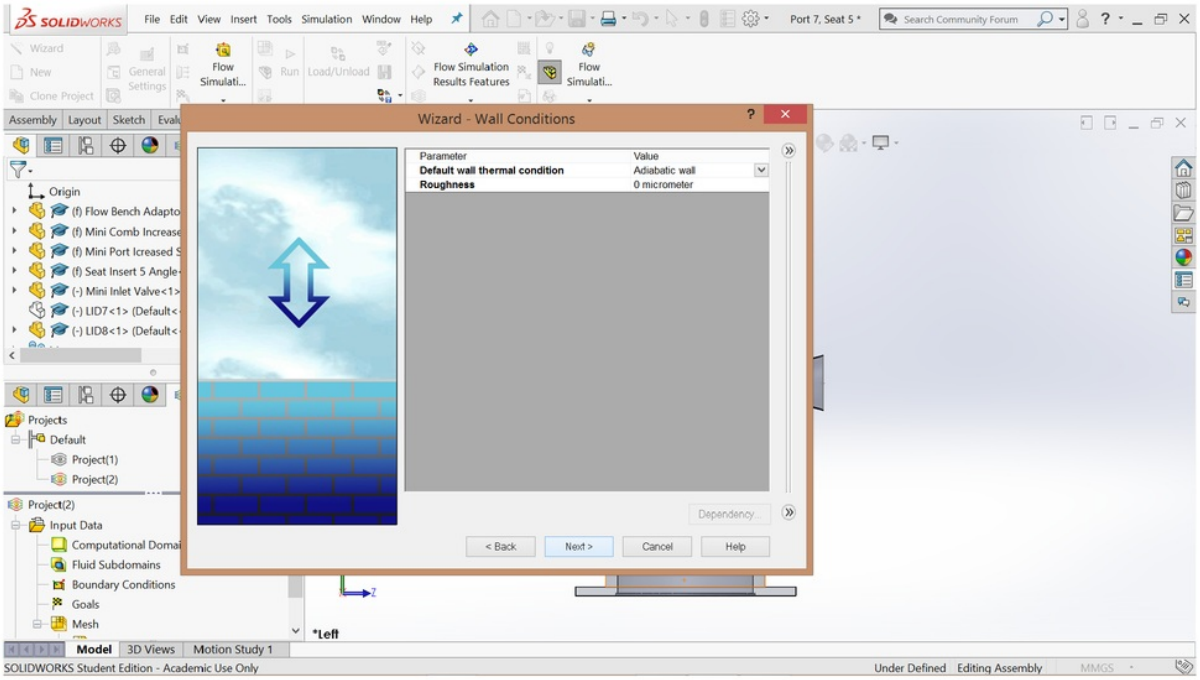
The next page to be completed is the analysis type. Internal should be selected.



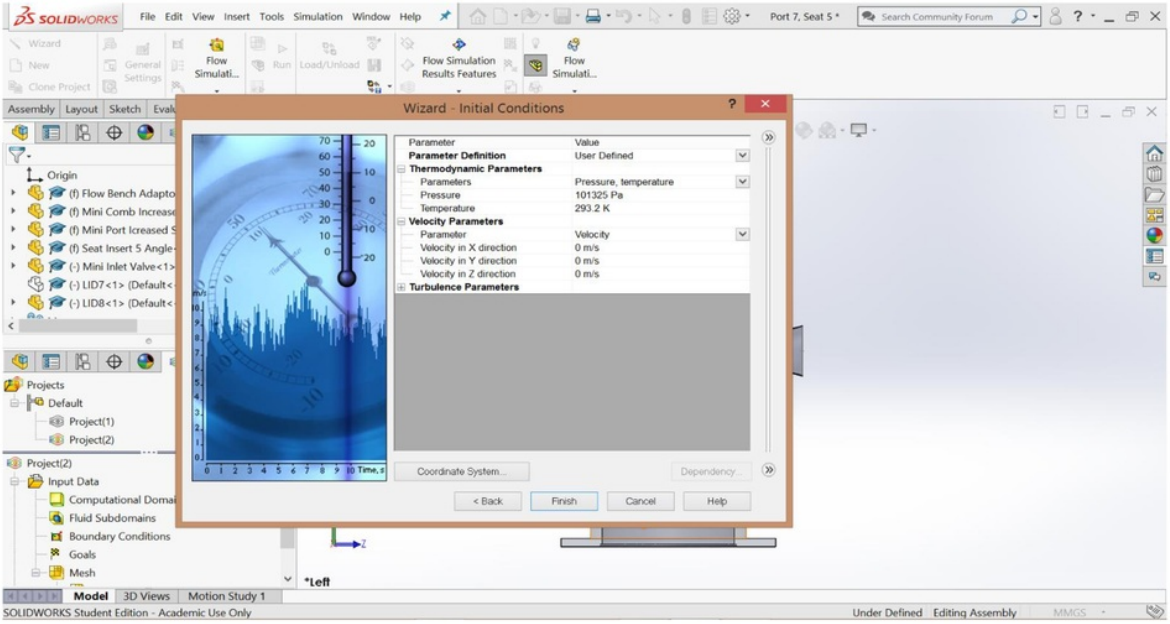
The fluid type options page is next, air should be selected.



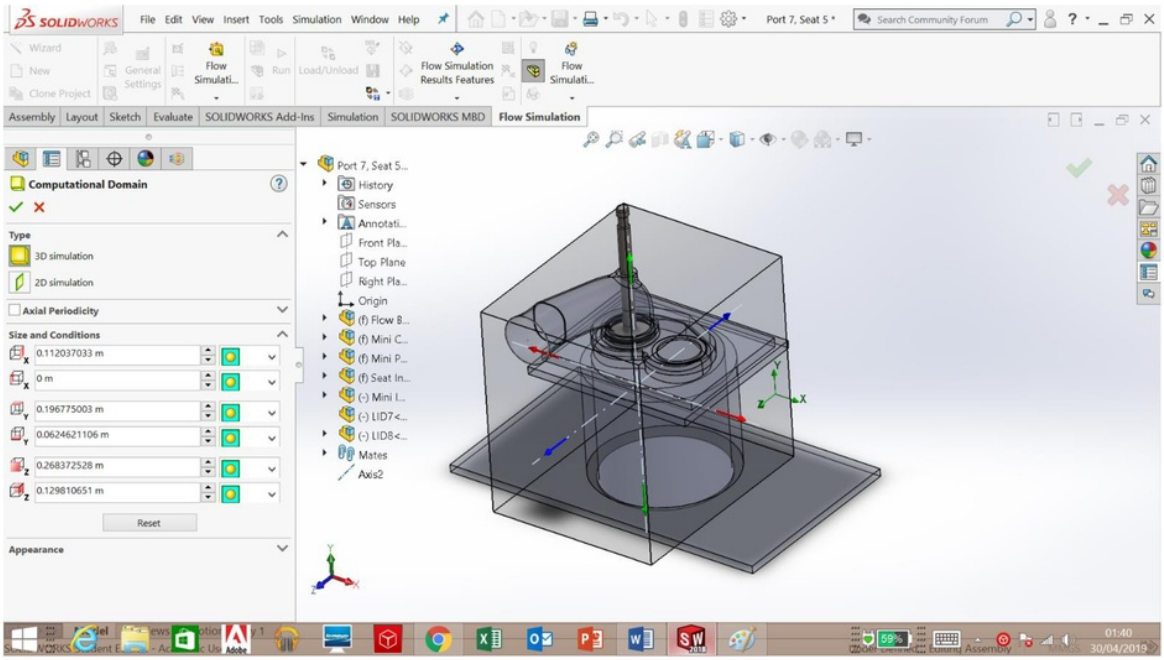
The next page is the wall conditions and should look like this.



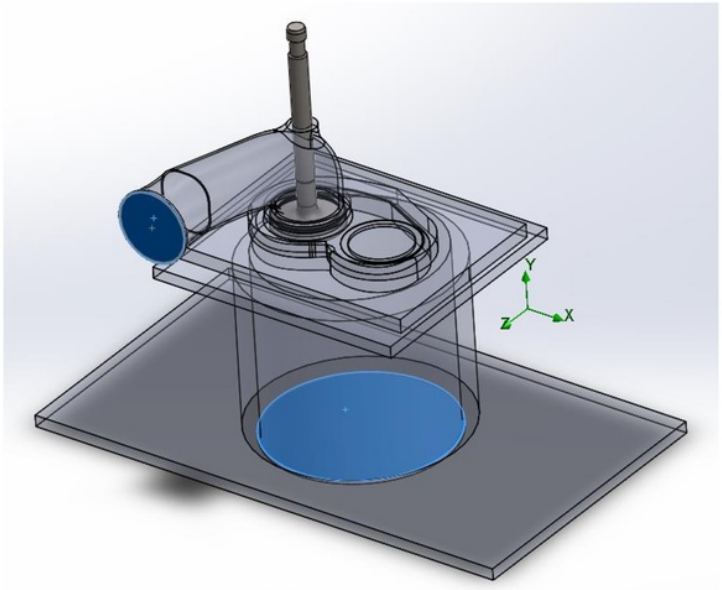
The final page is the initial conditions and should have the following parameters selected.



The computational domain now needs to be selected. This is the area in which the CFD analysis will take place.



Lids now need to be placed on the inside edge of both the orifices in the domain.



Under boundary conditions, the input parameters can be inputted, to create a suction through the assembly, the inlet orifice needs to be at environmental pressure. The pressure drop then needs to worked out. To calculate the pressure, drop the following equation can be used.

$$Pressure\ Drop = h\ \rho\ g$$

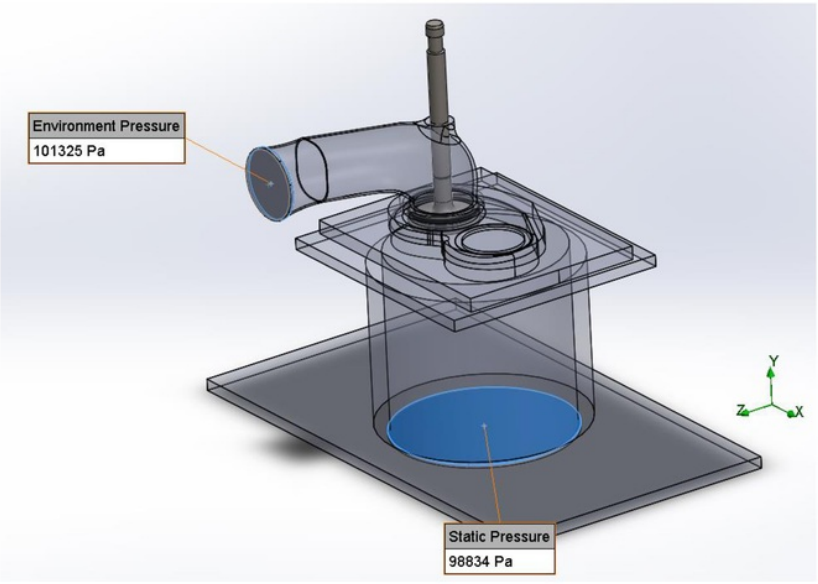
$$Pressure\ Drop = \left(\frac{10" \times 25.4}{1000}\right) \times 1000 \times 9.81$$

$$Pressure\ Drop = 2491$$

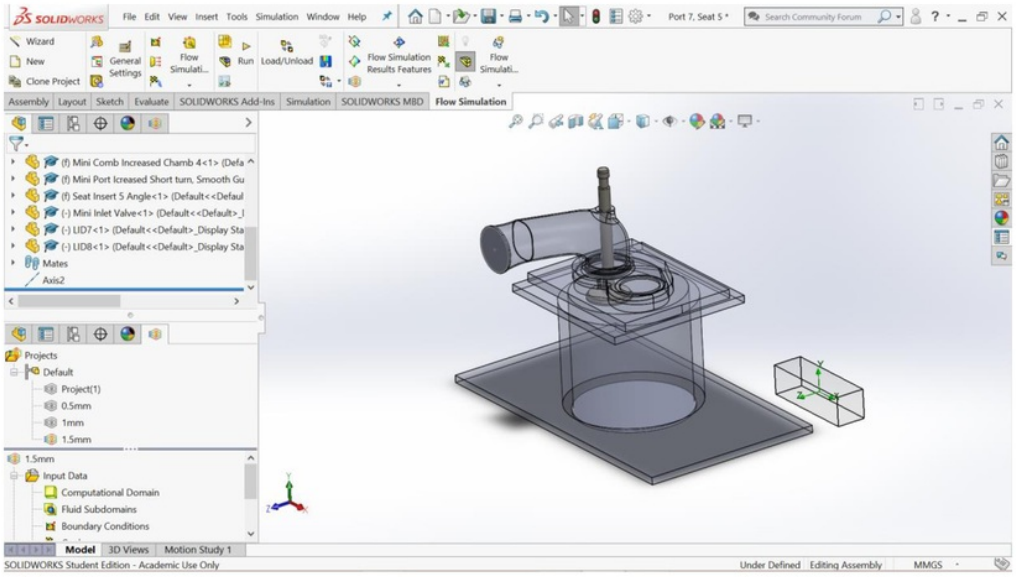
$$\text{Pressure at bottom orifice} = Enviromental\ Pressure - Pressure\ drop$$

$$\text{Pressure at bottom orifice} = 101325 - 2491$$

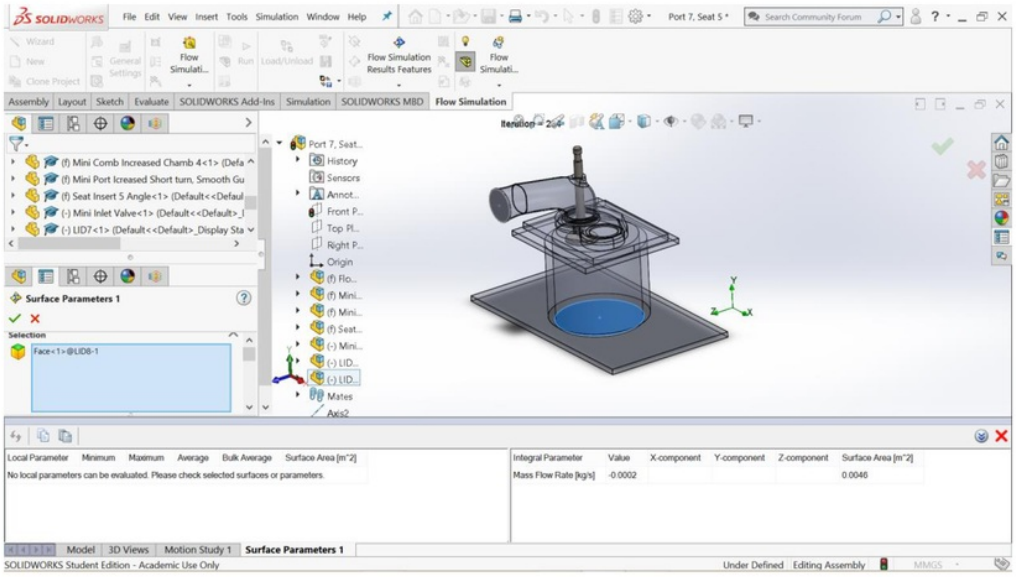
$$\text{Pressure at bottom orifice} = 98834\ \text{Pa}$$



Multiple projects can be run at different valve lifts from 0mm to 10mm



By clicking on the bottom lid, you can create a surface parameter. This can then be shown as a mass flow rate result.



To convert kg/s of air into cubic ft per minute the following calculations can be used:

Density of air at 20 Degrees = 1.2 (kg/m³)

$$kg/s \times 360 = kg/hr$$

$$kg/hr \times \left(\frac{1}{1.2}\, m^3/kg\right) = m^3/hr$$

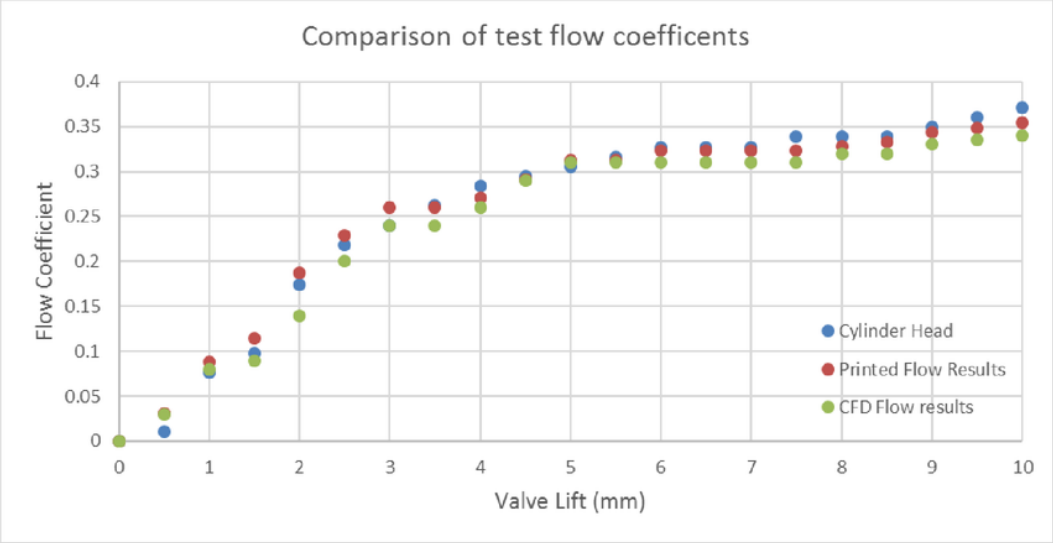
$$m^3/hr \times ft^3/m^3 = ft^3/\text{hr}$$

$$ft^3/\text{hr} \times \frac{1}{60} = ft^3/\text{min}$$

This number for CFM is then converted into a flow coefficient value

Each of the 8 port designs were tested with all 5 seats and all 4 combustion chambers, just like in the real-world testing on the flow bench, the CFD results compared to the flow bench results are below.

4.1 RESULTS COMPARISON



The image above shows the comparison between the three tests conducted. The flow bench test with the cylinder head, the flow bench test with the printed ports, and the flow test conducted using CFD This test in particular is the comparison between the standard mini combustion chamber and port with a single angle valve seat, the results are close to each other. For every real-life flow bench test, the same test using CFD was carried out. The results showed a consistent trend of being within 4% of each other for every test. From this we can say that the CFD analysis can be used as an accurate tool for flow testing and in order to see results for improving flow, physical components and test do not need to be carried out.

4.2 FURTHER WORK

If more time was and budget was allowed for this project there is some further work that would be beneficial to complete. Once the best seat, port and chamber combination has been decided, actually installing it on the physical cylinder head and testing it would be a great way of concluding whether the project was a success or not. Cutting the seats using a valve seat cutter is something that takes skill and specialised machinery which is something that is not available at the moment. The port could be ported by used of Dremel to the exact specification of the preferred cad drawing. The same method can also be applied to remove the inlet valve shrouding. These methods take substantial time and involvement, hence why they were not completed for the project. An investigation into port surface finish could also be conducted. Looking through various sources during the duration of the project has shown that considerable research and investment has been allocated into the surface finish. Leading further from this port dimpling is a relatively new, but growing idea, that by putting dimples along the inlet port turbulence is created and better flow is produced. Lastly, turbulence in a port is a key factor to the performance of an engine. This thesis has only investigated flow through the port. If further time was allocated a study into wether or not the best component combinations for flow aid or reduce the turbulence through the port would be undertaken. After this had been completed the most well-rounded design for flow and turbulence could be decided.

4.3 CONCLUSION

A few key points can be concluded from this study. By reducing increasing the angle of the short turn raidus, flow can be improved into the combustion chamber. This can also be said by increasing the angle of the long turn radius aswell. Valve shrouding restricts the amount of air into the cylinder for the mini cooper engine. Removing this shrouding can improve air flow. By increasing the radius of curvature of the valve seat, flow is allowed to stay attached to its path into the cylinder. A combination of all of the above

allows a significant increase of flow into the mini combustion chamber. The use of CFD Is a valid tool in designing and testing flow through a port, but attention must be paid to the accuracy of the drawing and setting up the test conditions.

4.3 EVALUATION

Overall the project was a success, a slow start did not help, and budget limitations also restricted the flow of the project at the beginning. There are plenty of other sources of information about individual elements that aid flow through a port, however there is no previous work on how all these individual elements work together. This is tricky when trying to compare your work and results with other as there is nothing else to compare to. Not having a clear path was a bit of a restriction at the start of the project but as weeks went by, and tasks were completed a final aim and goal was found. As the project picked up pace, new ideas and test procedures were implemented and tested. The hardest part of the project was trying to figure out a way to be able to test so many configurations with each other, both in real life and on the computer. Setting up the 3d printer was a challenge in itself and took a while to calibrate. The amount of time needed to complete a print was a massive restriction. Especially after waiting 6 hours to find out that the print had failed or wasn't correct. In the end the final designs turned out to work better than imagined and are a great way of being able to test flow both physically and on a flow bench. Being able to snap in and out components almost makes it like a puzzle and feels like a commercial product. the purpose in using CFD in the project was to be able to say that flow tests can be conducted accurately just by using computer analysis. At first the thought was the CFD would show the same result trends as the real-life tests but in fact it actually proved to be better than that as the results were very close to each other. This was unexpected and a nice surprise to be able to validate all three different tests.

4.4 BIBLIOGRAPHY

1 Fontana, G., Galloni, E., Jannelli, E. and Palmaccio, R. (2003) Influence of the Intake System Design on a Small Spark-Ignition Engine Performance: A Theoretical Analysis. SAE Paper No. 2003-1-3134.

2 Winterbone, D.E. and Pearson, R.J. (1999) Design Techniques for Engine Manifolds: Wave Action Methods for IC Engines. USA: Society of Automotive Engineers.

3 McLandress, A., Emerson, R., McDowell, P. and Rutland, C.J. (1996) Intake and InCylinder Flow Modeling: Characterization of Mixing and Comparison With Flow Bench Results. SAE Transactions, 105: 868–881

4 D. S. Oh and C. H. Lee, (2010) “Characteristics of Flow Coefficients in an Engine Cylinder Head with a Quasi-steady Flow Condition by Continuous Variation of the Valve Lift,” Journal of the KOSOS, vol. 25, no. 6. All.

5 D. S. Oh and C. H. Lee, (2011) “A comparative study of flow rate characteristics of an averaging Pitot tube type flow meter according to H parameters based on two kinds of differential pressure measured at the flow meter with varying air temperature,” Journal of Mechanical Science and Technology, vol. 25, no. 8, pp. 1961-1967.

6 El-Adawy, M.; Heikal, M.; Aziz, A.R.A.; Siddiqui, M.; Wahhab, H.A.A.(2017) Experimental study on an IC enginein-cylinder flow using different steady-state flow benches. Alex. Eng. J.

7 M.C.Bates and M.R. Helkal “A Knowledge-Based Model for Multi-Valve Diesel Engine Inlet Port Design” SAE Paper 2002-01-174

8 G J Micklow and W D Gong “Intake and in cylinder flow field modeling of a f our valve diesel engine” I MECH E Volume: 221 Part D Automobile Engineering. Page No:1425-1440 .

9 Selvara, B.SNS., Indraprakash, G., Senthilkumar, A. and Arvind P., 2011. Effects of Intake Port Geometry on the Performance of an SI Engine. JSAE 20119506 / SAE 2011-32-0506.

10 Semin, N.M.I.N. Ibrahim, Rosli A. Bakar and Abdul R. Ismail, In-Cylinder Flow through Piston-Port Engines Modeling using Dynamic Mesh, Journal of Applied Sciences Research, 4(1): 58-64, 2008.

11 Kumar C. R. and Nagarajan G. 2012. Investigation of flow during intake stroke of a single cylinder internal combustion engine. ARPN Journal of Engineering and Applied Sciences. 7 (2): 180-186.

12 Balakrishnan V. K., Morton S., Radavich, P., Sivagaminathan N. and Gopalakrishnan N. 2010. Air flow and charge motion study of engine intake port. 37th National and 4th International Conference on Fluid Mechanics and Fluid Power. Chennai, India. pp. 1-9